Deutsches Zentrum
für Luft- und Raumfahrt e.V.
in der Helmholtz-Gemeinschaft

EnMAP Ground Segment

Mission Quarterly Report #15

01.01.2026 to 31.03.2026

Public

Doc. ID	EN-GS-RPT-1115
Issue	1.0
Date	25.06.2026

Configuration Controlled: Yes

German Remote Sensing Data Center (DFD)
Remote Sensing Technology Institute (IMF)
German Space Operations Center (GSOC)
Helmholtz Centre for Geosciences (GFZ)
German Space Agency at DLR

TABLE OF SIGNATURES

Prepared

Emiliano Carmona Flores

Digitally signed by Emiliano Carmona Flores
DN: C=DE, CN=Emiliano Carmona Flores, GN=Emiliano, L=Koeln, O=Deutsches Zentrum fuer Luft- und Raumfahrt e. V., SN=Carmona Flores, ST=Nordrhein-Westfalen, E=emiliano.carmona@dlr.de, organizationIdentifier=VATDE-121965658
Reason: Prepared
Date: 2026.07.02 10:24:12+02'00'

Date — Emiliano Carmona, (DLR MF-ASP, EnMAP OMM)

Sabine Chabrillat

Digital unterschrieben von Sabine Chabrillat
Datum: 2026.07.02 15:13:26 +02'00'

Date — Sabine Chabrillat, (GFZ, EnMAP SciLead)

Reviewed

i. A. D. Schulze

Digital signiert von Daniel Schulze
Datum: 2026.07.06 08:46:41+02'00'

Date — Daniel Schulze, (DLR RB-MIB, dep. EnMAP OMM)

Sabine Engelbrecht

Digital signiert von Sabine Engelbrecht
DN: C=DE, CN=Sabine Engelbrecht, O=Deutsches Zentrum fuer Luft- und Raumfahrt e. V. (DLR), ST=Nordrhein-Westfalen, E=sabine.engelbrecht@dlr.de, postalCode=51147, street=Linder Höhe
Grund: Ich habe dieses Dokument geprüft
Ort: Oberpfaffenhofen
Datum: 2026.07.02 18:29:08+02'00'
Foxit PDF Editor Version: 14.0.4

Date — Sabine Engelbrecht, (DLR DFD-INF, EOC PAD)

Robert Größel

Digital signiert von Robert Größel
DN: C=DE, CN=Robert Größel, O=Deutsches Zentrum fuer Luft- und Raumfahrt e. V. (DLR), ST=Nordrhein-Westfalen, E=robert.groessel@dlr.de, postalCode=51147, street=Linder Höhe
Grund: Ich bin der Verfasser dieses Dokuments
Ort:
Datum: 2026.07.03 08:37:55+02'00'
Foxit PDF Reader Version: 2026.1.1

Date — Robert Größel, (DLR RB-CTA, GSOC PAD)

Karl Segl

Digital unterschrieben von Karl Segl
Datum: 2026.07.02 16:47:58 +02'00'

Date — Karl Segl, (GFZ, dep. EnMAP SciLead)

Approved & Released

i. A. Laura La Porta

2026.07.10
13:55:17+02'00'
14.0.4

Date — Laura La Porta, (DLR AR-AO, EnMAP MM)

DISTRIBUTION LIST

The document is publicly available via www.enmap.org.

CHANGE RECORD

Version	Date	Chapter	Comment
1.0	25.06.2026	All	First issue of Mission Quarterly Report #15 corresponding to 01.01.2026 to 31.03.2026.

Custodian of this document is Carmona, Emiliano.

CONTENTS

LIST OF FIGURES

LIST OF TABLES

1 Introduction

1.1 Purpose

This mission quarterly report (MQR) states information on the EnMAP mission status with regard to the registered user community, announcements-of-opportunities and observations as well as the status of the user interfaces, satellite (platform and payload), ground stations (S-band and X-band), processor (Archive, Level 1B, Level 1C, Level 2A (land and water)), calibration (spectral, radiometric, geometric), data quality control and validation of EnMAP.

Please visit www.enmap.org for further information on EnMAP.

1.2 Scope

This 15th Mission Quarterly Report (MQR) applies to the operations of EnMAP in the reporting period of Routine Phase (RP) from **01.01.2026 to 31.03.2026 (Q1 2026)**.

2 References

Reference Identifier	Document Identifier and Title
[1]	L. Guanter et al. (2015) The EnMAP Spaceborne Imaging Spectroscopy Mission for Earth Observation. Remote Sensing, Issue 7, pp. 8830-8857.
[2]	EN-GS-UM-6020 Portals User Manual, Version 1.4
[3]	EN-PCV-ICD-2009-2 Product Specification, Version 1.9
[4]	EN-PCV-TN-4006 Level 1B ATBD, Version 1.10
[5]	EN-PCV-TN-5006 Level 1C ATBD, Version 1.7
[6]	EN-PCV-TN-6007 Level 2A (land) ATBD, Version 2.4
[7]	EN-PCV-TN-6008 Level 2A (water) ATBD, Version 3.1
[8]	Chabrillat, S. et al. (2022) EnMAP Science Plan. EnMAP Technical Report, DOI: 10.48440/enmap.2022.001
[9]	Storch, T.; Honold, H.-P.; Chabrillat S., et al. The EnMAP imaging spectroscopy mission towards operations. Remote Sens. Environ. 2023, 294, 113632. DOI: 10.1016/j.rse.2023.113632
[10]	Brell, M.; Reiners, P.; Guanter, L.; et al. Assessment of EnMAP data quality through global product validation activities. Remote Sensing of Environment 342 (2026) 115459. https://doi.org/10.1016/j.rse.2026.115459

Table 2-1 References

3 Terms, Definitions and Abbreviations

Terms, definitions and abbreviations for EnMAP are collected in a database which is publicly accessible via Internet on www.enmap.org.

An Earth observation of swath length $n \times 30$ km (and swath width 30 km) is separated into n tiles of size 30 km × 30 km.

4 Mission

4.1 Mission Objectives

The primary goal of EnMAP (Environmental Mapping and Analysis Program) is to measure, derive and analyze quantitative diagnostic parameters describing key processes on the Earth's surface [1].

During the mission operations, with the successful launch on 1st of April 2022 and an expected operational mission lifetime of at least 5 years, EnMAP will provide valuable information for various application fields comprising soil and geology, agriculture, forestry, urban areas, aquatic systems, ecosystem transitions.

4.2 Mission Description

The major elements of the EnMAP mission are the EnMAP Space Segment, built by OHB System AG and owned by the German Space Agency at DLR, the EnMAP Ground Segment built and operated by DLR institutes DFD, MF, RB, and the EnMAP User and Science Segment represented by GFZ. The project management of the EnMAP mission is responsibility of the German Space Agency at DLR.

The EnMAP Space Segment is composed of

- the platform providing power and thermal stability, orbit and attitude control, memory, S-band uplink/downlink for TM/TC data transmission/reception, X-band downlink for payload data transmission, and

- the payload realized as a pushbroom imaging dual-spectrometer covering the wavelength range between 420 nm and 2450 nm with a nominal spectral resolution ≤ 10 nm and allows in combination with a high radiometric resolution and stability to measure subtle reflectance changes.

The EnMAP satellite is operated on a sun-synchronous repeat orbit to observe any location on the globe with comparable illumination conditions. This allows a maximum reflected solar input radiance at the sensor with an acceptable risk for cloud coverage.

The EnMAP Ground Segment is the interface between Space Segment and User and Science Segment. It comprises functionalities to

- perform planning of imaging, communication and orbit maneuver operations, provision of orbit and attitude data, command and control of the satellite, ground station networks (in particular: Weilheim, Germany, for S-band and Neustrelitz, Germany, for X-Band), receive satellite data, perform long-term archiving and delivery of products, and

- perform processing chain (for systematic and radiometric correction, orthorectification, atmospheric compensation), instrument calibration operations, and the data quality control of the products.

The EnMAP mission interfaces to the international science and user community through the EnMAP Portal www.enmap.org with official information related to EnMAP by DLR and GFZ-Potsdam (as the document in hand) and links for ordering observations and products.

The EnMAP Science Segment is represented by the EnMAP Science Advisory Group chaired by the mission principal investigator at the GFZ-Potsdam. The Science Segment addresses aspects such as

- supporting and performing validation activities to improve sensor performance and product quality

- developing scientific and application research to fully exploit the scientific potential of EnMAP [8] including provision of software tools for EnMAP data processing and analyses (EnMAP-Box) and provision of teaching and education materials (HYPERedu)

- Organizing workshops, summer schools and in general information, training and networking activities for the user community

The EnMAP User Segment is the community of German and international users ordering acquisitions and accessing products of EnMAP.

4.3 Mission Status Summary

The mission successfully finished the commissioning phase (CP) on 01.11.2022 and entered its routine phase (RP) on 02.11.2022. For an overview of the EnMAP mission and the activities and results of the Launch and Early Orbit and Commissioning Phases, check [9]. For an overview of the EnMAP product validation activities during the commissioning phase and the first two years of the operational phase check [10].

In the reporting period, from 01.01.2026 to 31.03.2026, there have been no major issues affecting the instrument or the satellite, only some minor issues have caused the loss of a small fraction of observation time. The Ground Segment services have been operating normally, with some very minor exceptions.

During the period 01.01.2026 to 31.03.2026 (90 days in total), no issues resulted in an extended loss of acquisitions. During normal operations, the mission is regularly surpassing the initially planned maximum acquisition capacity of 5000 km / day. Nevertheless, the average number of acquisitions is reduced compared to previous quarters as a result of the introduction of the new cloud strategy to reduce the presence of clouds in the EnMAP imagery. On the Neustrelitz receiving station three passes were lost due to a problem on the downconverter. This resulted in the loss of 20 acquired datatakes during transmission on the 04.01.2026 (6 datatakes) and 05.01.2026 (14 datatakes).

In this period, 1345 Earth observations of 30 km swath width and up to 990 km swath length were successfully performed which resulted in 15709 archived Earth observation tiles of 30 km × 30 km and 20 calibration acquisitions. In addition, 22004 products were delivered from catalog orders. In total, 22871 Earth observations were performed until 31.03.2026 by the EnMAP team and the 5289 registered users with at least one active user role. This results in 209458 archived Earth observation images (249846 products including the different versions of the re-processed products) and 401673 Earth products delivered from observations requests (217021) and catalogue orders (184652) since the start of the mission. More details are presented in sections 5 and 6.

The mission acquisition process was updated at the end of November 2025 to improve cloud forecast handling during planning. The forecast request window to obtain cloudiness predictions from the German Meteorological Service (DWD) has been reduced to ensure EnMAP acquisitions are planned with the most up-to-date information. Additionally, acquisitions with negative forecasts (predicted cloudiness exceeding the threshold specified in the request) are now excluded from planning, whereas previously they could still be considered and scheduled if no better alternative was available. As a result, the total number of acquisitions has decreased in future quarters, but the quality of acquired has improved significantly thanks to a reduced cloud presence in the EnMAP products. Data shows that user requests in the period 01.01.2025 – 15.05.2025 had a cloudiness median of 20% (20% clouds of less in 50% of the user tasked scenes), while in the same period of 2026 (01.01.2026 – 15.05.2026) the cloudiness median is 2%.

No major limitations are applicable at 31.03.2026. For minor limitations affecting data processing, check section 7.4. Other effects observed in the data by our Quality Control team are reported in section 7.6 where they are investigated in more detail.

Activities within the EnMAP Mission and in particular the Ground Segment are periodically reported in conferences and workshops. More details are available in Section 9.

The following changes were implemented in the reporting period:

- New processor version (**V01.05.06**). For more details on this new version see section 7.4.
- Implementation of updated FGM flightlines and switch to normal mode (from winter mode)

- Implementation of stricter policy concerning use of private emails for registration as an EnMAP user. Registration as a EnMAP user now requires the use of an institutional mailing address (e.g. University or research center).
- Reprocessing of L0 products to L2A ARD products with processor version **V01.05.02** in progress. It is expected that all L2A ARD products in EOC-Geoservice are updated to a version **≥ V01.05.02** until the end of July 2027. During this re-processing, L1B and L1C ARD products for the complete EnMAP archive will also be generated and made available along 2026.

The list of changes introduced in this and previous processor updates is available at:

https://www.enmap.org/data/doc/EnMAP_processor_changelog.pdf

Since August 2024, EnMAP L2A ARD products have been available for download through the EOC Geoservice (https://geoservice.dlr.de/) and the EO-Lab platform (https://eo-lab.org/). These possibilities allow the direct download of EnMAP L2A products generated by the EnMAP Ground Segment with a standard set of parameters. Since these L2A products are already processed, users can directly download these products without waiting times, allowing a fast way to get large amounts of EnMAP products from the mission archive. Notice that both EOC Geoservice and EO-Lab are not part of the standard services offered by the EnMAP mission but are accessible with the GS/IPS EnMAP account. More information on the number of products downloaded through Geoservice can be found in section 6.2.1.

The following changes are expected to be performed in the next quarters:

- A campaign support webpage will be available to register campaigns and get support from the Foreground Mission program for these campaigns. Users are encouraged to make use of this tool and register their campaigns in this tool.
- Implementation of new linearity calibration (and updated calibration) to improve the VNIR-SWIR matching between spectrometers, specially at low radiances.

5 Users and Announcements-of-Opportunities

5.1 Users

	Country/Continent (No of Countries) *(of reporting period)*	Reporting Period 01.01.2026 to 31.03.2026		Country/Continent (No of Countries) *(since beginning of routine phase)*	Since beginning of routine phase until 31.03.2026 (end of reporting period)
Total European Users	**Europe (22)**	**140**		**Europe (35)**	**2161**
European Countries	• *Germany*	*54*		• Germany	797
	• *France*	*16*		• *France*	*206*
	• *Italy*	*11*		• *Italy*	*195*
	• *Spain*	*11*		• *United Kingdom of Great Britain*	*136*
	• *United Kingdom of Great Britain*	*10*		• *Spain*	*134*
	• *Finland*	*5*		• *Netherlands*	*103*
	• *Hungary*	*5*		• *Poland*	*90*
	• *Netherlands*	*5*		• *Finland*	*51*
	• *Greece*	*3*		• *Greece*	*45*
	• *Poland*	*3*		• *Belgium*	*41*
	• *Romania*	*3*		• *Switzerland*	*40*
	• *Austria*	*2*		• *Austria*	*36*
	• *Belgium*	*2*		• *Czechia*	*34*
	• *Norway*	*2*		• *Norway*	*34*
	• *Bulgaria*	*1*		• *Hungary*	*33*
	• *Croatia*	*1*		• *Sweden*	*33*
	• *Others (6)*	*6*		• *Others (18)*	*152*
Non European	North America (4)	49		North America (11)	647
	South America (9)	35		South America (11)	316
	Asia (22)	187		Asia (37)	1684
	Africa (15)	45		Africa (34)	272
	Oceania (2)	11		Oceania (3)	209
	Total (74)	467		**Total(131)**	**5289**

Table 5-1 Number of registered users per continent with **at least one active user role** (number of user countries during reporting period)

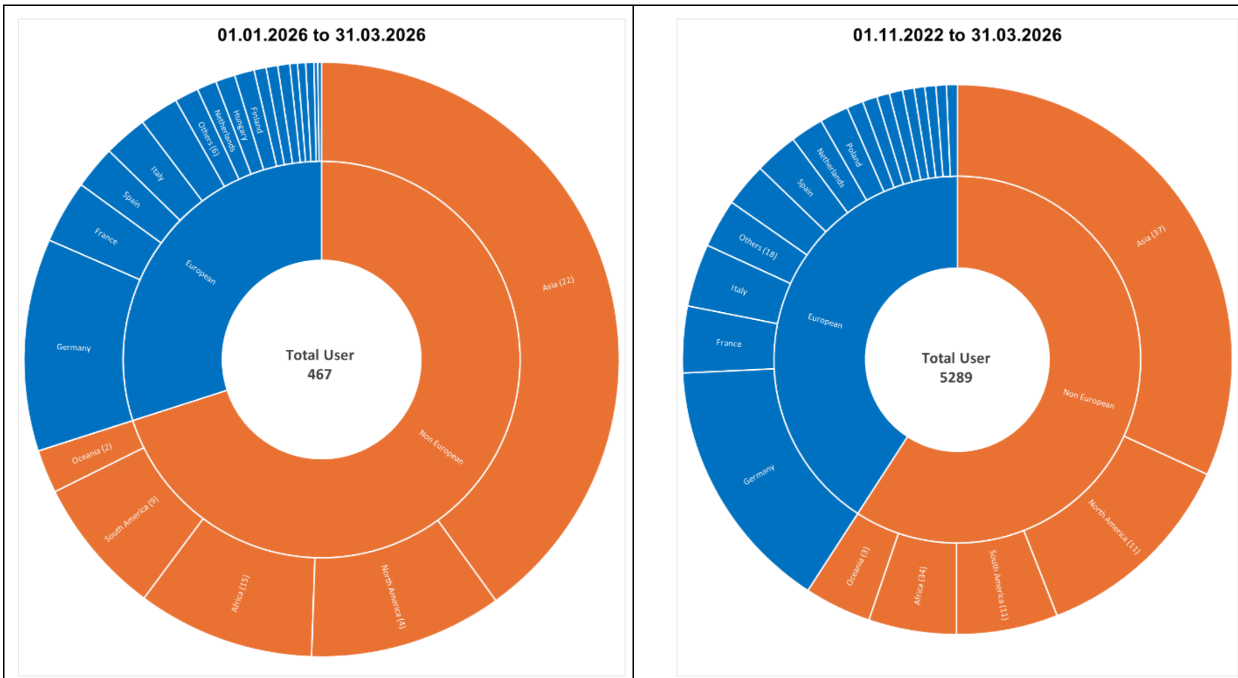

Reporting Period 01.01.2026 to 31.03.2026 with a total of 467 Users of 74 different countries.	Since beginning of operational phase until 31.03.2026 (end of reporting period) with total of 5289 Users of 131 different countries.

Figure 5-1 Number of registered users (with at least one active user role) per country

User per Category		New within reporting period 01.01.2026 to 31.03.2026	Since beginning of routine phase start until 31.03.2026 (end of reporting period)
Registered users	Total*	665	7699
	with active role assignment**	495	5289
Cat-1 Science	Total	396	5160
	AO Process 00001**	387	4293
	AO Process 00002**	0	641
	AO Process 00003**	0	225
Cat-2 Commercial	Total	19	73
Cat-1 Distributor***	Total	315	3949

Table 5-2 Number of registered users and number of released user roles per category (Cat-1 Science, Cat-2 Commercial and Cat-1 Distributor)

* Registered users inhibited user accounts excluded

**Registered users with at least one active user role

***Catalogue User, ordering EnMAP data from archive

Notice that registered users belong to different categories, therefore the sum of Cat-1 Science and Cat-1 Distributors or other categories does not correspond to the total registered users.

5.2 Announcements-of-Opportunities

Announcement -of-Opportunity	New within reporting period 01.01.2026 to 31.03.2026		Since beginning of routine Phase until 31.03.2026 (end of reporting period)	
	Proposals	Total tiles granted	Proposals	Total tiles granted
A00001	79	5345	996	46705
A00002	0	0	126	10395
A00003	0	0	4	127
Total	79	5345	1126	57227

Table 5-3 Number of released science proposals per Announcement-of-Opportunity (AOs#) and total number of granted tiles per AO#.

Icon	Topic	New within reporting period 01.01.2026 to 31.03.2026		Since beginning of routine Phase until 31.03.2026 (end of reporting period)	
		Proposal	Total tiles granted	Proposal	Total tiles granted
	ATMOSPHERE	5	977	62	4545
	CAL/VAL	0	0	41	5675
	GEO/SOIL	23	397	369	10966
	HAZARD/RISK	1	24	26	1116
	METHODS	4	1344	28	2312
	SNOW/ICE	0	0	25	1589
	URBAN	1	18	18	709
	VEGETATION	38	2186	431	24592
	WATER	7	399	126	5723
	Total	**79**	**5345**	**1126**	**57227**

Table 5-4 Number of accepted science proposals and total number of granted tiles per topic

6 Archived and Delivered Observations

The following table shows the number of archived Earth Observation and Calibration products and their sizes within the specified time frames.

Acquisition Type	Archived	Reporting Period 01.01.2026 to 31.03.2026		Since beginning of Commissioning Phase until 31.03.2026 (end of reporting period)	
		Number Tiles / Observations	Size (in GB)	Number Tiles / Observations	Size (in GB)
Earth Observation (EO)	Total	15845 / 1345	7720.76	249846 / 22871	121741.95
	Average / Day	176.06 / 14.95	85.79	171.01 / 15.65	83.33
Calibration (CAL)	Total	20	83.51	508	2121.27
	Average / Day	0.22	0.98	0.35	1.45

Table 6-1 Number and size of archived and not archived products (more than one version of the same image can be archived)

The following table shows the number of delivered products and their sizes within the specified time frames. Product deliveries result either directly from acquisition orders (“Acquisition”) or catalog orders (“Archive”).

Acquisition Type	Order Type		Reporting Period 01.01.2026 to 31.03.2026		Since beginning of Commissioning Phase until 31.03.2026 (end of reporting period)	
			Number Tiles / Observations	Size (in GB)	Number Tiles / Observations	Size (in GB)
Earth Observation (EO)	Acquisition	Total	16434 / 1328	7447.42	217021 / 19816	96434.82
		Average / Day	182.6 / 14.75	82.74	148.54 / 13.56	66.01
	Catalogue	Total	22004	7763.86	184652	68320.87
		Average / Day	244.48	86.26	126.38	46.76
Calibration (CAL)	Acquisition	Total	20	84.51	339	1436.65
		Average / Day	0.22	0.93	0.23	0.98
	Catalogue	Total	0	0.0	77	394.94
		Average / Day	0.0	0.0	0.052	0.27

Table 6-2 Number and size of delivered products

6.1 Archived Acquisitions

The following figures show the heatmaps for the whole world and for Europe within the specified time frames. The heatmaps represent the frequencies of products at a geographic location, where the number of products increases from blue over red to yellow.

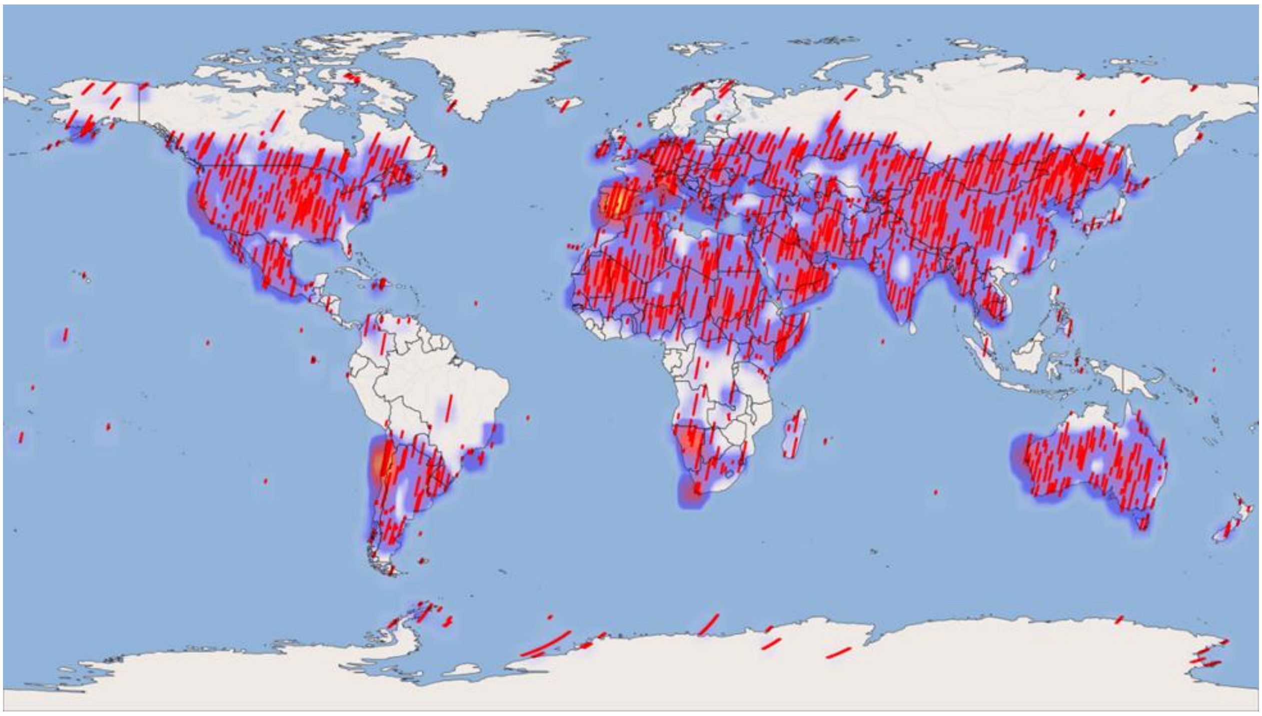

reporting period 01.01.2026 to 31.03.2026

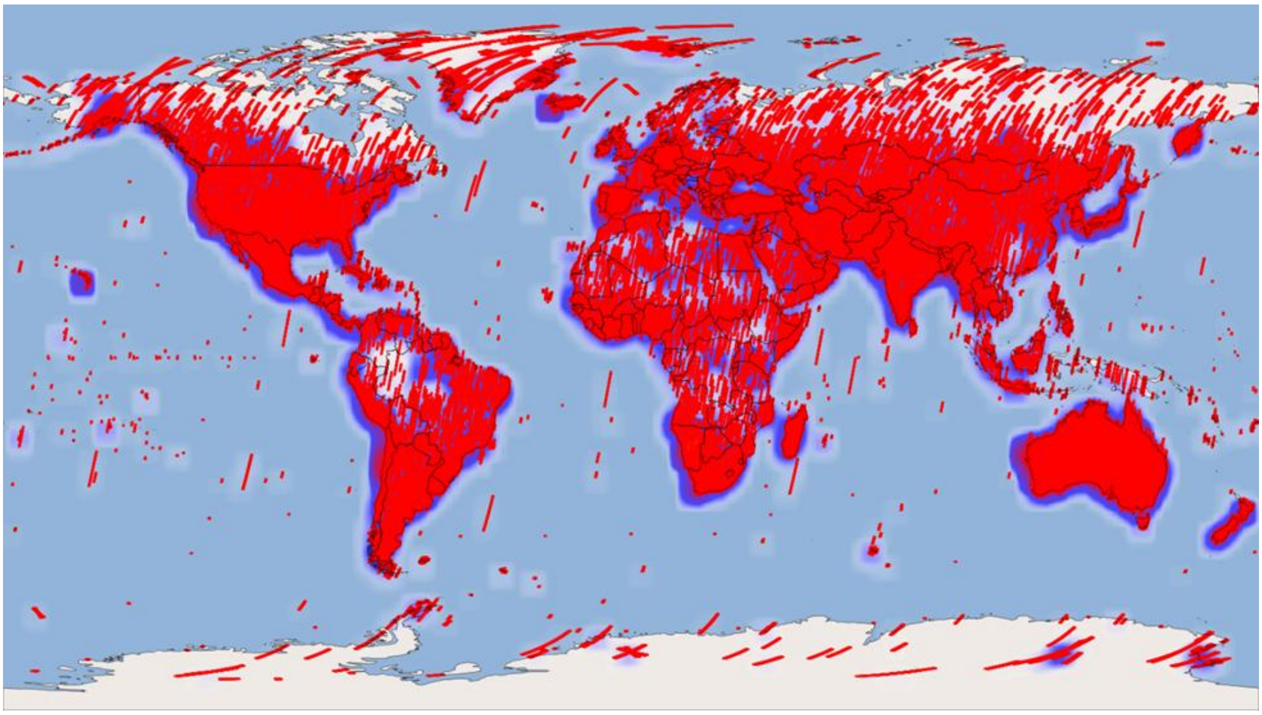

reporting period 2022-04-01 to 31.03.2026 includes commissioning phase acquisitions and different versions of the same tiles)

Figure 6-1 Geographic location of all Earth observation tiles archived, World

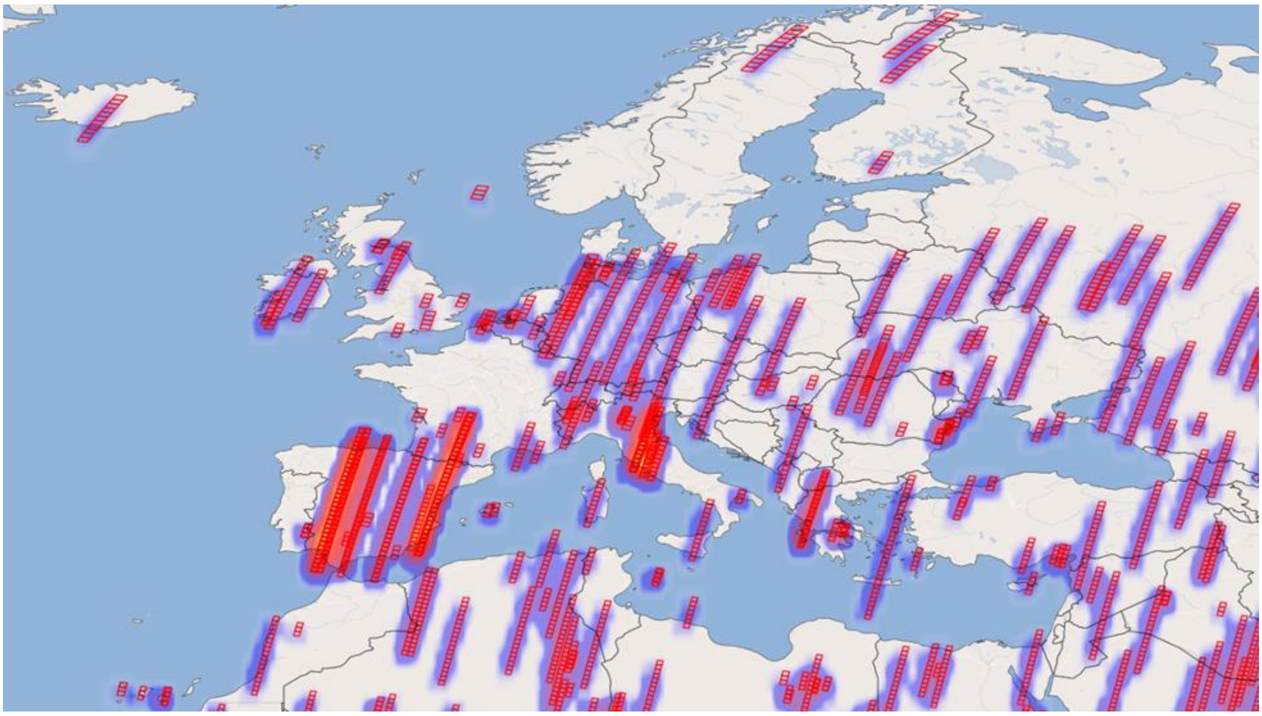

reporting period 01.01.2026 to 31.03.2026 Europe

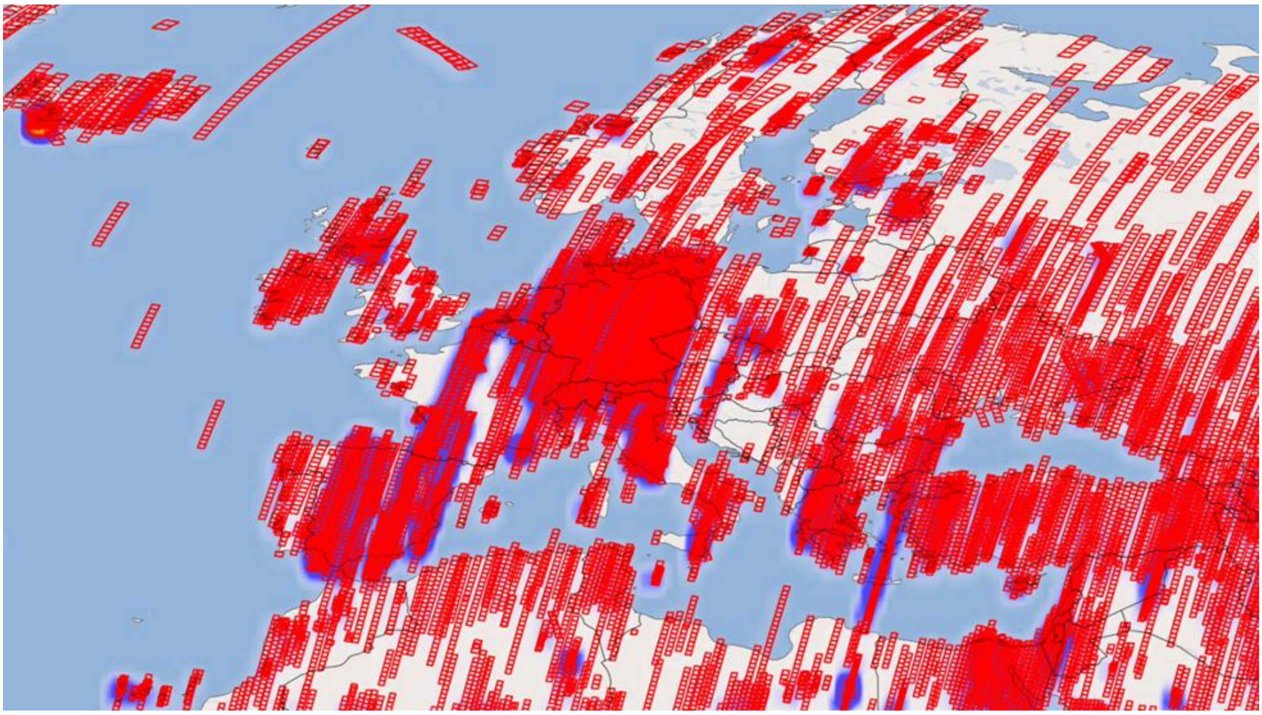

reporting period 2022-04-01 to 31.03.2026 Europe (includes commissioning phase acquisitions)

Figure 6-2 Geographic location of all Earth observation tiles archived, Europe

The following figures show the distribution of cloud coverage for the archived products.

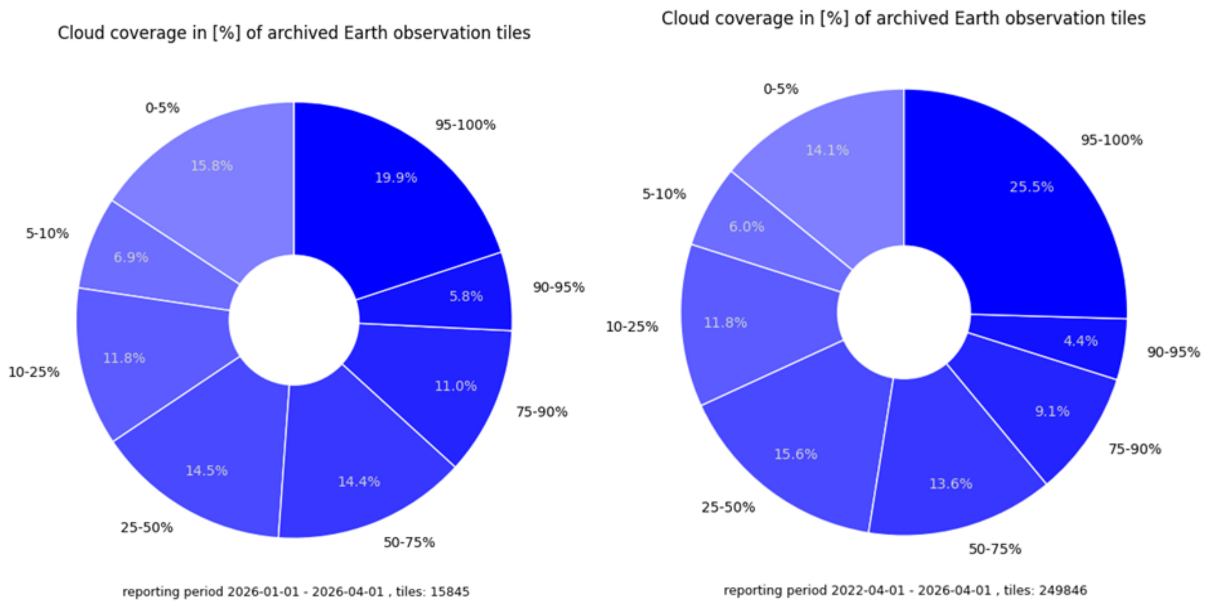

Figure 6-3 Cloud coverage in [%] of archived Earth observation tiles

The following figures show the distribution of observation angles for the archived products.

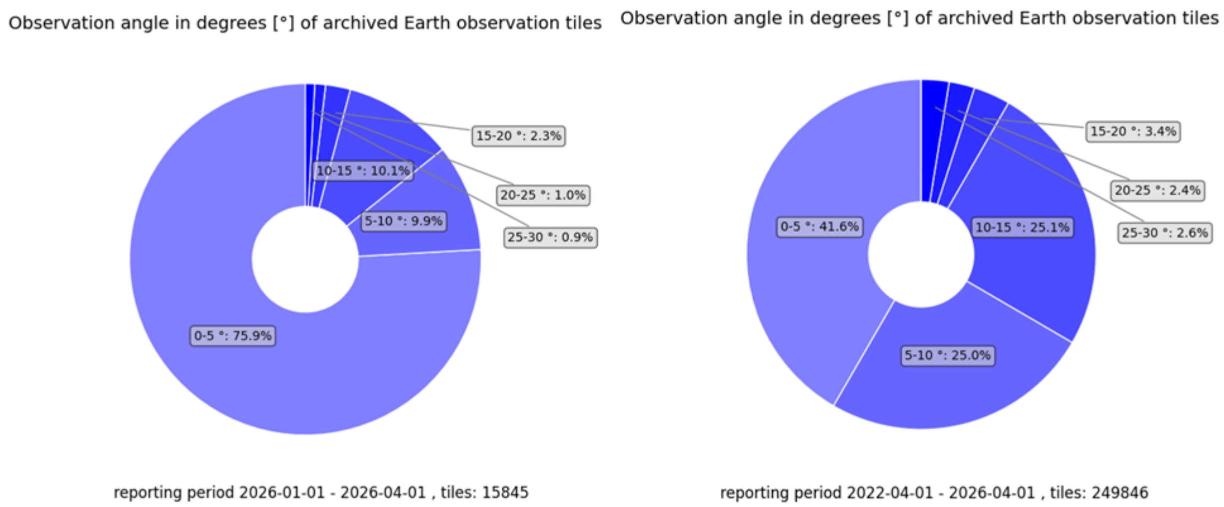

Figure 6-4 Observation angle of archived Earth observation tiles

6.2 Delivered Observations

The following figures show the distribution of processing level of the delivered products from acquisition orders.

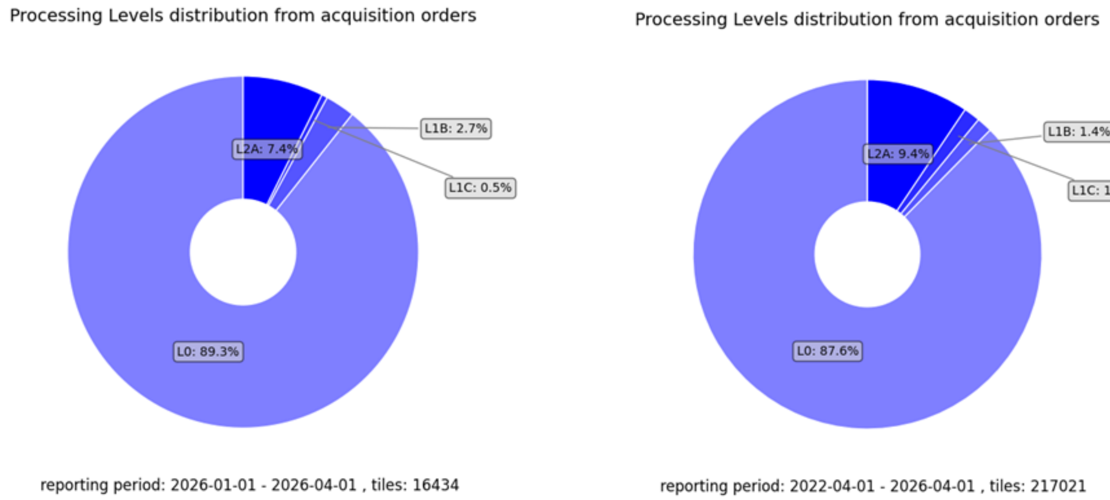

Figure 6-5 Levels of delivered Earth observation tiles from acquisition orders

The following figures show the distribution of processing level and correction type (for L2A) of the delivered products from catalog orders.

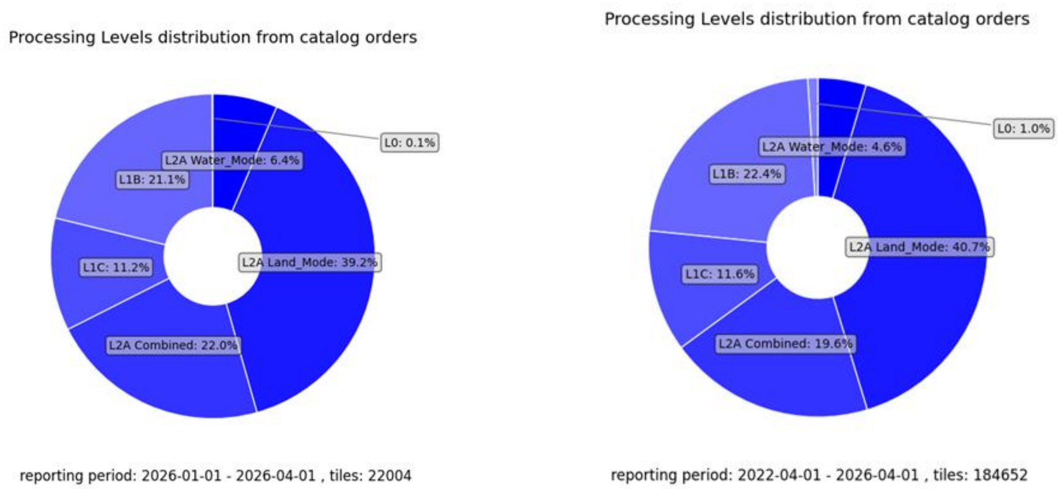

Figure 6-6 Levels of delivered Earth observation tiles from catalog orders

6.2.1 Delivered L2A products from the Download service (EOC Geoservice)

The Ground Segment also produces products already processed with standard parameters. CEOS certified L2A ARD products are available for direct download using the EOC Geoservice and the EOLab platforms. Since July 2025, the IPP account credentials also grant access to the EOC Geoservice to download EnMAP products.

EnMAP's Ground Segment processes all recorded data to L2A ARD format, saving computational and processing time. The default processing parameters of the L2A ARD are the following:

Product_Format = **GeoTIFF+Metadata**
Map Projection = **UTM_Zone_of_Scene_Center**
Image Resampling = **Bilinear_Interpolation**
Correction Type = **Land_Mode**
Cirrus Haze Removal = **No**
Band Interpolation = **No**
Terrain Correction = **Automatic**
Season = **Automatic**
Ozone column = **Automatic**

Table 6-3 Processing parameters used for the L2A ARD products in Geoservice / EOLab

In addition, take into account that:

- the versions of the L2A ARD products may differ depending on their generation time. The processor changelog (https://www.enmap.org/data/doc/EnMAP_processor_changelog.pdf) provides an overview of the software changes. During re-processing of the L2A ARD products, new versions of the products will replace older versions of the products. Currently a re-processing is in progress that shall bring all L2A products to at least version **V01.05.02**.

- No L2A-water products are available as L2A ARD products in Geoservice. For the moment water processing is only available using the on-demand processing options in EOWeb.

- The L2A ARD archive is now complete. All EnMAP products available in the Mission archive are also available as L2A ARD products at Geoservice / EOLab.

The total number of downloads* using the EOC Geoservice is **2370099** for this reporting period (01.01.2026 to 31.03.2026). Number of monthly downloads for this quarter are given in Table 6-4 and the graph with their evolution since the start of the service is shown in Figure 6-76-7.

Product	Month	# Downloads
ENMAP-L2A	2026-01	4324494
ENMAP-L2A	2026-02	2722780
ENMAP-L2A	2026-03	774874
Total in period		7822148

Table 6-4 Absolut amount of downloads in Geoservice.

*Downloads count the download of a file from the EOC Geoservice. A EnMAP L2A product consists of 13 different files

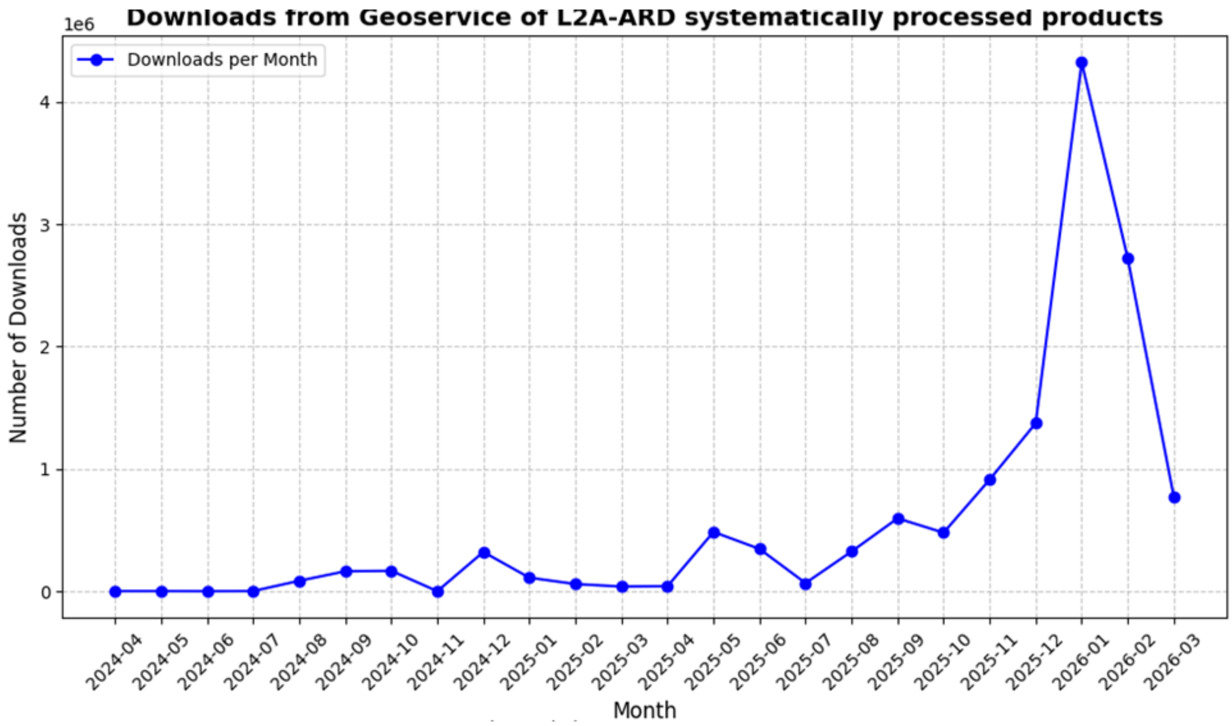

Figure 6-7 Downloads in Geoservice per month

In the current period, there is a remarkable increase in the download numbers as CloudFerro (EOlab) currently downloads all data for CodeDE3.

7 Detailed Status

7.1 Satellite

During the reporting period the mission has experienced no HSI SAFE_ERROR events that have resulted in the loss of observation time. No DSHA Safety Mode event took place during the reporting period. As reported in all the previous events of these types, no consequences on the image or data quality are observed as a result of these events. For more details on data quality see sections 7.6 and 8.

The sporadic cancellation of acquisitions when the satellite is coming from the eclipse phase (known as "3-minute events"), has been observed during the reporting period, as it was expected given the seasonal variability of this phenomenon. A total of 14 image acquisitions were cancelled due to this issue. Due to its seasonal variability, towards the end of Q1 2026 these issues disappeared with the last of the observed events on 08.03.2026.

An update of the Sun calibration procedure was performed on 12.02.2026. With this change, the exposure of the sun diffuser during solar calibrations is minimized. This change has no influence on the calibration results.

More details about different satellite aspects are reported in the following subsections.

7.1.1 Orbit and Attitude Maneuvers

The reference orbit is a Sun-synchronous polar orbit with a mean local time of descending node of 11:00 hrs and a repeat cycle of 398 revolutions in 27 days at an altitude of 643 km.

The satellite orbit is controlled with respect to an Earth-fixed reference track over the entire orbit, analogous to a rim, with a control box of +/- 6 km in radial direction and +/- 22 km in normal direction.

During Q1 2026, a total of 1433 ACS Precise Modes were executed onBoard, compared to 1696 during the previous quarter. Due to the implementation of Back-to-Back Image Acquisitions, the number of ACS Precise Modes does not represent the number of performed activities. By executing two or three Images as one sequence, the total number of ACS Precise Modes decreases whereas the number of Image Acquisitions remains stable or increases. Over the whole mission, a total of 24487 ACS Precise Modes have been successfully executed.

During Q1 2026, one in-plane and four out-of-plane maneuvers were executed. No collision avoidance maneuvers were required. The resulting performance error off all maneuvers was estimated by FDS to range between -0.41% and +0.85%. No actuations of the Ball Latch Valve or other OCS configuration changes were performed during Q1 2026**.**

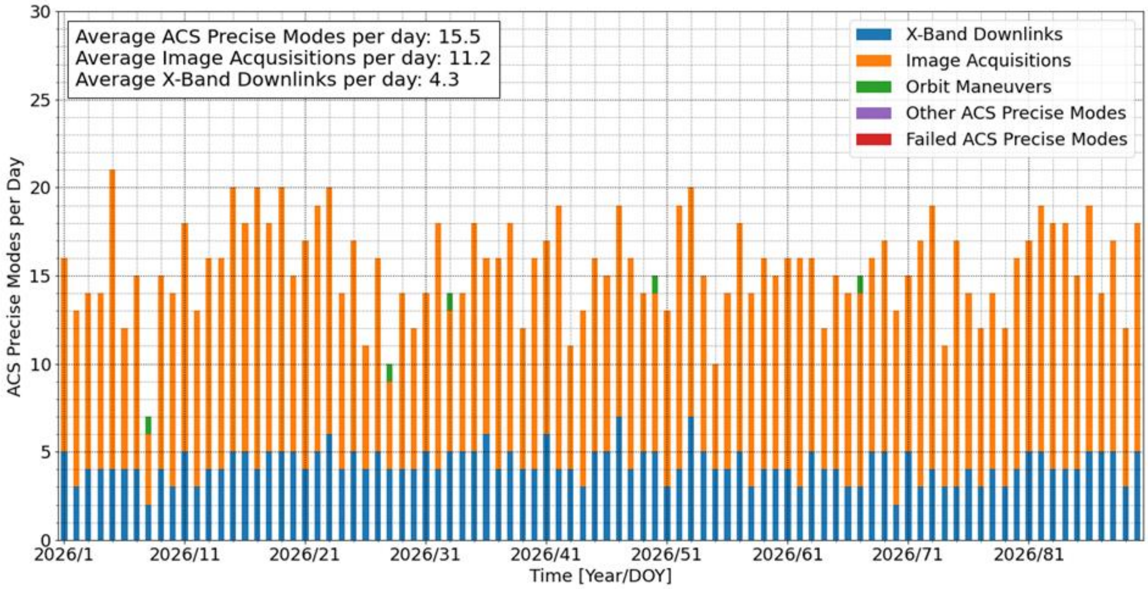

Figure 7-1 Number of ACS Precise Modes per day during Q1 2026

7.1.2 Life Limited Items

The life cycle of the life limited items is evaluated depending on their use. The life-limited items include the following optical and mechanical components:

Life-Limited Item	01.01.2026 to 31.03.2026	until 31.03.2026	Estimated minimum total lifetime / health of the system
Fuel(*)	+0.7 kg	10.0 kg	17.1 years
Battery and Solar Cells(**)	nominal	nominal	Nominal
Thruster thermal cycles	+5	92	333 qualifies cycels
Shutter Usage	+1.55%	26.66%	15.0 years (@ daily use)
FAD movements	+1.00%	33%	15.2 years (@ bimonthly use)
Diffuser exposure time based on sole measurement time(***)	+1.67%	55.00%	8.5 years (@ bimonthly use to reach 100% originally planned used)
Diffuser exposure time based on real cyclogram duration(***)	+1.67%	65.63%	7.4 years (@ bimonthly use to reach 100% originally planned used)
On-Board Calibration Equipment Usage	On-board calibration equipment:		
- OBCA SPC lamp 1	+1.41%	19.47%	19.4 years (@ biweekly use)
- OBCA RAD lamp 1/LED 1	+1.57%	38.61%	13.0 years (@ biweekly use)
- FPA LEDs 1	+0.56%	8.99%	44.5 years (@ monthly use)

Table 7-1 Status of life-limited items

(*) During periods with higher temperature and pressure fluctuations due to e.g., an Instrument shutdown and startup, the calculation of the propellant mass via the Pressure-Volume-Temperature method contains a relatively large margin of errors.

(**) The Power Subsystem is working nominally and as expected. Voltage stays above any critical level.

(***) A 100% Sun diffuser exposure time corresponds to a total planned exposure of 2 hours after 5 years when performing monthly Solar calibrations. The contribution of the diffuser to the total radiometric uncertainty after reaching the reference 100% value is estimated to be **0.6%** according to the instrument manufacturer. This value is significantly below the 5% total radiometric uncertainty requirement, which indicates that the diffuser will not be a relevant contributor to the total radiometric uncertainty of the instrument even if the diffuser were to be used significantly above the originally allocated 2 hours of exposure time (reference 100% value). Nevertheless, the use of the diffuser is continuously monitored and accounted for in the Life-Limited Item list and thanks to the instrument stability the Sun calibration frequency is adjusted to reduce the number of necessary Solar calibrations.

The consumed resources (except fuel) are calculated based on the processed L0 product metadata, i.e. only successfully processed calibrations can be considered.

7.1.3 Redundancies

To date, the SWIR wavelength range is covered by SWIR-A (SWIR-B can be activated using a one-time switch mechanism).

All satellite subsystems are using nominal configurations.

7.2 Ground Stations

7.2.1 S-Band

S-Band Ground Stations	01.01.2026 to 31.03.2026		
	Total Passes	Non-Routine Passes (e.g. Anomaly Handling/SW Updates)	Failed Passes
All stations (Weilheim-Germany, Neustrelitz-Germany, Inuvik-Canada, O'Higgins-Antarctica, Svalbard-Norway)	560 (153 WHM, 245 NSG, 156 INU)	6	1

Table 7-2 S-Band Ground Station Passes

7.2.2 X-Band

X-Band Ground Stations	01.01.2026 to 31.03.2026	
	Executed Passes	Successful Passes
All stations (Neustrelitz-Germany, Inuvik-Canada)	385 (276 NZ, 109 INU)	384 (276 NZ, 108 INU)

Table 7-3 X-Band Ground Station Passes

Inuvik (Canada) station was integrated in Q4 2023 into the regular operations of the EnMAP Ground Segment for X-Band and S-Band downlinks. After integration, more data and more flexibility in S-band and X-band data reception is achieved, especially concerning image acquisitions over Europe.

7.3 User Interfaces

Further improvements to the user interfaces are continuously on-going and will be reported in this section.

During the reporting period the Ground Segment of EnMAP continues to update the information on future high priority observations of the EnMAP mission (*Foreground Mission*). The tool displaying this information is available at the EnMAP web site (under https://www.enmap.org/data_tools/foreground_mission/).

With this tool the users can get informed weeks in advance about future priority observations with EnMAP. Initially, a set of long flight-lines (990km) over Germany and other European countries have been identified together with the user community and will be regularly scheduled. Since July 2024, the Foreground mission has expanded to include additional European regions. The foreground mission continued in Q1 2026 to focus on Europ. It started in the so-called *winter mode* (since November 2025), when it shifts to southern Europe and the southern hemisphere during winter time. At the end of Q1 2026 returned to the normal mode, using the new configuration of monthly and bi-monthly regular flightlines that was the result of the Foreground Mission Survey that took place at the start of 2026.

At the end of Q1 2026, the registering conditions for new users were updated. Since end of March 2026, new users have to provide an email address affiliated to an institution (e.g. University, research center) or related to commercial sector (cat-2 users).

7.4 Processors

Reference [3] provides the product specification and [4], [5], [6], [7] the algorithm theoretical basis for Level 1B, Level 1C and Level 2A (land / water).

In the reporting period (01.01.2026 to 31.03.2026) there has been one update in the EnMAP processing chain. A new version of the EnMAP processing software, **V01.05.06**, was available to the users since **06.02.2026**.

The following changes are part of the **V01.05.06** release:

- Fixed creation of black L2A products under certain (rare) conditions.
- Switched the entries for scene azimuth and zenith angles for the lower corners in the metadata files for Lx products (they are now all in clock-wise order)

The changelog document was updated during Q1 2026 to include the list of changes. The document contains the history of EnMAP processor updates and shows the updates performed in the processing software. The document can be downloaded from the EnMAP website:

https://www.enmap.org/data/doc/EnMAP_processor_changelog.pdf

The following changes are expected to be performed in the future quarters:

- Update of the linearity calibration and other adjustments to improve the matching between VNIR and SWIR spectrometers.

7.5 Calibrations

Table 7-4 summarizes the radiometric calibration observations acquired in this quarter and which will be described in the rest of this section. The calibration acquisitions were generally acquired according to the routine operations plan.

Category	01.01.2026 to 31.03.2026	
	Number of Archived Observations	Size (in GB)
Total	22	91.1
Deep Space	4	5.2
Rel. Radiometric	7	27.3
Abs. Radiometric	1	1.3
Linearity	3	51
Spectral Calibration	7	6.3

Table 7-4 Number and size of archived radiometric and spectral calibration observations

The continuous degradation of the VNIR sensor was monitored and quantified. The rate of degradation is constantly decreasing as illustrated in Figure 7-27-2 and by the end of March 2023 it has reached the point where it is practically negligible and has been kept that way during the reporting period. It shall be noted, though, that this average trend is different at different parts of the detector as illustrated for individual pixels in Figure 7-37-3. The effect on the radiometric calibration coefficients of a few selected bands is shown in Figure 7-47-4.

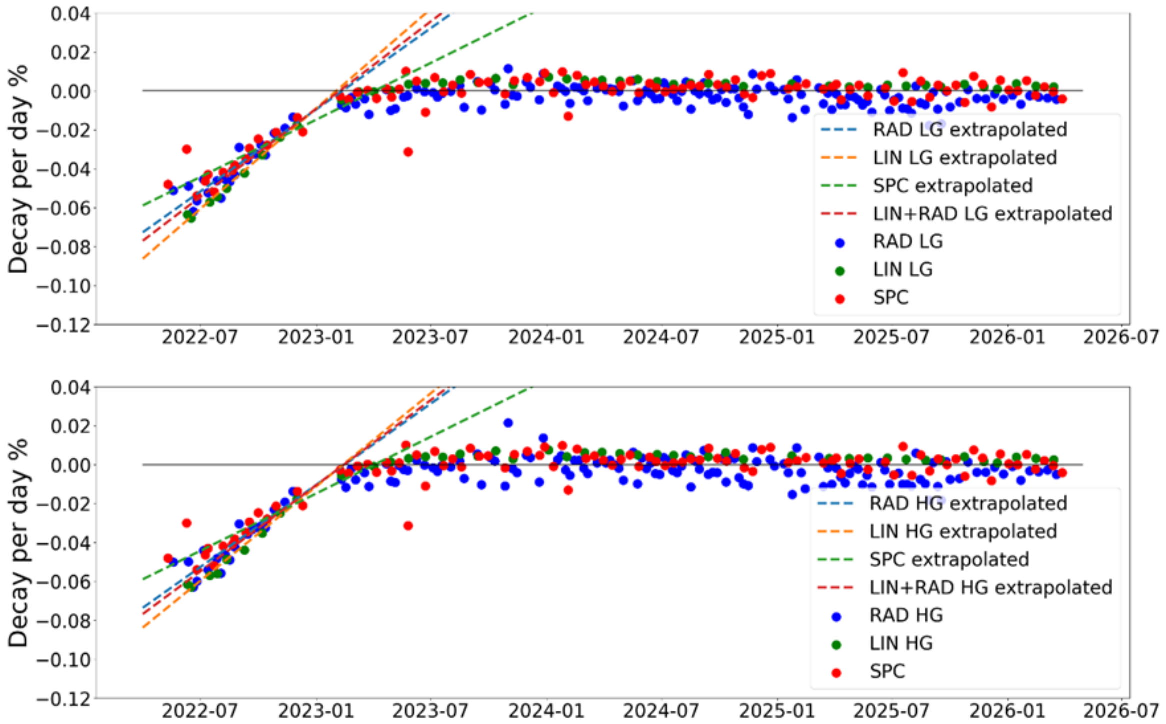

Figure 7-2 Decay per day from Lamp (RAD), Linearity (LIN) and Spectral (SPC) measurements for low gain (top) and high gain (bottom)

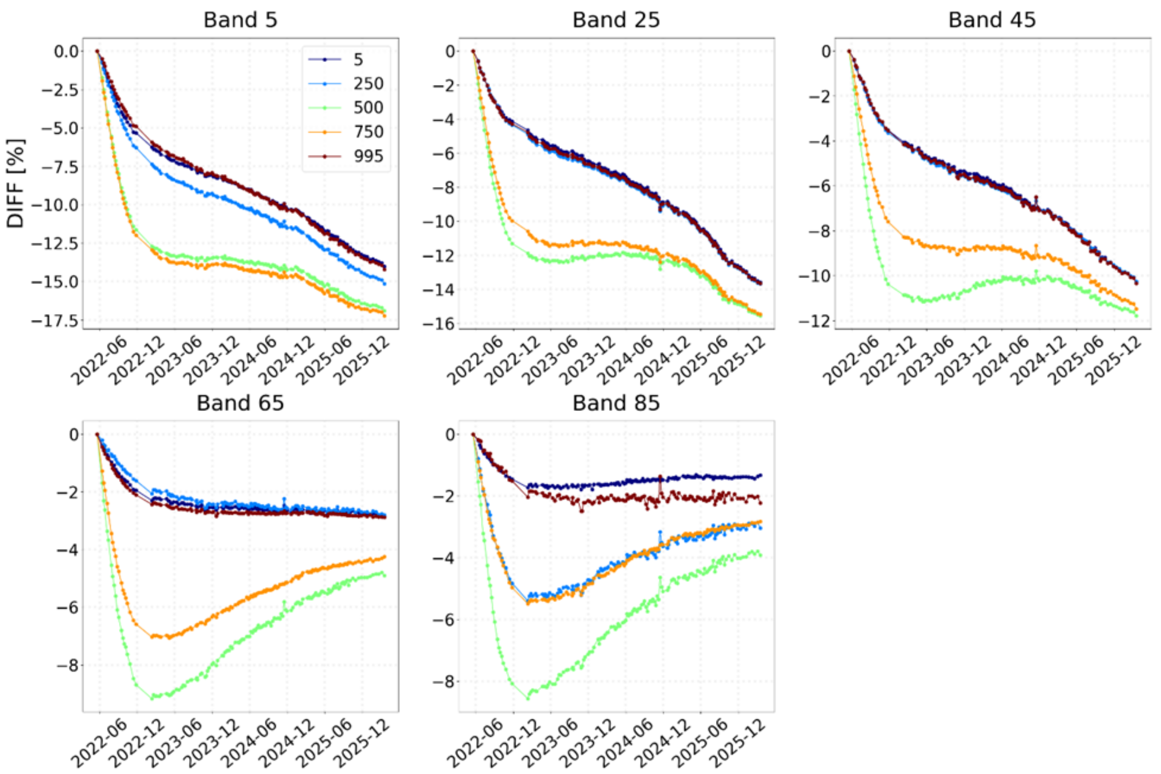

Figure 7-3 Change in percentage for individual pixels based on OBCA-Lamp measurements given for 5 bands and 5 cross track elements (coloured lines).

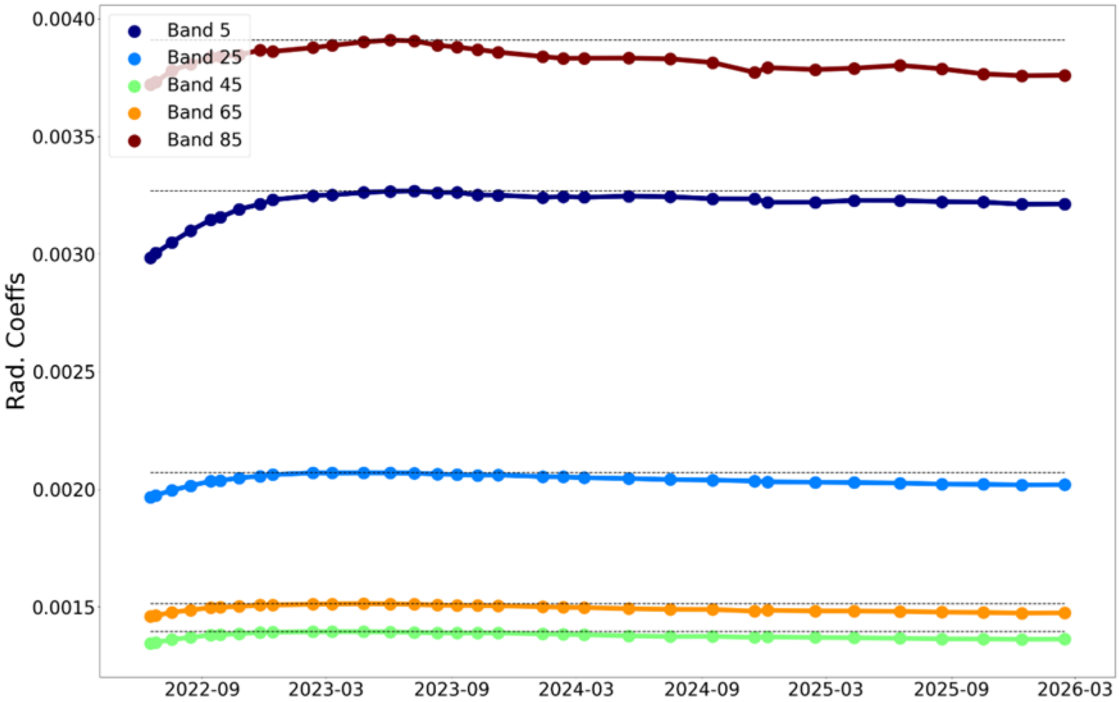

Figure 7-4 Average percentage change in the VNIR radiometric coefficients for five selected bands since launch

7.5.1 Dead Pixels

The following table shows the number and percentage of dead pixels. Figure 7-57-5 and Figure 7-67-6 show the position of the dead pixels in the focal plane of VNIR and SWIR sensors respectively. There have been no updates since 31.08.2022.

Defect Pixels	01.01.2026 to 31.03.2026	
	Number of Pixels	Percent
Total	1921	0.8
VNIR	137	0.2
SWIR	1784	1.2

Table 7-5 Number and percent of dead pixels

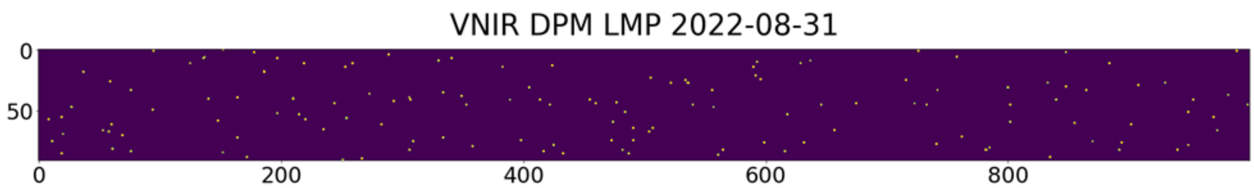

Figure 7-5 VNIR Dead Pixel Mask

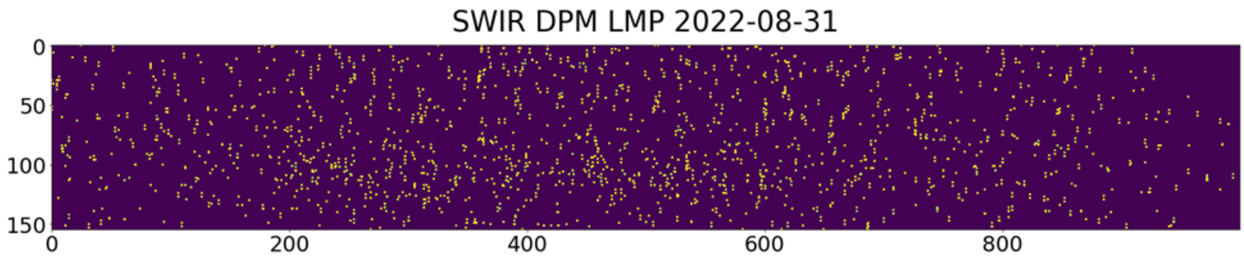

Figure 7-6 SWIR Dead Pixel Mask

There are no clusters of more than three spectrally or spatially adjacent dead pixels.

7.5.2 Spectral Calibration

Remark: In the following figures, OBCA is abbreviation for On-Board Calibration Assembly for spectral and radiometric calibrations.

Category	01.01.2026 to 31.03.2026	
	Number of Archived Observations	Size (in GB)
Total	7	6.3
Spectral Calibration	7	6.3

Table 7-6 Number and size of archived spectral calibration observations

The spectral properties – in particular center wavelength (CW) (see Figure 7-77-7 and Figure 7-87-8) and full width at half maximum (FWHM) (see Figure 7-107-9) for each band (spectral coordinate) and pixel (spatial coordinate) – have been characterized, considering all bands and pixels provided in Level 1B, Level 1C and Level 2A products.

The major conclusions of the monitoring of the spectral performance are summarized as follows:

- During the reporting period, 7 spectral calibration measurements were made which took place on: 02.01.2026, 16.01.2026, 30.01.2026, 14.02.2026, 27.02.2026, 13.03.2026 and 27.03.2026.
- The VNIR spectral range in this reporting period was found to be 418.4 – 993.3 nm over 91 bands (Figure 7-77-7). The average spectral sampling distance was 6.4 nm with a total range of 4.7 – 8.2 nm. This meets the requirement for overall wavelength coverage [HSI-POSS-0210], average spectral sampling distance [HSI-POSS-0310] and spectral sampling distance range [HSI-POSS-0320].
- The SWIR spectral range in this reporting period was found to be 902.1 – 2445.4 nm over 155 bands (Figure 7-77-7). The average spectral sampling distance was 10.0 nm with a total range of 7.5 – 12.0 nm. This meets the requirement for overall wavelength coverage [HSI-POSS-0210], average spectral sampling distance [HSI-POSS-0310] and spectral sampling distance range [HSI-POSS-0320].
- The spectral calibration measurements from this quarter show good temporal stability – measurements showed an absolute <0.15 nm change from the VNIR sensor and <0.31 nm change in SWIR (Figure 7-87-8) with respect to current spectral calibration table. All changes were below 0.5 nm between measurements for VNIR and below 0.5 nm SWIR. Long-term VNIR and SWIR spectral shifts are reported in Figure 7-9. This meets the requirement for consecutive spectral stability [HSI-POSS-0510] and overall spectral stability [HSI-POSS-0520].
- FWHM for VNIR and SWIR (Figure 7-107-9) are shown below but are not recalculated inflight.
- A VNIR degradation pattern is not clearly visible between consecutive spectral reference measurements acquired in this period, but there are positive and negative changes across the detector and on average the signal appears to have increased by 0.01% across all pixels from 19.12.2025 to 27.03.2026. A comparable change was reported in the previous quarter (0.08%). Although now very small, the monitoring of this behavior will continue in the next reporting period.

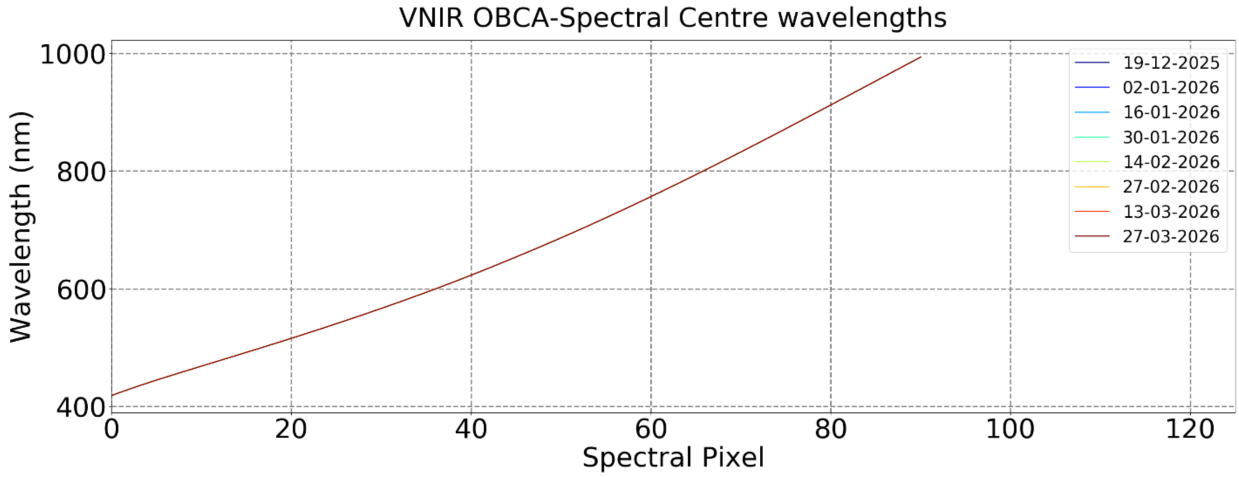

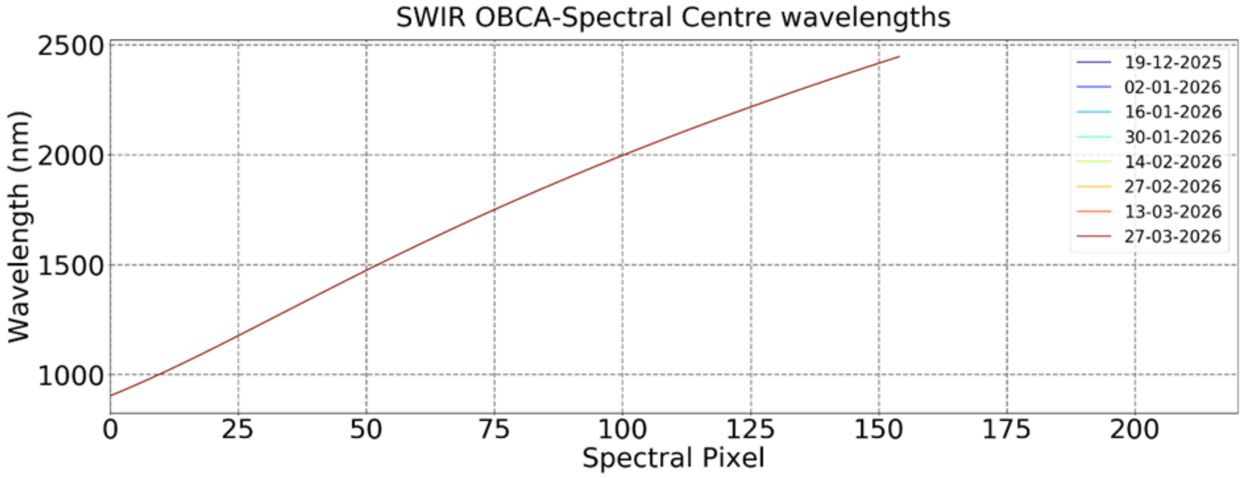

Figure 7-7 VNIR (top) and SWIR (bottom) center wavelength in nm

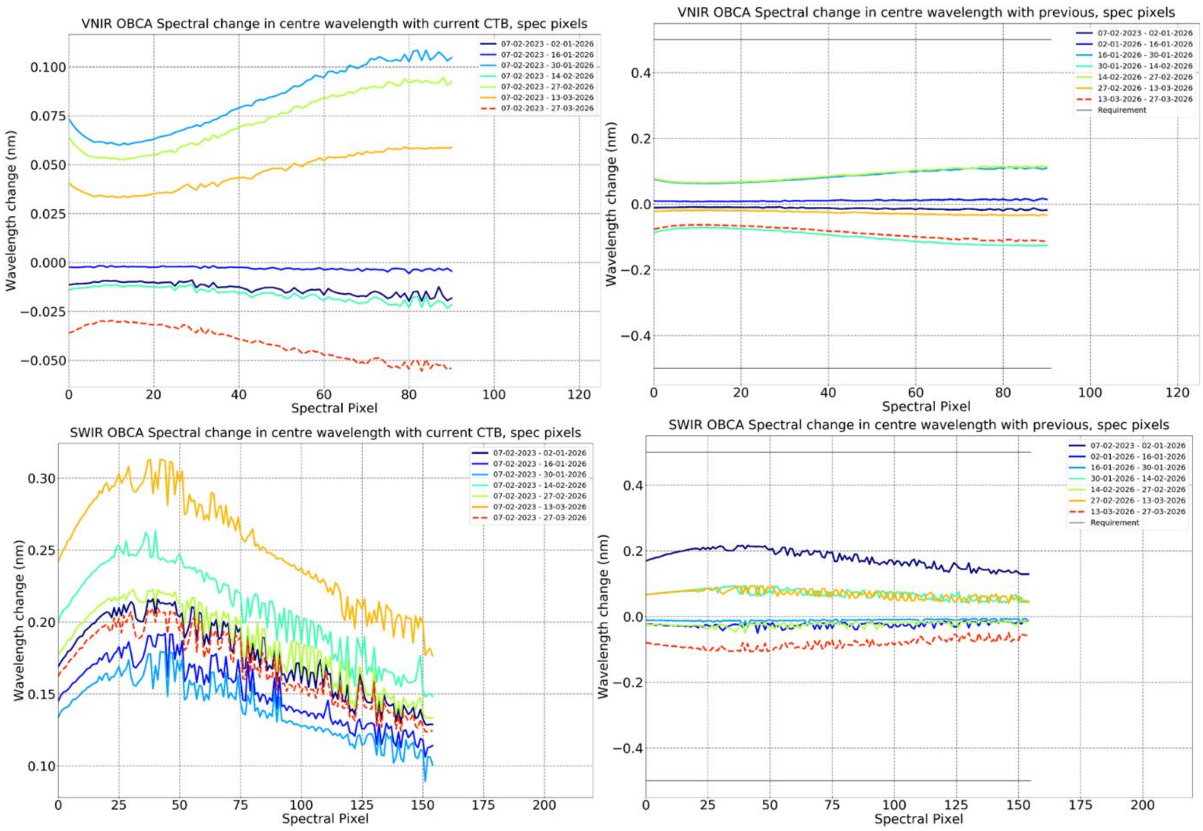

Figure 7-8 Change in center wavelength per spectral pixel for VNIR (top) and SWIR (bottom). Left panels show the changes with respect to current spectral calibration table in use and right panels with respect to the previous measurements.

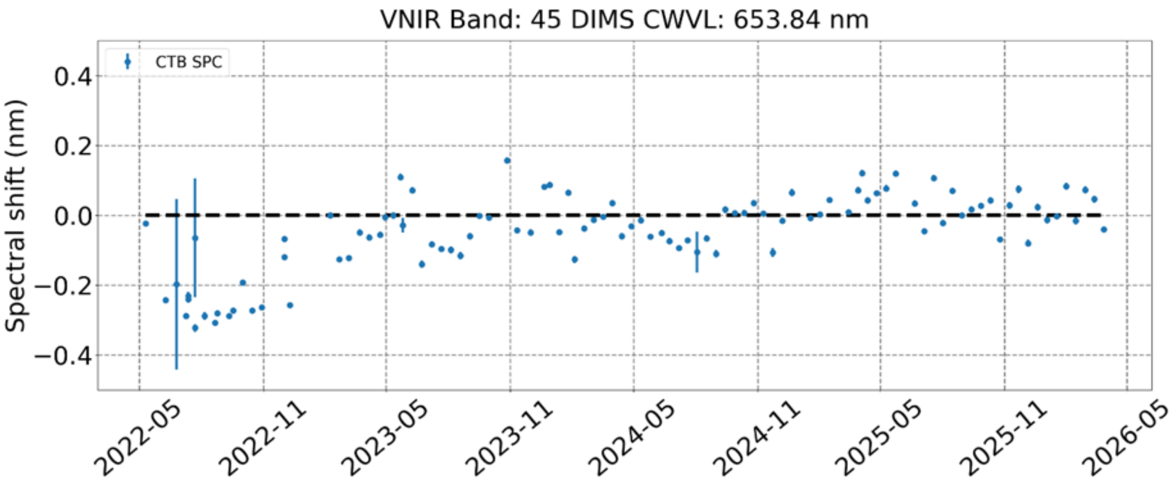

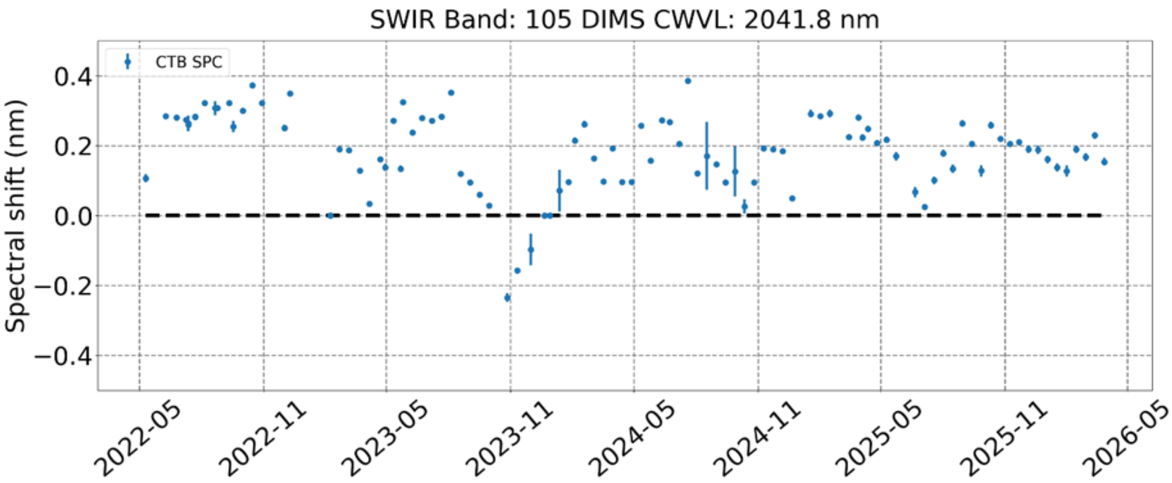

Figure 7-9 Long-term VNIR (top) and SWIR (bottom) spectral shifts since the beginning of the mission for VNIR band 45 at 654 nm and SWIR band 105 at 2042 nm.

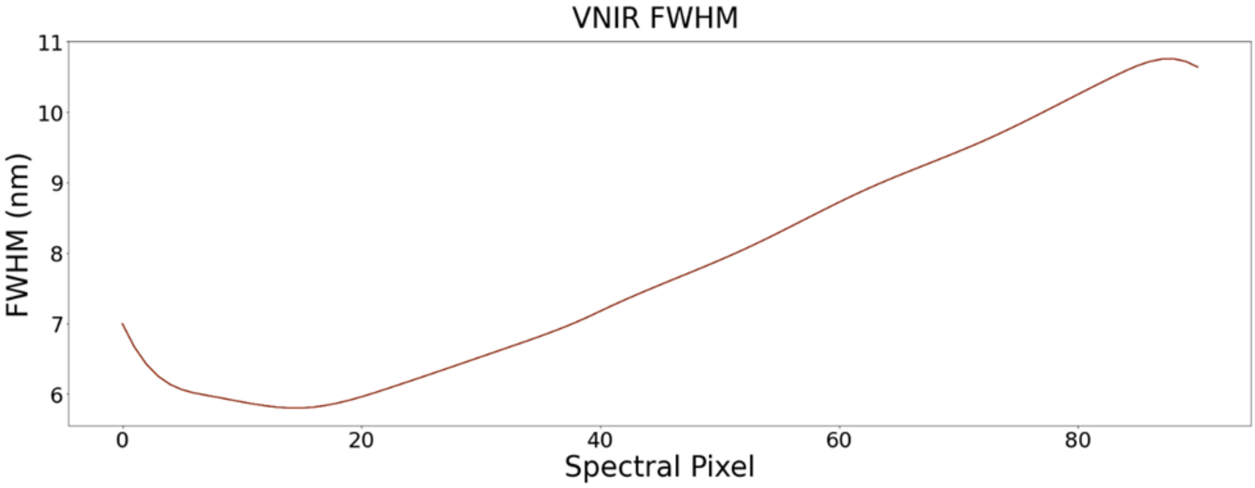

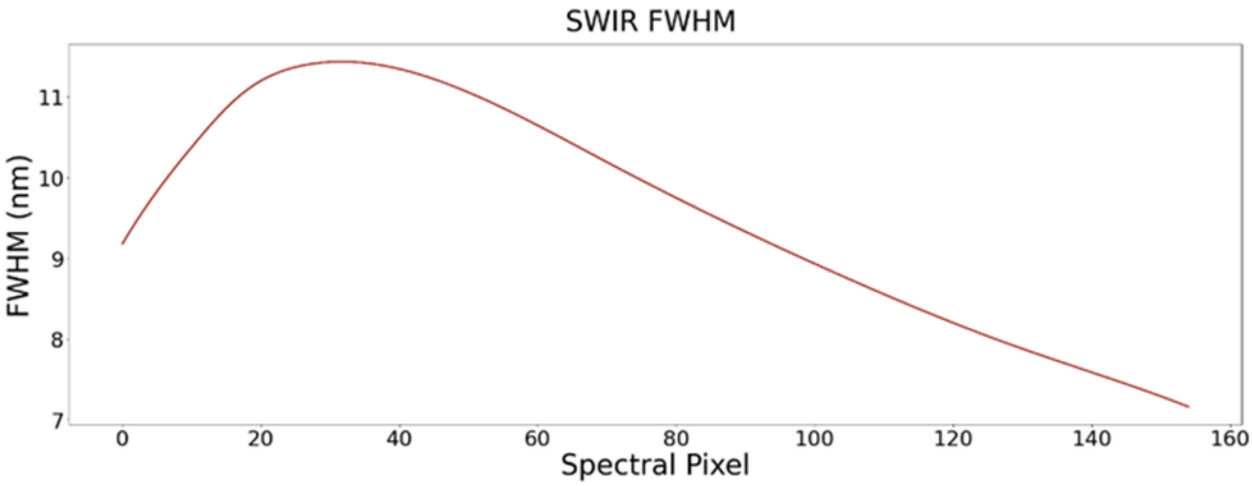

Figure 7-10 VNIR (top) and SWIR (bottom) FWHM in nm

CW and FWHM are available in the spectral calibration tables (see Table 7-7) and System Response Functions (SRF) per band are modelled by a Gaussian shape using those parameters.

Spectral calibration updates

No new calibration products were generated and delivered during the reporting period.

Product	Type	Date of Generation	Date of Validity Start	Date of Validity End	Delivered to
none					

Table 7-7 Generated spectral calibration tables

7.5.3 Radiometric Calibration

Category	01.01.2026 to 31.03.2026	
	Number of Archived Observations	Size (in GB)
Total	15	84.8
Deep Space	4	5.2
Rel. Radiometric	7	27.3
Abs. Radiometric	1	1.3
Linearity	3	51

Table 7-8 Number and size of archived radiometric calibration observations

The radiometric properties – characterized in particular by the calibration coefficient for each band (spectral coordinate) and pixel (spatial coordinate) and radiance – during this reporting period are investigated, considering all bands and pixels and radiances provided in Level 1B, Level 1C and Level 2A products.

Radiometric calibration coefficients (see Figure 7-117-10, Figure 7-127-11 and Table 7-10) and VNIR RNU (response non-uniformity, see Figure 7-147-13) were affected by the degradation of the VNIR sensor during commissioning but have stabilized from Q1 2023. In-flight, the gain matching coefficients (see Figure 7-137-12), the SWIR calibration coefficients, and the SWIR RNU (response non-uniformity, see Figure 7-147-13) have been stable.

During the reporting period, one Absolute Radiometric Calibration measurement was obtained. It took place on: 14.02.2026.

Albeit now relatively small in magnitude, changes in the VNIR sensor have led to the creation of new calibration and reference tables for the new absolute radiometric measurement.

Although the VNIR degradation has almost stopped, the overall effects are visible in the reference measurements of the sun. However geometric conditions (sun-earth distance, pointing angle) also play a role in the absolute magnitude so the degradation cannot be quantified with these reference measurements.

The major conclusions of the monitoring of the absolute performance are summarized as follows:

- Changes in the VNIR sensor have affected the absolute Radiometric calibration coefficients: the increasing signal in the VNIR sensor, although not homogeneous, has resulted in decreasing radiometric coefficients. In this reporting period, the calibration coefficients increased by only 0.03% to offset the increase in absolute (Figure 7-117-10 and Figure 7-127-11). Regarding RNU, the degradation features are still visible in the focal plane (Figure 7-147-13). Lastly, the Gain Matching correction has been relatively stable during this reporting period (Figure 7-137-12).

- The SWIR sensor has shown good stability during this reporting period, with no significant changes in the gain matching, RNU or radiometric calibration coefficients (Figure 7-117-10 and Figure 7-127-11).

- Regarding the total change in calibration corrections as a result of the VNIR degradation, almost all pixels experienced a change of less than 2.5% between consecutive measurements as set in requirement [HSI-POSR-0410]. The only pixels which exceeded this value were already marked as dead during inflight assessment. No SWIR pixels experienced a change of more than 2.5% between consecutive absolute calibration measurements.

- New VNIR and SWIR calibration and reference tables were created for the absolute radiometric measurements from 14.02.2026, despite the small changes seen in the calibration coefficients. The VNIR radiometric calibration coefficients have decreased in this reporting period to offset the increasing VNIR signal. If the VNIR (and SWIR) calibration continues to behave in a stable manner, it will not be necessary to create new calibration tables for every Absolute Radiometric calibration measurement.

- Since April 2024, Absolute Radiometric Calibration measurements are planned at intervals of two months, following the stable performance of both sensors, and to allow for the extension of the lifetime of the solar diffuser.

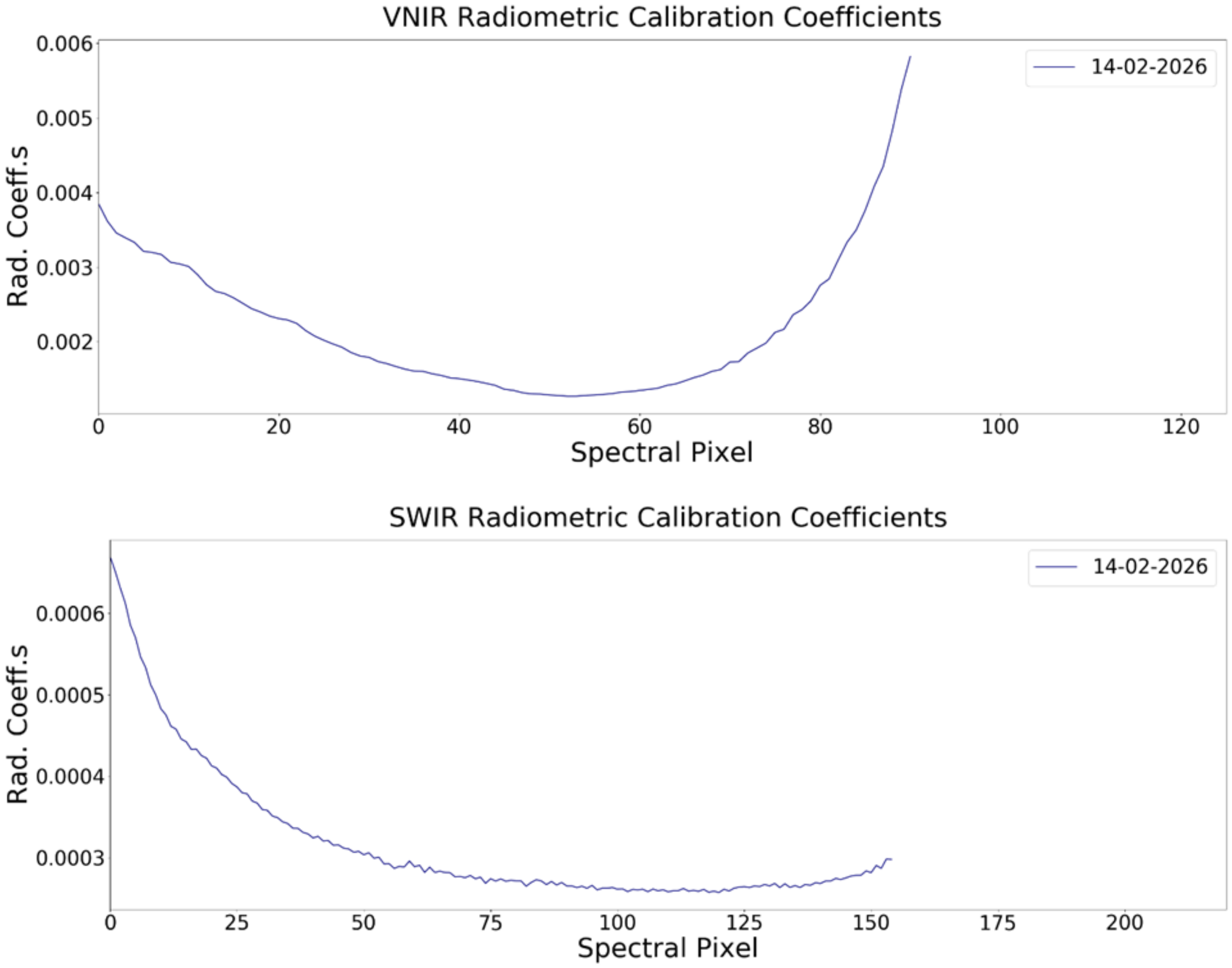

Figure 7-11 VNIR (top) and SWIR (bottom) calibration coefficient in mW/cm²/sr/µm

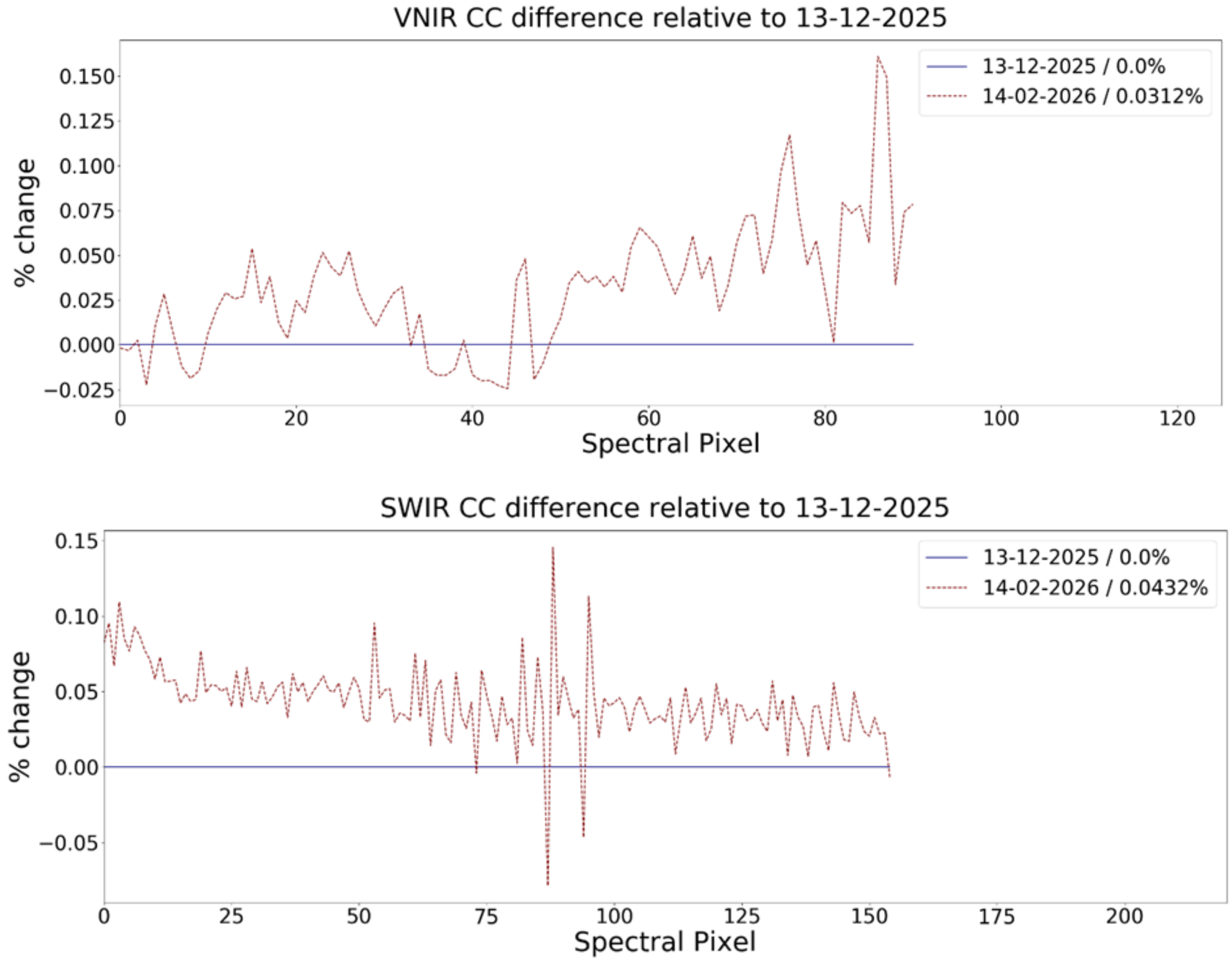

Figure 7-12 Percentage change in VNIR Calibration Coefficients (top) and SWIR Calibration Coefficients (bottom)

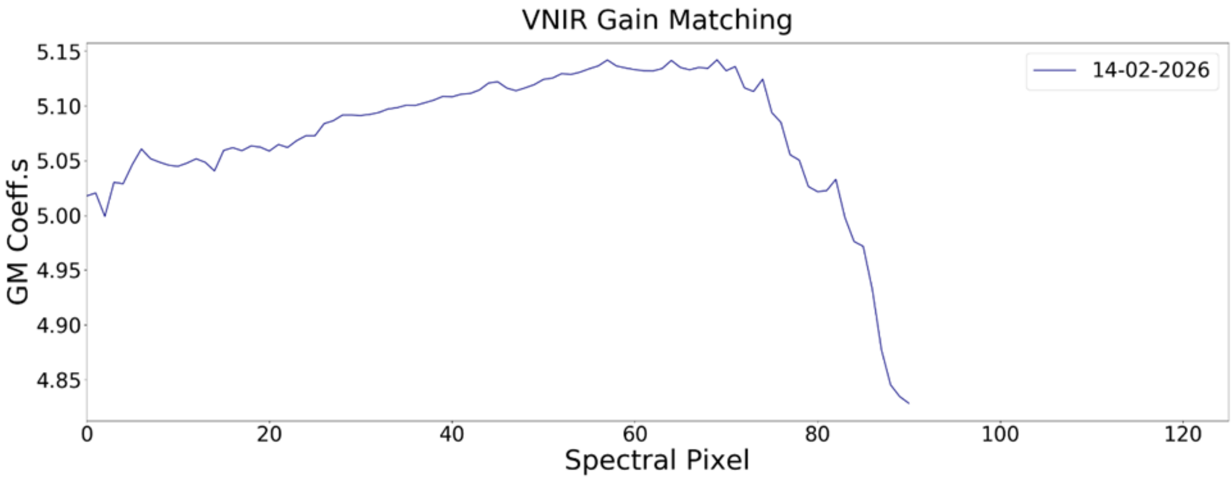

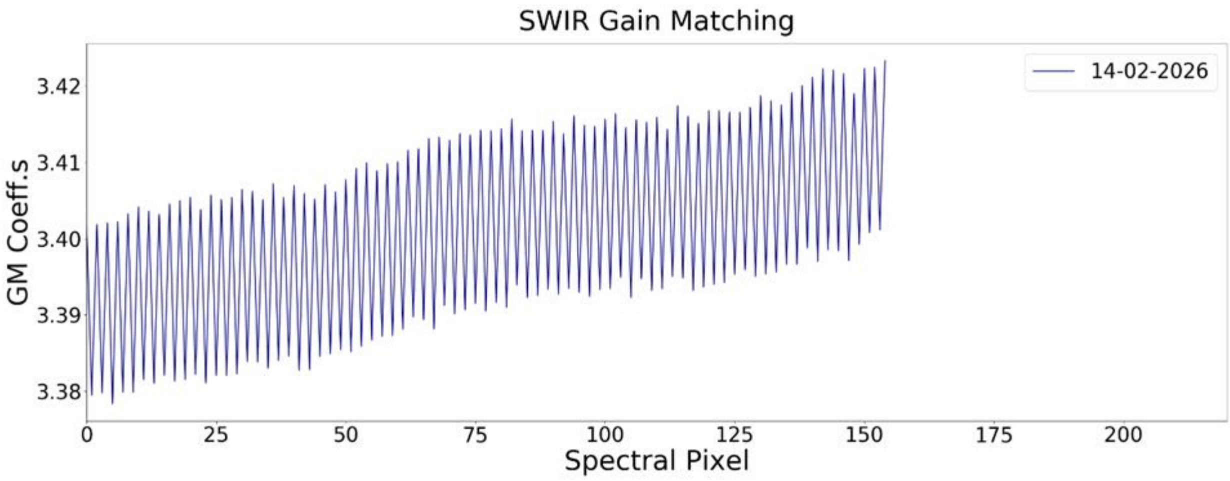

Figure 7-13 VNIR (top) and SWIR (bottom) gain matching calibration coefficients

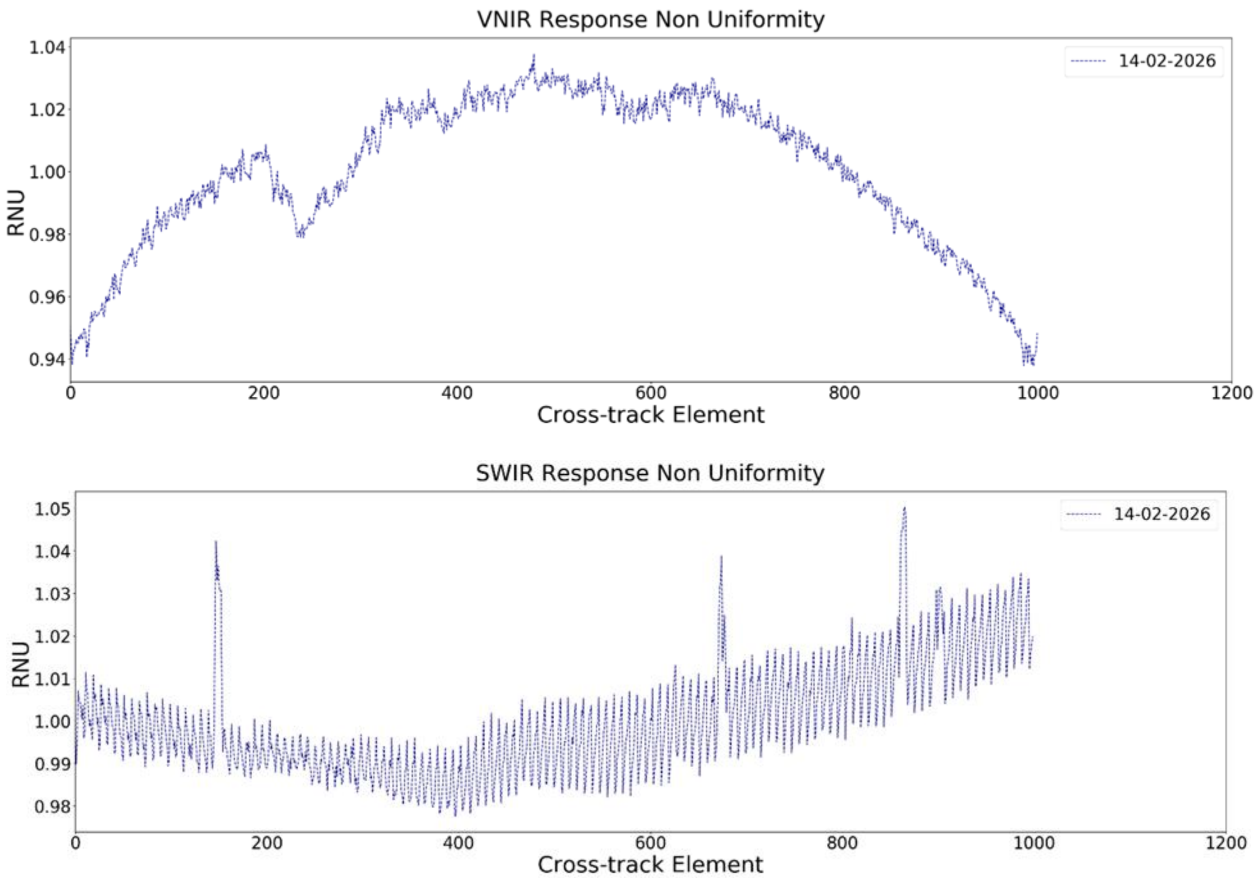

Figure 7-14 VNIR (top) and SWIR (bottom) response non-uniformity coefficients

Signal-to-Noise Ratio

The Signal-to-Noise Ratio (SNR) is derived from the Linearity reference measurements. This is not a perfect set-up for the assessment of the SNR as the linearity measurements only cover a single wavelength and light level at increasing integration times. However, it is well constrained, covering a wide range of radiances including the levels of the reference radiance spectrum that is used to evaluate the requirements (30%

reflectance, 30° sun incidence angle, 21 km visibility, target 500 m above sea level). The lamp reference measurements are not used, as the reference spectrum is not well covered at the radiances of the lamp and extrapolation would be required to test the performance at the SNR requirements. Those requirements are: SNR greater than 500 at 495 nm in VNIR for the reference spectrum value given a 10 nm pixel; and SNR greater than 150 at 2200 nm in SWIR for the reference spectrum given a 10 nm pixel.

For the VNIR sensor, SNR is computed from the linearity calibration measurement. SNR values are shown as a contour map with the reference radiance spectrum as a blue line. Contour lines with SNR values of 150 and 500 are also shown in black. The plot in low gain mode includes the mission requirement which is evaluated at 495 nm for a radiance value of 36 mW/cm^2/μm/sr and is expected to be greater than 500: the calculated value here is **590**. The radiance value used here for the evaluation is the value at 495 nm of the reference radiance spectrum after bandwidth normalization to a 10 nm pixel (see Figure 7-167-15).

For the SWIR sensor, SNR is also computed from the linearity calibration measurement. SNR values for the high gain mode are shown as a contour map with the reference radiance spectrum as a blue line. Contour lines with SNR values of 150 and 500 are also shown in black. The plot in high gain mode includes the mission requirement which is evaluated at 2200 nm for a radiance value of 0.5 mW/cm^2/μm/sr and is expected to be greater than 150: the calculated value here is **248**. The radiance value used here for the evaluation is the value at 2200 nm of the reference radiance spectrum after bandwidth normalization to a 10 nm pixel (see Figure 7-177-16).

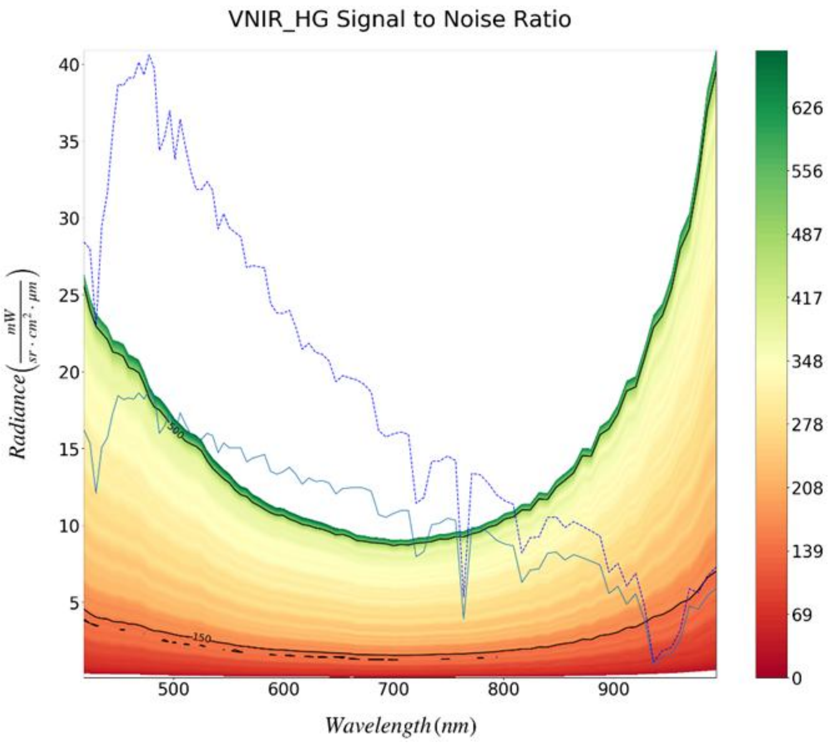

Figure 7-15 SNR contour map for VNIR high gain from the LED linearity observations observed on 14.03.2026. The reference radiance is shown with a blue line and after bandwidth normalization to a 10 nm pixel (dotted). Contour lines with SNR values of 150 and 500 are also shown in black.

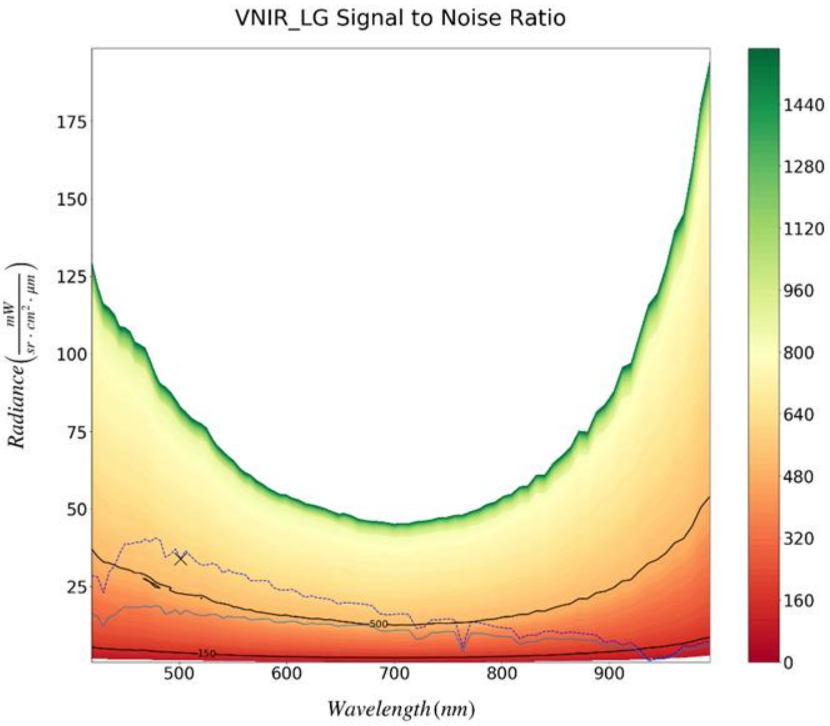

Figure 7-16 SNR contour map for VNIR low gain from the LED linearity observations observed on 14.03.2026. The reference radiance is shown with a blue line and after bandwidth normalization to a 10 nm pixel (dotted). Contour lines with SNR values of 150 and 500 are also shown in black. The mission requirement is evaluated at 495 nm for a radiance value of 36 mW/cm^2/μm/sr (marked with a black cross) and is expected to be greater than 500.

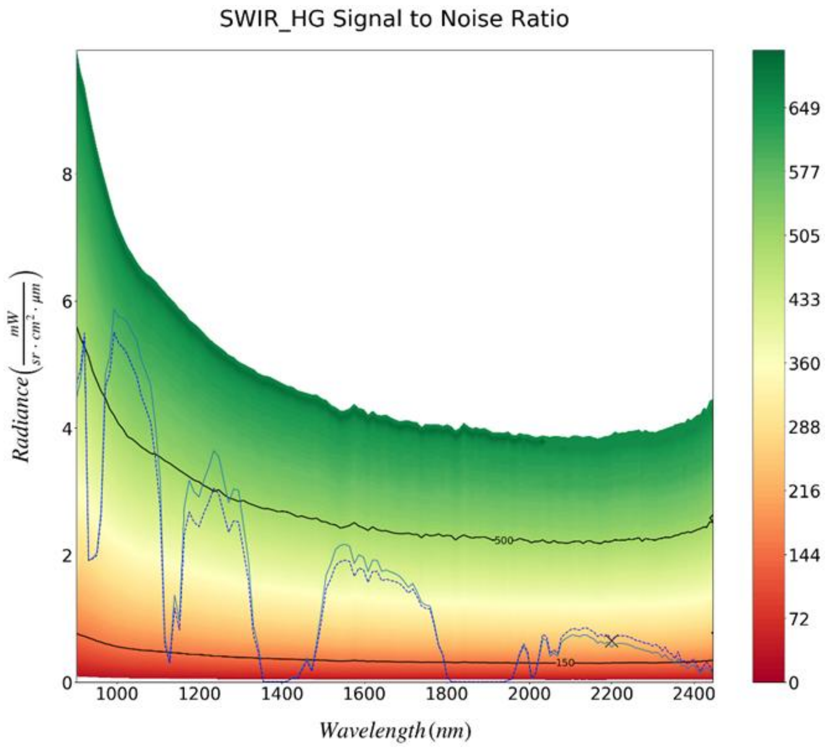

Figure 7-17 SNR contour map for SWIR high gain from the LED linearity observations observed on 14.03.2026. The reference radiance is shown with a blue line and after bandwidth normalization to a 10 nm pixel (dotted). Contour lines with SNR values of 150 and 500 are also shown in black. The mission requirement is evaluated at 2200 nm for a radiance value of 0.5 mW/cm^2/μm/sr (marked with a black cross) and is expected to be greater than 150.

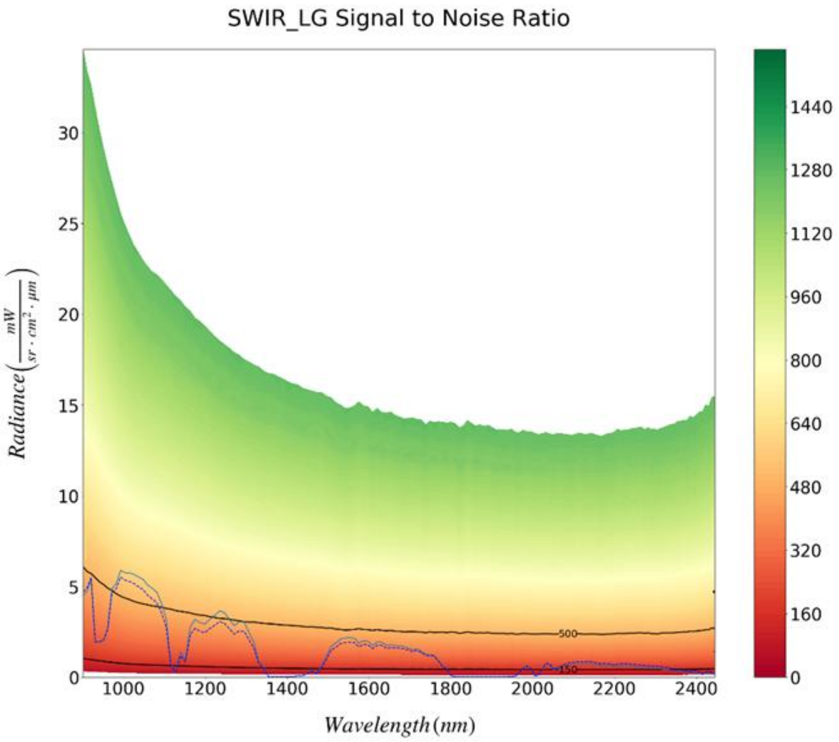

Figure 7-18 SNR contour map for SWIR low gain from the LED linearity observations observed on 14.03.2026. The reference radiance is shown with a blue line and after bandwidth normalization to a 10 nm pixel (dotted). Contour lines with SNR values of 150 and 500 are also shown in black.

The SNR values at the reference radiance spectrum are given in the table below (Table 7-9). The SNR is not determined in absorption regions and when the reference is too low or too high relative to the measured values in the linearity calibration.

Sensor	Wavelength (nm)	Reference Radiance (mW/sr/cm2/µm)	SNR Low gain	SNR High gain
VNIR	418.42	15.62	300.53	310.70
VNIR	424.04	15.32	300.89	312.61
VNIR	429.46	12.09	263.44	281.56
VNIR	434.69	15.07	303.88	315.41
VNIR	439.76	15.69	312.17	340.23
VNIR	444.7	17.29	331.67	342.62
VNIR	449.54	18.44	354.28	368.17
VNIR	454.31	18.18	352.69	367.02
VNIR	459.03	18.29	369.06	374.51
VNIR	463.73	18.2	370.27	374.48
VNIR	468.41	18.62	378.18	375.87
VNIR	473.08	18.2	381.83	383.14
VNIR	477.74	18.8	391.82	
VNIR	482.41	18.42	395.79	
VNIR	487.09	15.98	370.43	375.75
VNIR	491.78	16.46	379.99	403.49
VNIR	496.5	17.36	395.09	
VNIR	501.24	15.97	383.45	466.39
VNIR	506.02	17.31	414.31	

VNIR	510.83	16.57	403.47	
VNIR	515.67	15.92	395.81	
VNIR	520.55	15.48	390.28	
VNIR	525.47	15.6	397.25	
VNIR	530.42	15.98	423.25	
VNIR	535.42	15.84	431.91	
VNIR	540.46	14.72	417.40	
VNIR	545.55	15.36	445.09	
VNIR	550.69	15.03	445.66	
VNIR	555.87	15.02	460.96	
VNIR	561.11	15.03	465.06	
VNIR	566.41	14.13	450.97	
VNIR	571.76	14.36	464.41	
VNIR	577.17	14.47	466.73	
VNIR	582.64	14.61	475.55	
VNIR	588.17	13.5	465.49	
VNIR	593.77	13.32	465.77	
VNIR	599.45	13.48	469.11	
VNIR	605.19	13.77	477.40	
VNIR	611.02	13.33	465.48	
VNIR	616.92	12.67	466.92	
VNIR	622.92	13.07	469.39	
VNIR	628.99	12.85	467.42	
VNIR	635.11	12.9	473.98	
VNIR	641.3	12.76	477.29	
VNIR	647.54	12.04	464.89	
VNIR	653.84	12.4	479.67	
VNIR	660.21	12.43	492.26	
VNIR	666.64	12.48	486.55	
VNIR	673.13	12.41	481.09	
VNIR	679.69	12.21	483.91	
VNIR	686.32	10.69	444.51	
VNIR	693.02	10.52	448.47	
VNIR	699.78	10.76	450.67	
VNIR	706.62	10.96	459.24	
VNIR	713.52	10.96	460.91	
VNIR	720.5	7.95	365.59	377.86
VNIR	727.54	8.29	375.45	367.27
VNIR	734.65	10.03	413.28	
VNIR	741.83	10.13	410.56	
VNIR	749.06	10.45	426.00	
VNIR	756.35	10.32	414.89	
VNIR	763.7	3.91	227.82	277.21
VNIR	771.11	9.86	395.65	

VNIR	778.57	9.87	390.38	
VNIR	786.08	9.53	370.30	417.31
VNIR	793.64	9.01	363.44	382.64
VNIR	801.25	8.78	336.17	359.25
VNIR	808.91	8.66	328.12	344.44
VNIR	816.61	6.28	280.76	311.68
VNIR	824.36	7.09	291.37	312.06
VNIR	832.15	7.15	284.95	312.96
VNIR	839.98	8.18	303.86	327.67
VNIR	847.85	8.25	296.55	309.82
VNIR	855.76	7.74	285.55	303.67
VNIR	863.7	8.09	284.64	309.11
VNIR	871.68	7.88	267.84	296.62
VNIR	879.69	7.66	256.25	283.45
VNIR	887.73	7.41	246.44	270.24
VNIR	895.79	5.56	199.94	244.93
VNIR	903.87	6.03	205.30	244.90
VNIR	911.97	4.85	169.73	220.26
VNIR	920.08	5.54	182.12	227.76
VNIR	928.2	3.8	133.19	162.81
VNIR	936.34	0.89		68.62
VNIR	944.47	1.48		83.59
VNIR	952.61	1.65		88.36
VNIR	960.75	2.58	86.97	103.15
VNIR	968.89	4.74	127.66	133.63
VNIR	977.04	4.53	117.39	144.11
VNIR	985.19	5.41	120.68	145.78
VNIR	993.34	5.87	123.19	144.94
SWIR	901.96	6.12	504.20	
SWIR	911.57	4.75	445.36	
SWIR	921.32	5.38	484.48	
SWIR	931.2	1.91	259.50	
SWIR	941.22	1.95	273.12	
SWIR	951.36	2.03	287.55	
SWIR	961.63	2.7	347.91	
SWIR	972.02	4.85	505.49	
SWIR	982.52	5.13	531.99	
SWIR	993.14	5.87	583.16	
SWIR	1003.88	5.75	585.29	
SWIR	1014.72	5.73	592.40	
SWIR	1025.66	5.66	595.62	
SWIR	1036.7	5.51	590.55	
SWIR	1047.84	5.38	588.69	
SWIR	1059.07	5.07	574.96	

SWIR	1070.39	4.89	569.83	
SWIR	1081.78	4.67	554.79	
SWIR	1093.26	4.06	515.10	
SWIR	1104.81	3.18	451.78	
SWIR	1116.43	0.67	159.97	
SWIR	1128.11	0.35	94.91	
SWIR	1139.84	1.37	276.60	
SWIR	1151.62	0.97	217.98	
SWIR	1163.44	2.76	434.49	
SWIR	1175.3	3.18	477.17	
SWIR	1187.2	2.99	463.10	
SWIR	1199.11	2.91	458.12	
SWIR	1211.05	3.18	488.26	
SWIR	1223	3.39	508.90	
SWIR	1234.97	3.64	536.60	
SWIR	1246.95	3.54	529.01	
SWIR	1258.94	3.18	499.44	
SWIR	1270.93	2.82	468.75	
SWIR	1282.92	3.04	493.86	
SWIR	1294.91	3.02	497.07	
SWIR	1306.89	2.46	444.98	
SWIR	1318.87	1.92	383.52	
SWIR	1330.85	0.89	231.76	
SWIR	1342.82	0.56	166.46	
SWIR	1354.76	0.01		
SWIR	1366.69	0.01		
SWIR	1378.59	0.01		
SWIR	1390.47	0.01		
SWIR	1402.33	0.01		
SWIR	1414.17	0.01		
SWIR	1425.95	0.07		
SWIR	1437.7	0.06		
SWIR	1449.43	0.23	82.92	
SWIR	1461.1	0.38	127.09	
SWIR	1472.74	0.2	75.39	
SWIR	1484.33	0.61	187.61	
SWIR	1495.9	1.11	290.93	
SWIR	1507.41	1.68	377.86	
SWIR	1518.87	1.86	405.54	
SWIR	1530.29	2.09	436.66	
SWIR	1541.67	2.15	450.88	
SWIR	1553.02	2.17	448.74	
SWIR	1564.3	2.14	444.41	
SWIR	1575.55	1.87	404.84	

SWIR	1586.77	2	427.94	
SWIR	1597.91	1.97	422.71	
SWIR	1609.03	1.74	397.63	
SWIR	1620.08	1.92	418.75	
SWIR	1631.1	1.91	422.27	
SWIR	1642.07	1.74	399.47	
SWIR	1653	1.76	401.74	
SWIR	1663.87	1.73	398.78	
SWIR	1674.69	1.71	396.64	
SWIR	1685.46	1.67	394.30	
SWIR	1696.19	1.59	380.15	
SWIR	1706.88	1.49	365.61	
SWIR	1717.5	1.55	379.40	
SWIR	1728.07	1.42	356.33	
SWIR	1738.59	1.25	336.40	
SWIR	1749.08	1.21	324.16	
SWIR	1759.52	1.19	321.88	
SWIR	1769.9	0.91	269.59	
SWIR	1780.21	0.59	197.30	
SWIR	1790.5	0.44	152.89	
SWIR	1800.73	0.07		
SWIR	1810.92	0.01		
SWIR	1821.06	0		
SWIR	1831.16	0		
SWIR	1841.2	0		
SWIR	1851.19	0		
SWIR	1861.16	0		
SWIR	1871.06	0		
SWIR	1880.92	0		
SWIR	1890.73	0		
SWIR	1900.52	0		
SWIR	1910.22	0		
SWIR	1919.91	0		
SWIR	1929.55	0		
SWIR	1939.15	0		
SWIR	1948.69	0.02		
SWIR	1958.19	0.04		30.26
SWIR	1967.66	0.23		120.24
SWIR	1977.07	0.43		186.10
SWIR	1986.45	0.56		222.91
SWIR	1995.79	0.45		193.84
SWIR	2005.08	0.06		41.28
SWIR	2014.33	0.1		57.80
SWIR	2023.54	0.37		174.11

SWIR	2032.7	0.68		252.52
SWIR	2041.83	0.66		247.25
SWIR	2050.92	0.4		184.31
SWIR	2059.96	0.46		197.33
SWIR	2068.96	0.4		183.30
SWIR	2077.93	0.63		242.39
SWIR	2086.85	0.68		253.94
SWIR	2095.74	0.71		263.81
SWIR	2104.59	0.74		270.65
SWIR	2113.41	0.73		263.46
SWIR	2122.17	0.71		262.75
SWIR	2130.91	0.74		269.49
SWIR	2139.6	0.74		267.03
SWIR	2148.27	0.7		260.91
SWIR	2156.89	0.68		253.47
SWIR	2165.46	0.61		239.95
SWIR	2174.03	0.64		245.22
SWIR	2182.54	0.61		236.97
SWIR	2191.02	0.63		245.42
SWIR	2199.45	0.55		222.25
SWIR	2207.86	0.59		232.98
SWIR	2216.24	0.61		235.92
SWIR	2224.58	0.61		234.67
SWIR	2232.89	0.6		235.09
SWIR	2241.16	0.59		229.50
SWIR	2249.41	0.57		224.60
SWIR	2257.61	0.54		216.94
SWIR	2265.8	0.53		213.22
SWIR	2273.93	0.51		212.02
SWIR	2282.05	0.49		205.11
SWIR	2290.13	0.49		204.51
SWIR	2298.17	0.46		196.26
SWIR	2306.18	0.47		201.83
SWIR	2314.17	0.45		195.58
SWIR	2322.14	0.39		174.99
SWIR	2330.06	0.43		188.33
SWIR	2337.94	0.36		168.82
SWIR	2345.81	0.35		161.38
SWIR	2353.64	0.29		139.97
SWIR	2361.43	0.37		169.56
SWIR	2369.2	0.24		124.63
SWIR	2376.94	0.26		127.66
SWIR	2384.66	0.21		111.20
SWIR	2392.34	0.26		126.55

SWIR	2399.99	0.27		134.33
SWIR	2407.61	0.19		101.50
SWIR	2415.21	0.12		69.08
SWIR	2422.79	0.19		101.01
SWIR	2430.32	0.24		115.82
SWIR	2437.83	0.19		94.94
SWIR	2445.31	0.18		89.91

Table 7-9 SNR values per wavelength for VNIR and SWIR low and high gains

Radiometric calibration updates

The following calibration products were generated and delivered:

Product	Type	Date of Generation	Date of Validity Start	Date of Validity End	Delivered to
ENMAP01-CTB_RAD-20260224T000000Z_V040100_20260223T130838Z	CTB_RAD	23.02.2026	24.02.2026	-	DIMS
ENMAP01-REF_SUN-20260224T000000Z_V040100_20260223T130838Z	REF_SUN	23.02.2026	24.02.2026	-	DIMS

Table 7-10 Generated radiometric calibration tables

7.5.4 Geometric Calibration

There have been no new geometric calibration tables generated in the reporting period.

Type of Calibration Table	ID of Calibration Table	Date of Generation	Date of Validity Start	Date of Validity End
None				

Table 7-11 Generated new geometric calibration tables

The performance of the geometric calibration table is assessed in chapter 7.6.3.

7.6 Internal Quality Control

7.6.1 Archive

Within the given time period (01.01.2026 to 31.03.2026), 1754 datatakes with a total of 19123 tiles were acquired and archived (remark: additional datatakes acquired during this period but for which the archiving is pending might be missing in the statistics).

The overall quality rating statistics are listed in Table 7-12, and in relation to the Solar Zenith Angle (SZA) in Table 7-13. Also these ratings are further detailed for the VNIR and SWIR detector in Table 7-14, showing a nominal performance rating for the given quality thresholds.

In addition, the rating for the atmospheric conditions for the scenes are depicted in Table 7-15. When setting the atmospheric quality rating in relation to the illumination conditions (i.e., large SZA) during data acquisition (Table 7-16), For the reporting period, a slight increase of “low quality” scenes can be observed, but the numbers are still very small, 396 scenes (2.07%) compared to 88 scenes (0.4%) in Q3; this increase is related both to the increase in scenes with low light conditions (100% of the “low quality” scenes), and to a slight increase in the detected general radiometric artefacts.

Parameter	Value	Number of tiles	Percentage
overallQuality	Nominal	10937	99,71%
	Reduced	2	<0.02%
	Low	30	0.27%

Table 7-12 Overall quality rating statistics

Parameter	Sub-Parameter	Number of tiles	Percentage
overallQuality = Low		30	
	Thereof with SZA > 70°	30	100%

Table 7-13 Overall quality rating in relation to Sun Zenith Angle (SZA)

Parameter	Sub-Parameter	Number of tiles	Percentage
overallQuality = Reduced		2	
	Thereof with qualityVNIR nominal	0	0%
	Thereof with qualitySWIR nominal	2	100%
overallQuality = Low		30	
	Thereof with qualityVNIR nominal or reduced	4	13.33%
	Thereof with qualitySWIR nominal or reduced	24	80.00%

Table 7-14 Reduced and low quality rating statistics

Parameter	Value	Number of tiles	Percentage
QualityAtmosphere	Nominal	4633	42.24%
	Reduced	1542	14.06%
	Low	4794	43.70%

Table 7-15 QualityAtmosphere rating statistics

Parameter	Sub-Parameter	Number of tiles	Percentage
overallAtmosphere = Reduced		1542	
	Thereof with SZA > 65°	0	0%
	Thereof with SZA > 70°	0	0%
	Thereof with SZA > 80°	0	0%
overallAtmosphere = Low		4794	
	Thereof with SZA > 65°	1225	25.55%
	Thereof with SZA > 70°	294	6.13%
	Thereof with SZA > 80°	50	1.04%

Table 7-16 QualityAtmosphere rating in realtion to Sun Zenith Angle (SZA)

Parameter	Sub-Parameter	Number of tiles	Percentage
overallAtmosphere = Reduced		1542	
	Thereof with Cloud Cover > 66%	0	0%
	Thereof with DDV warnings	954	61.87%
overallAtmosphere = Low		4794	
	Thereof with Cloud Cover > 66%	2628	54.82%
	Thereof with DDV warnings	4001	83.46%

Table 7-17 QualityAtmosphere rating in relation to Cloud Cover and DDV availability

Remark about definition of EnMAP low quality collection

The quality rating of EnMAP products is based on image parameters, such as illumination conditions (i.e., sun elevation angle) and image defects, and on possible anomalies in the image data or instrument telemetry. These parameters are retrieved during the pre-processing and are added to the metadata and quality layers for every archived L0 product. In EOWEB GeoPortal two collections of EnMAP L0 products are available: “EnMAP-HSI (L0)” and “EnMAP-HSI (L0), Low Quality”. An L0 product is assigned to the low-quality collection if the corresponding metadata item qualityFlags.overallQuality is equal to 2 (low quality). This happens for products with a significant number of striping, saturation, artefact or dead pixels, when the screening of data and instrument indicates non-nominal behavior or, in the majority of cases, when the sun elevation angle is less than or equal to 0 (e.g., night scenes). A detailed definition of qualityFlags. overallQuality is given in Sec. 4.4.9 in the L1B ATBD (EN-PCV-TN-4006).

7.6.2 Level 1B

7.6.2.1 Radiometric Performance

Defective / de-calibrated detector elements

Using the Detector Map components, an offline check of possibly defective or de-calibrated detector elements is conducted. In particular, a detector element is identified as “possibly defective” if it is suspicious in at least 75% of the useful tiles. Note that this analysis is based on L1B_RAD data, so no dead / defective pixel interpolation was carried out. Within the given reporting period, the following indications for defective pixels are found for the VNIR and the SWIR camera:

VNIR (total of 16021 tiles, with 15891 suitable for analysis):

Newly found suspicious pixels in green, previously detected in **black**, no longer present ones in ~~red~~.

Band	Cross-track element
19	187
85	14
89	395

Note that the band index starts at 1.

SWIR (total of 15432 tiles, with 15244 suitable for analysis):

Newly found suspicious pixels in green, previously detected in **black**, no longer present ones in ~~red~~.

NOTE: due to the change in SWIR band configuration within the period Q3 2023, the band index from band 45 till 75 did change by +1 (with bands 45, 74 & 75 newly added) w.r.t. the reports before Q3 2023.

Band	Cross-track element	Band	Cross-track element	Band	Cross-track element
1	817	33	560	~~85~~	~~525~~
2	235, 286, 593, 673	38	241, 919	89	285
3	381	48	511	91	973
4	362, 363, 418	50	311, 344, 395	92	677, 973
5	687	51	155	96	341, 819
7	472, 910	53	97, 98	101	318

8	801	54	941	106	107
9	124	56	221, 965	107	265, 764
11	715	58	632, 667, 922	108	886
14	29, 684	59	89, 90	111	315
16	535	61	312	~~118~~	~~837~~
29	855, 928	63	123		
30	360, 855	66	93		
31	360	69	864		
		72	801, 845		
		75	737		

Dead detector elements

Within the given reporting period, the statistics for dead pixels are provided in Table 7-18 and Table 7-19. When comparing these numbers to the estimates in Ch. 7.5.1, one must bear in mind that the latter is based on the full detector readout configuration, while the numbers provided in the following are related to the standard readout configuration as provided in the user product. Because of the smaller readout area, these following dead pixel numbers are lower in comparison.

Parameter	Value (number of pix)	Number of tiles	Percentage
DeadPixelsVNIR	137	10969	100%

Table 7-18 Dead pixel statistics, VNIR

Parameter	Value (number of pix)	Number of tiles	Percentage
DeadPixelsSWIR	1509	10969	100%

Table 7-19 Dead pixel statistics, SWIR

Saturation and radiance levels

Within the given reporting period, no indications for increased saturation defects are found for the VNIR and the SWIR camera (see Table 7-20 and Table 7-21).

Parameter	Value (per mille of scene)	Number of tiles	Percentage of tiles
SaturationCrosstalkVNIR	0	10732	97.84%
	> 0 per mille	237	2.16%
	> 10 per mille	29	0.26%

Table 7-20 Saturation statistics, VNIR

Parameter	Value (per mille of scene)	Number of tiles	Percentage of tiles
SaturationCrosstalkSWIR	0	10800	98.46%
	> 0 per mille	169	1.54%
	> 10 per mille	8	0.07%

Table 7-21 Saturation statistics, SWIR

Other radiometric artifacts

Within the given reporting period, the striping performance is similar to the one encountered during the Commissioning Phase. Within PCV, different de-striping approaches were tested, and the selected one by M. Brell (GFZ) is implemented in processor version V01.02.00 (07.03.2023).

Apart from this, no indications for an increase in general radiometric artifacts are found for the VNIR and the SWIR camera (see following tables).

Parameter	Value (number of pix)	Number of tiles	Percentage
generalArtifactsVNIR	0	0	0%
	> 0	10969	100%
	> 10	341	3,11%
	> 100	31	0,28%
	> 1000	0	0%

Table 7-22 Artifacts statistics (without striping), VNIR

Parameter	Value (number of pix)	Number of tiles	Percentage
generalArtifactsSWIR	0	0	0%
	> 0	10969	100%
	> 10	10969	100%
	> 25	331	3.02%
	> 100	41	0.37%
	> 1000	0	0%

Table 7-23 Artifact statistics (without striping), SWIR

7.6.2.2 Spectral Performance

For the analysis of the spectral stability, the Detector Maps of all Earth datatakes acquired in the reporting period were used. Note that no smile correction was applied, so the analysis shows only on the instrument characteristics. At the wavelengths of stable atmospheric features (760 nm Oxygen absorption and CO2 absorption at ~2050 nm), simulations of spectral shifts were carried out by resampling the absorption in the interval of +/- 3.0 nm with steps of 0.05 nm. Then the signal of the Detector Maps and the simulated shifted absorptions were normalized, and a least-square fit was used where the sensed absorption matches the simulations. Also an additional polynomial fitting was applied, as especially the CO2 absorption band region has low signal an is thus significantly influenced by noise.

For the VNIR, when aggregating the shifts (Figure 7-197-18) the mean derivation is almost constant in across-track direction and -as before- around 0.5 nm towards shorter wavelengths, underpinning the consistency with the in-orbit spectral calibration and especially regarding the shape of the spectral smile. Note that of course these results are consistent within the limitations of this vicarious approach. Additionally, the variability of the vicariously estimated spectral calibration can be expressed as the standard deviation at 1 sigma is below 0.3 nm, which includes the spectral stability of EnMAP and as well the variations of the used Earth datatakes and the limitations of the method.

In summary, for the VNIR the estimated differences to the CTB_SPC consistent with the results of previous reporting periods, confirming the validity of the spectral calibration and the spectral stability of the instrument taking into accounts the limitations of the vicarious approach.

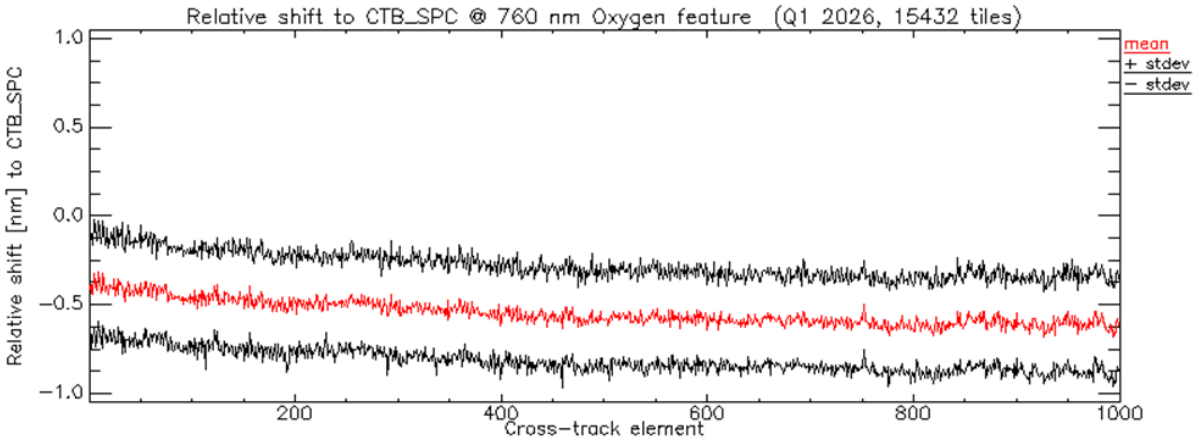

Figure 7-19 VNIR estimated spectral shift at 760 nm w.r.t the valid spectral calibration table (CTB_SPC), and relative spectral stability expressed at 1 sigma (Q1 2026, 15920 tiles)

For this analysis, the reference is thus not the nominal center wavelengths (i.e., a single number per band), but the CW per cross-track pixel, thus explicitly including the spectral smile (see Figure 7-207-19).

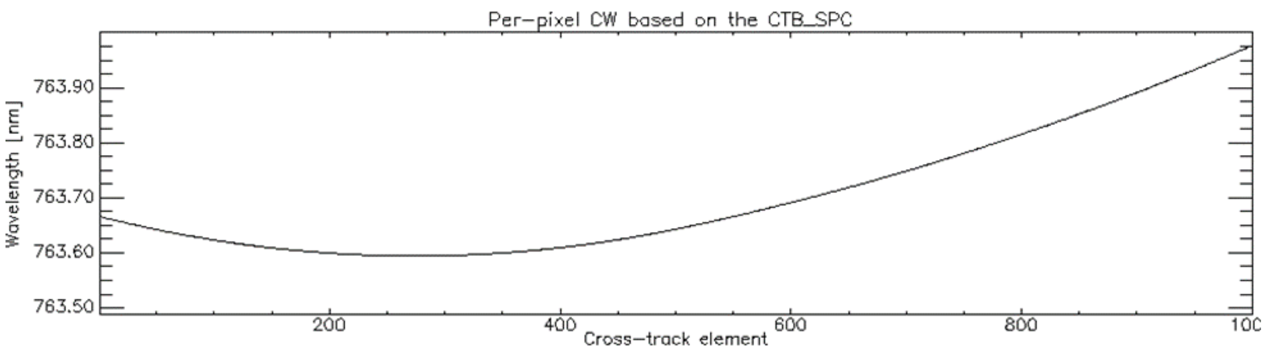

Figure 7-20 Center wavelengths per cross-track pixel based on the spectral calibration table (VNIR band 62) in the calibration table (CTB_SPC).

For the SWIR having less pronounced atmospheric absorption features, more influence of the background and a much lower signal level, the fitting also results in more clutter, as shown in Figure 7-217-20.

In order to demonstrate that the mean derivation to the CTB_SPC is within the spread of the data, the mean and standard deviation are calculated using the relative values, as shown in Figure 7-217-20. For Q1 2026, a small shift of ~0.35 nm towards longer wavelengths is visible when comparing to CTB_SPC (Figure 7-227-21) , and having a standard deviation of ~0.5 nm. This shift is equal for all cross-track elements, so the shape of the spectral smile did not change and is well represented in the CTB_SPC. When comparing this small spectral shift to the results in the past quarter, the mean shift to the CTB_SPC is slightly reduced by ~0.07 nm. As before, the spectral shift is the same for all cross-track elements, so the shape of the spectral smile did not change and is well represented in the CTB_SPC. In addition, the spread around the estimated mean with a standard deviation of ~ 0.5 nm (1 sigma) indicates no significant change of the good overall stability of the instrument.

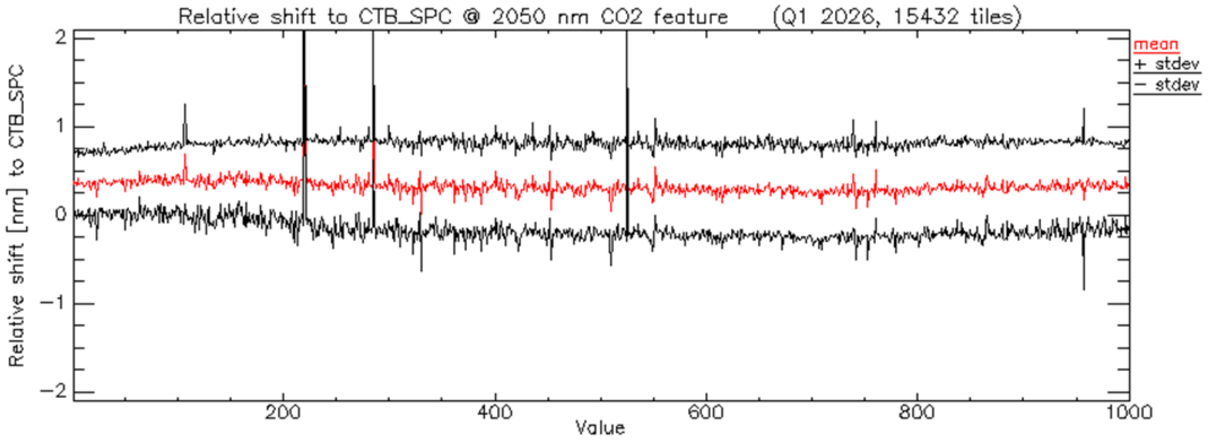

Figure 7-21 SWIR estimated spectral shift at 2050 nm w.r.t the valid spectral calibration table (CTB_SPC, shown below), and relative spectral stability expressed at 1 sigma (Q1 2026, 17894 tiles)

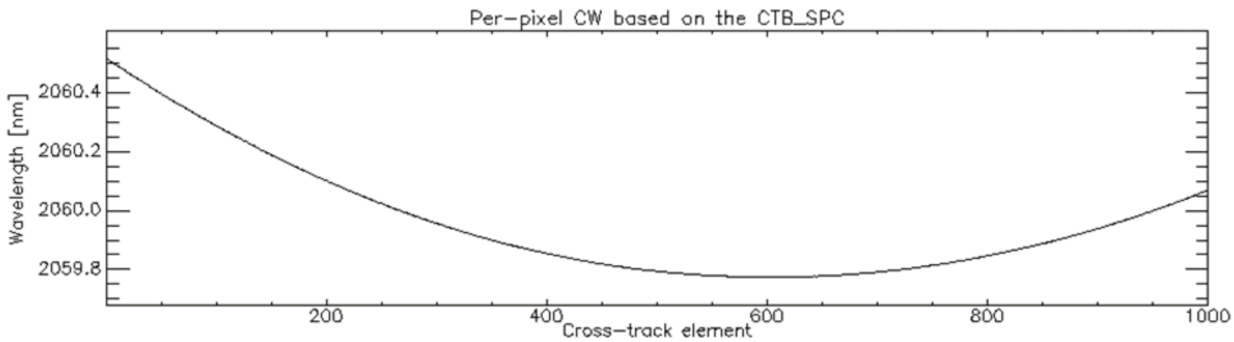

Figure 7-22 Center wavelengths per cross-track pixel based on the spectral calibration table (SWIR band 86).

7.6.3 Level 1C

This report covers the timeframe from 01.01.2026 to 31.03.2026. No geometric calibration was performed during this period.

In the timeframe of this report, 1355 datatakes have been acquired. In 1180 of those datatakes (~87 %), enough ground control points (GCP) and independent check points (ICP) were found to perform a geometric accuracy assessment. The datatakes without enough GCPs were not assessed quantitatively, but a random subset of them was inspected visually. The vast majority of those datatakes was either almost fully covered with clouds or showing only water, desert or rain forest. The behavior is thus as expected.

The assessment of the RMSE values in the metadata is shown below in Figure 7-237-23.

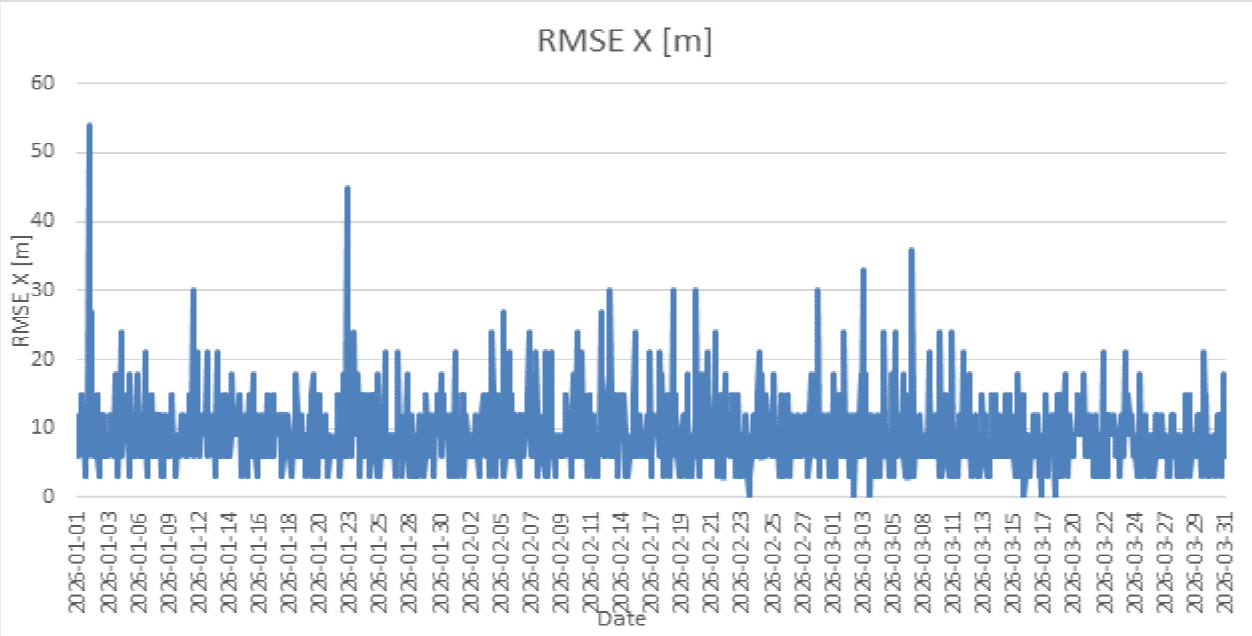

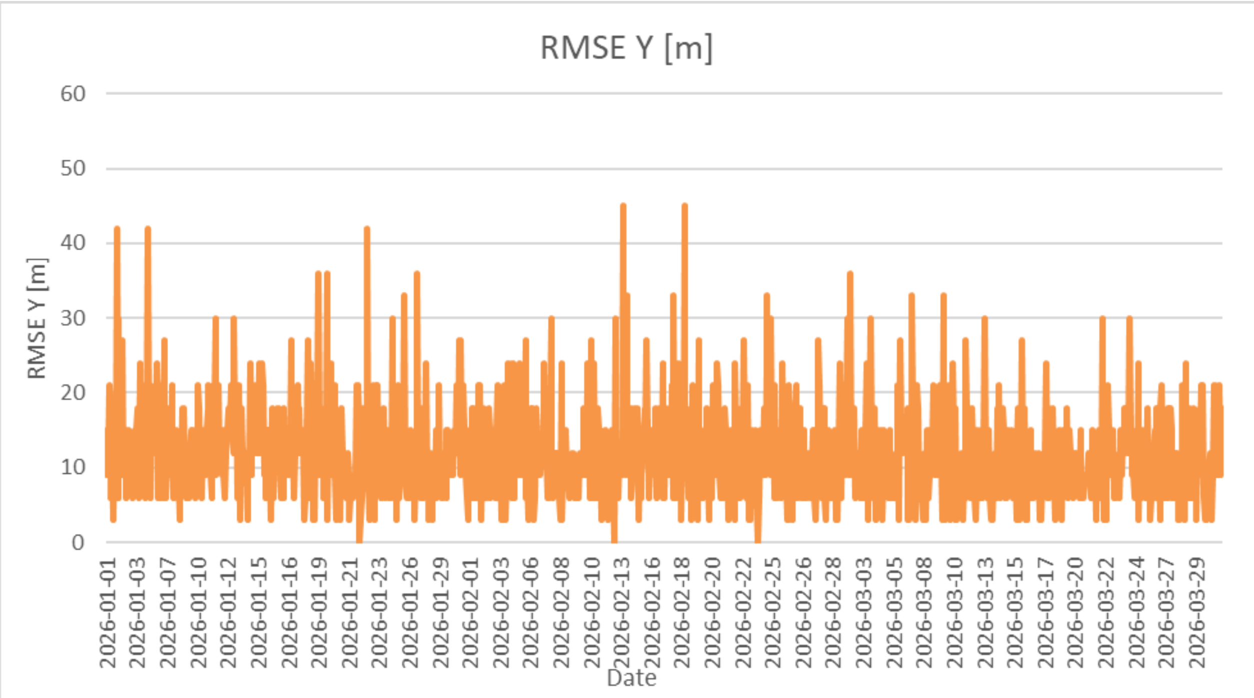

Figure 7-23 Assessment of RMSE X values (top) and RMSE Y values (bottom), calculated based on found ICPs, for all datatakes where ICP could be found

In x-direction, 4 datatakes (~0.3%) had an RMSE value above 30 m (1 GSD), whereas in y-direction, 15 datatakes (~1.3%) are above this threshold. For most of those datatakes, only very few GCP and ICP could be found during processing, making the results less reliable. The mean values are 9.24 m in x-direction and 11.91 m in y direction. This shows a very high geolocation accuracy for the datatakes where matching was possible. The requirement GRD-PCV-0155 (1 GSD) is thus fulfilled.

The average boresight angles, which can be interpreted as the correction and thus the error of the scene if no GCPs could have been found, correspond to approximately -4 m in x direction with a standard deviation of approximately 20 m and -45 m in y direction with a standard deviation of approximately 20 m on ground. It is reasonable to assume that the scenes where no GCPs could be found are in the same accuracy range and thus well within the requirement of 100 m (GRD-PCV-0150). Note that the x and y direction mentioned in this report are not in the image coordinate system but in UTM, as the evaluation is done on L1C products.

7.6.3.1 **Geometric accuracy**

EnMAP L1C products are matched against a reference image (Sentinel-2 data, if not stated otherwise) by using image matching techniques to assess the geometric accuracy. At the obtained checkpoints (CP), statistics are calculated to provide mean and RMSE values (Figure 7-247-24) for each scene. Note that the obtained accuracy in the analysis is always w.r.t. the reference image. This report covers EnMAP data from 01.01.2026 to 31.03.2026. A random sample of 565 L1C tiles was selected based on visual inspection of the catalogue quicklooks (e.g. to avoid cloudy images).

The requirement GRD-PCV-0155 shall be fulfilled:

The geolocation accuracy at nadir look direction of level 1C and 2A products shall be better than 1 GSD (1 sigma) in each direction with respect to reference images provided that reference images are available and sufficient similarity.

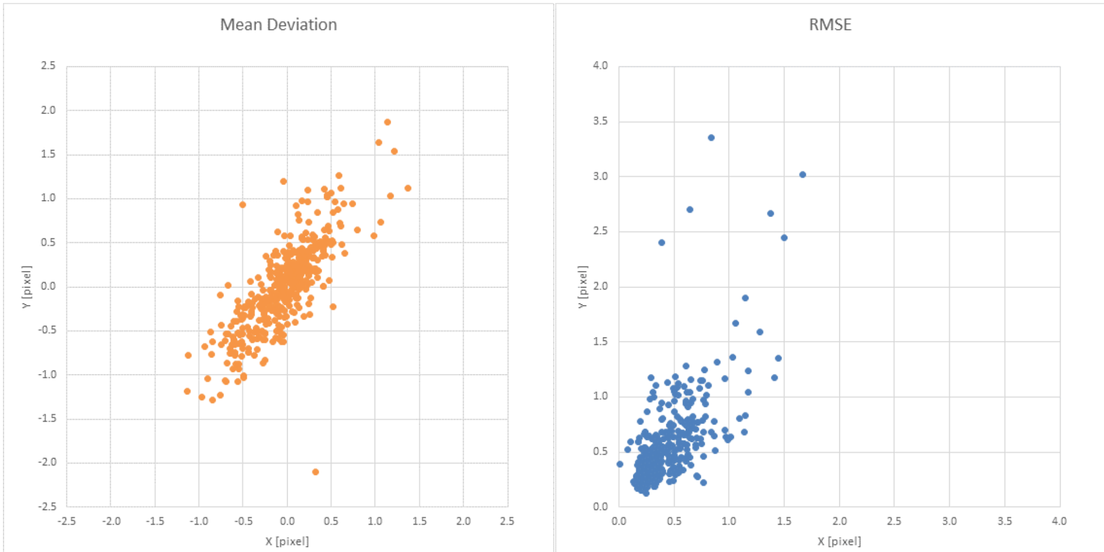

Figure 7-24 Mean deviation of EnMAP L1C products in pixel (left). RMSE value for EnMAP L1C products in pixel (right)

Note, that during processing the boresight angles and the geometric accuracy related quality flags are calculated on datatake level while in the figures and tables above, the accuracy is assessed per tile. The mean values over all 483 L1C tiles are -0.03 and 0.02 pixel in mean deviation with a standard deviation of 0.37 and 0.51 pixel while the mean RMSE values are 0.40 and 0.53 pixel, all in x and y direction respectively. The data show that for the vast majority of scenes the accuracy wrt. reference image is better than one pixel and thus the requirements are fulfilled. Compared to the last geometric QC report, the values are very stable (see Figure 7-267-26).

7.6.3.2 **Co-registration accuracy**

In this section, the co-registration accuracy is checked against the Space Segment requirement SRDS-PIM-0050 (EN-KT-RFW-003 is also to be considered here):

*The HS-Imager shall be designed such, that the geometric co-registration is ≤ 20 % of the nominal Ground Sampling Distance (0.2 * GSD linear displacement in both directions).*

For the assessment of co-registration accuracy, the SWIR data of EnMAP L1C products are matched against the corresponding VNIR data and the mean deviation values shown in this section (Figure 7-257-25).

This report covers EnMAP data from 01.01.2026 to 31.03.2026. A random sample of 568 L1C tiles was selected based on visual inspection of the catalogue quicklooks (e.g. to avoid cloudy images).

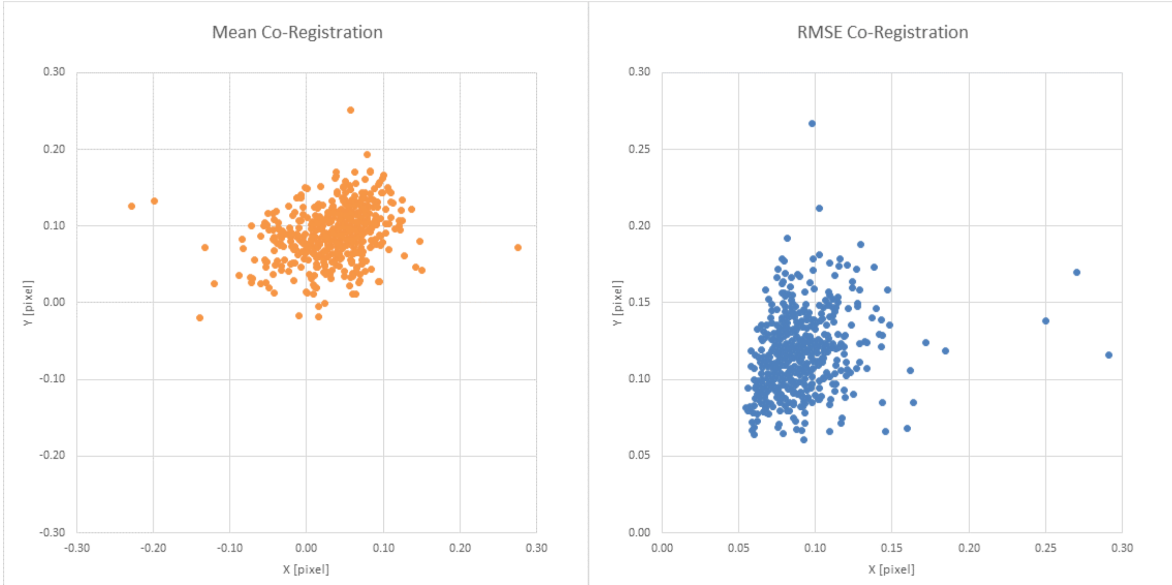

Figure 7-25 Mean deviation in pixel between VNIR and SWIR data of EnMAP L1C products (left). RMSE in pixel between VNIR and SWIR data of EnMAP L1C Products (right)

The data show, that the mean co-registration is well within the requirement. Note that the theoretical accuracy of the used matching algorithm is 0.1 pixel, and as can be seen in the RMSE values, still some mismatches were not removed by the blunder detection techniques that were applied. The mean deviation over all analyzed tiles are 0.03 pixel in x-direction with a standard deviation of 0.05 pixel and 0.09 pixel in y direction with a standard deviation of 0.04 pixel. Compared to the results in the previous geometric QC report, the values are very stable as can be seen in Figure 7-267-26.

7.6.3.3 Development of geometric performance

Since the launch of EnMAP on April 1st 2022, the geometric performance has been improved significantly. This was achieved by different geometric calibrations and processor updates. Table 7-2426 shows the measures performed, their date and their effect.

Date	Measure	Effect
01.08.2022	Fix of attitude processing	Improvement of absolute geolocation (w/o matching)
20.09.2022	Boresight Calibration	Improvement of absolute geolocation (w/o matching)
03.11.2022	1st Geometric Calibration	Improvement of absolute geolocation (w/o matching) Improvement of VNIR/SWIR co-registration (~0.8 pix -> ~0.4 pix)
11.02.2023	2nd Geometric Calibration	Improvement of VNIR/SWIR co-registration (~0.4 pix -> ~0.15 pix)
29.03.2023	Processor update (v01.02.00)	Improvement of VNIR/SWIR co-registration (~0.15 pix -> ~0.06 pix)
05.05.2023	Processor update (v01.03.01)	Improvement of geolocation accuracy

Table 7-24 Improvement of geometric performance

Figure 7-267-26 shows the development of the co-registration accuracy, measured as described in previous section. Again, after a significant improvement since commissioning phase, over the last report periods the accuracy has been very stable.

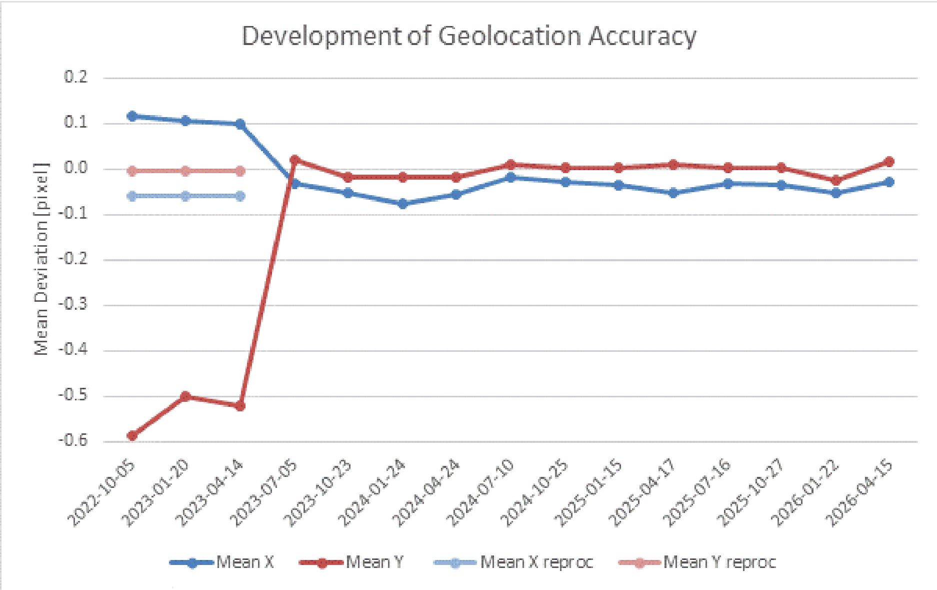

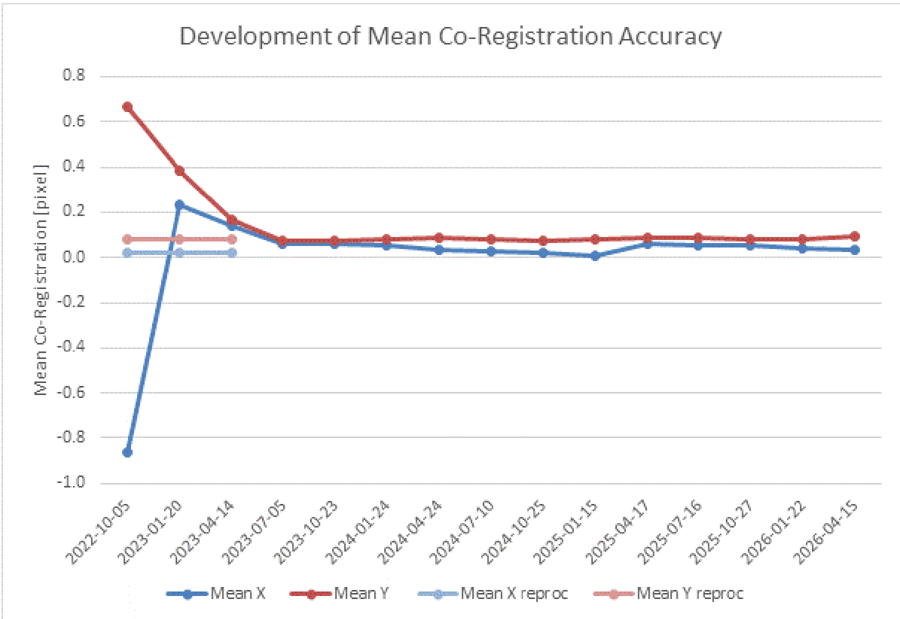

Figure 7-26 Development of co-registration accuracy based on the previous geometric QC reports. The values with re-processed L0 data and archived version ≥V01.03.00 are also shown

As most of the geometric processing – especially the matching against a reference image – is done on datatake level during L0 processing, the geometric accuracy and co-registration of data acquired earlier during the mission is not automatically improved when higher level products (L1B, L1C, L2A) are processed with the current processor version. However, after completing the L0 reprocessing of the whole archive, the geometric processing is executed with the latest processor version and geometric calibration table to make sure that the best geometric quality and co-registration is reached also for the reprocessed data. Today, the geometric performance of the products available in the Mission Archive with date earlier than 29.03.2023 is the same as for the products acquired after that date. Users can recognize reprocessed data by checking the metadata tag **archivedVersion**: if the version is 01.03.00 or higher, then the geometric performance should be as analyzed in this report, regardless of the acquisition date of the product.

7.6.4 Level 2A

7.6.4.1 **Validity of generated L2A “water” data**

7.6.4.1.1 Analyzed scenes

The following scenes were taken into consideration:

DataTake - ID	Tile - ID	Location	L2A Option	Cirrus / Haze Removal	Overall Quality
179591	03	2026-02-17	ITA, Venice	Water mode, water type “clear”	Cirrus
177473	13	2026-02-07	AUS, Agnes Water	Water mode, water type “clear”	Cirrus
176781	04	2026-01-23	JAP, Hota	Water mode, water type “clear”	Cirrus
182665	06	2026-03-12	DE, Peenemünde	Water mode, water type “clear”	Cirrus
177810	20	2026-02-10	USA, Martinsville	Water mode, water type “clear”	Cirrus

Table 7-25 Datatake IDs of analyzed water products

The below listed parameters were checked for above mentioned scenes by EOMAP:

Parameter	Check
Masking (Land, Water, Clouds, etc.)	No issues found.
Adjacency correction	No issues found.
Retrieval of atmospheric properties	No issues found.
Cirrus – correction	No issues found.
Retrieval of water leaving reflectance	No issues found.
Quality Mask	No issues found.

*Details to the updates are presented below.

7.6.4.1.2 Data Checks

For the checks described in the following, multiple scenes were used. The corresponding scene - IDs and locations can be found in Table 7-2527. Every scene was processed using the EnMAP Processor 01.05.06 and MIP version 1.4.2.

- Masking

First, the geo mask is checked. The different parts of the scene shown masked (see Figure 7-27 and Figure 7-28Figure 7-28) are classified as expected.

Figure 7-27 Scene-ID 182665; RGB-Quicklook with Bands 611.02nm – 550.69nm – 463.73nm

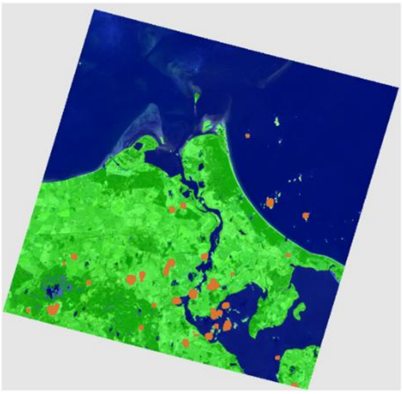

Figure 7-28 Scene-ID 182665; Geo Mask with Blue – Water, Green – Land, Light Blue - Shadows, Orange – Clouds, Dark Green – Cirrus, White – NA

- Cirrus and Adjacency Correction

Next, we check for the cirrus and adjacency correction using the two sites ‘AC1’ and ‘AC2’ shown in Figure 7-27.

The coordinates of the sample locations are as follows:

AC 1: LAT 54.05876118 | LON 13.92655405

AC 2: LAT 54.18371098 | LON 13.98696014

For sampling, we choose two locations, one located over shallow water, the other over deep water (see Figure 7-27 for the sample locations).

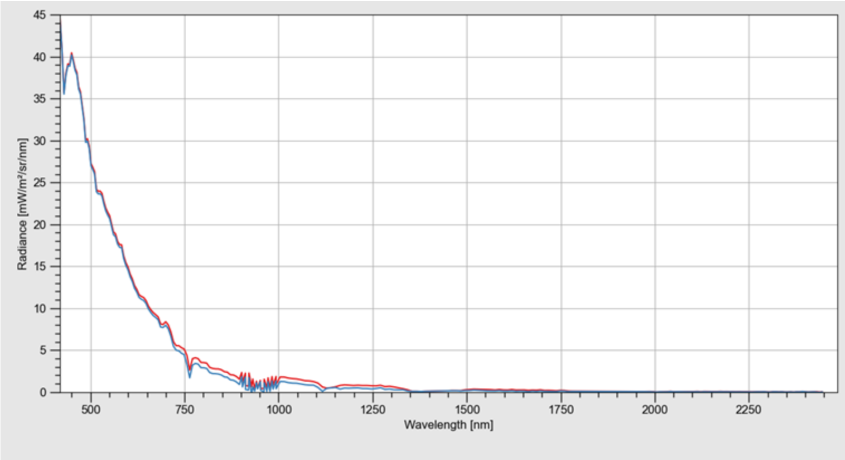

Figure 7-29 Scene-ID 182665; At-sensor-radiance sampled at location AC 1; red: measured, blue: adjacency corrected

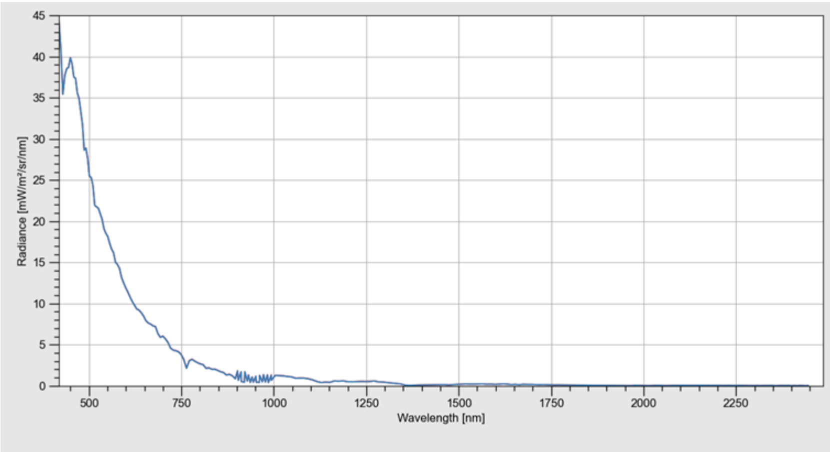

Figure 7-30 Scene-ID 182665; At-sensor-radiance sampled at location AC 2; red: measured, blue: adjacency corrected

Figure 7-29 and Figure 7-30 depict the sampled at-sensor-radiance - signal for location AC 1 and AC 2, respectively. The effect of the adjacency correction is clearly depicted in Figure 7-29. This is what we expect, since the sample location was placed near high reflective terrestrial objects. In contrast, a differentiation between the two plotted signals in Figure 7-30 is not possible, since the effect here is near zero. Due the sample – placement in an offshore region, this is as well the behavior we expect.

Thus, overall, the adjacency correction works as intended.

- Reflectance Product

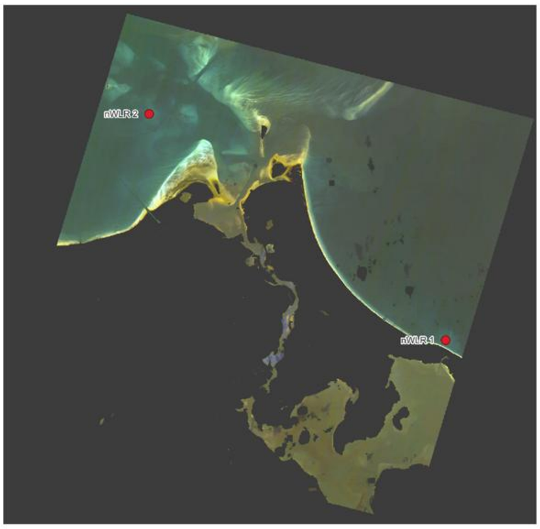

Figure 7-31 Normalized Water Leaving Reflectance of scene-ID 182665; wavelengths for RGB: 611.02nm – 550.69nm – 463.73nm

For the labeled locations in Figure 7-32, the sampling coordinates are as follows:

nWLR 1: LAT 54.07377048 | LON 13.97305438

nWLR 2: LAT 54.21523716 | LON 13.64634771

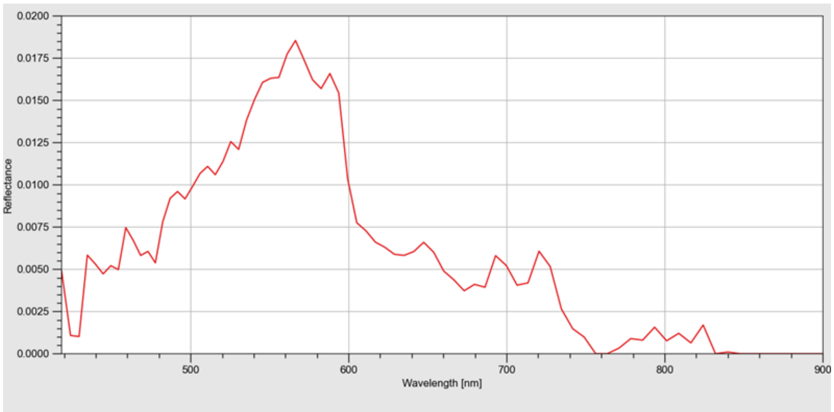

Figure 7-32 Scene-ID 182665; nWLR sampled at location nWLR 1

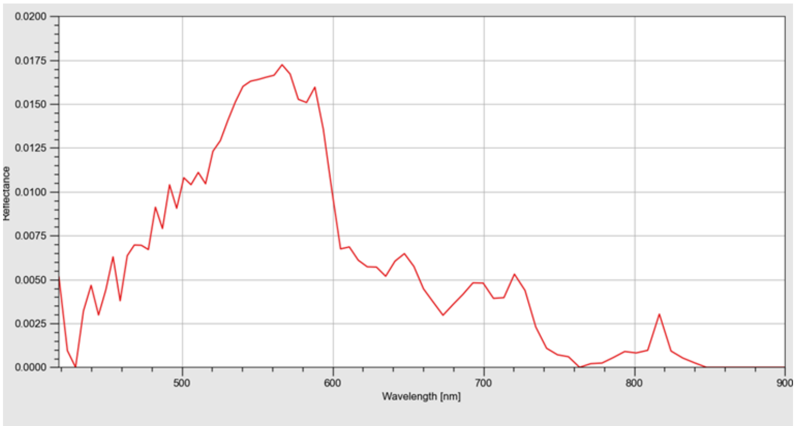

Figure 7-33 Scene-ID 182665; nWLR sampled at location nWLR 2

Figure 7-32 and Figure 7-33 Figure 7-34Figure 7-35depict the normalized water leaving reflectance sampled at location nWLR1 and nWLR 2, respectively. The fact that the scene at hand suffers from a sun angle of around 57.5° (measured from zenith) explains that some of the peaks, for example around 650nm or 720nm, are more pronounced than usual. This is due to the distance the light has to travel through the atmosphere until reaching the water surface. In case of such high sun angles, this distance is very high and leads to a more pronounced effect of the atmosphere on the signal. Thus, scenes captured under comparable sun angles have to be used with care. This is of course already indicated by the overall quality, which in this case equals zero.

Summing up, the atmospheric correction workflow works as we expect it to.

7.6.4.2 **Validity of generated L2A "land" data**

7.6.4.2.1 Analyzed scenes

Within the time interval between 01.01.2026 to 31.03.2026, an interactive in-depth analysis has been conducted for the following scenes:

Datatake-ID	Tile-ID	date	location	L2A option	cirrus and haze removal	Archived Version	processor version	Overall Quality	Quality Atm
177995	002	2026-02-10	Antarctica	land	no	01.05.06	V010506	Reduced	Low (SZA 65°)
180304	007, 008	2026-02-20	Kantaunggyi, Myanmar	land	no	01.05.06	V010506 "EOWeb"	Nominal	Nominal
180304	007, 008	2026-02-20	Kantaunggyi, Myanmar	land	no	01.05.06	V010506 "Geoservice"	Nominal	Nominal
189005	005	2026-04-21	North Euboean Gulf, Greece	land	no	01.05.06	V010506	Reduced	Nominal

(*): note: quality atm. rating for L0 is "low"; reasons for this discrepancy are currently investigated.

Table 7-26 Datatake IDs of analyzed land products

For the selection of L2A data, several data takes acquired within the reporting period and covering different landscapes at different conditions were analyzed.

7.6.4.2.2 Data Checks

In the following, the different tiles were checked for the shape and magnitude of the BOA_ref spectra, and also the quality of the generated masks is evaluated when meaningful.

For all tiles the visual image impression is fine. For the masking, there are known issues of mis-classifications which are currently being investigated. The BOA_ref spectra all show the typical shape and magnitude, indicating the correct L2A correction.

- **Antarctica (DT177995, 2026-02-10)**

The selected scene at the shoreline of Antarctica was chosen as the scene content is challenging regarding the correct separation and masking of snow & ice, dark rocks, open water and clouds, while also showing the typical lower radiance levels due to low sun conditions (SZA 65°) and thus more noise.

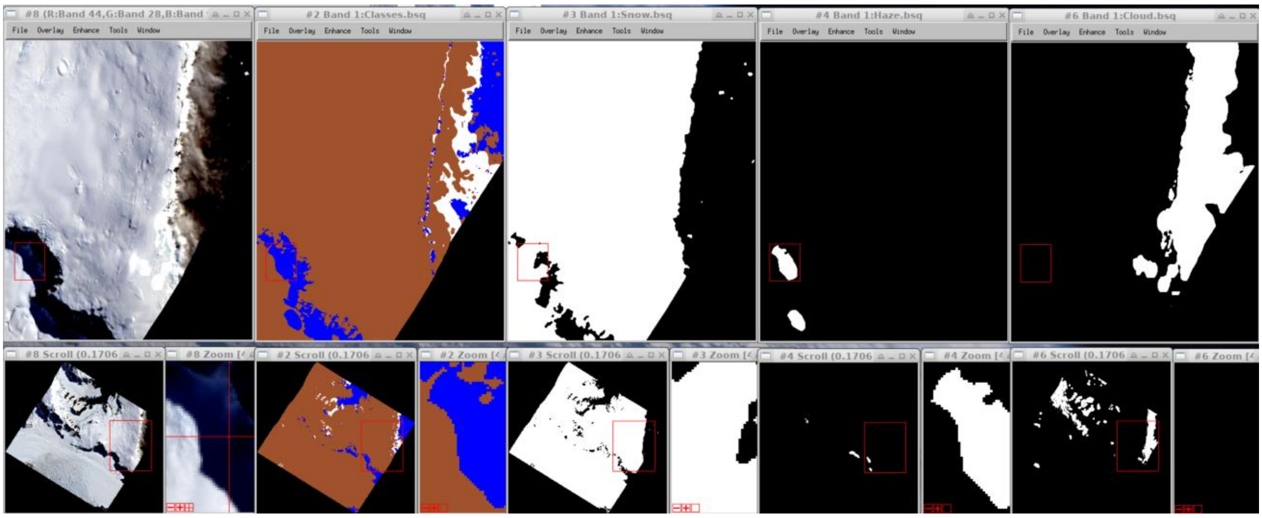

Figure 7-34 DT177995, from left to right: TrueColorComposite; QualityClasses (blue: water, brown: land, white: other), Snow Mask, Haze Mask, Cloud Mask. The CirrusMaks and CloudShadowMask are correctly empty.

Regarding this masking (Figure 7-34), the Snow Mask is well representing the inland snow and ice areas. Around the coastline, submerged or swimming ice areas are incorrectly included in the Cloud Mask, which is due to the quite unusual spectral signatures. Next, a few smaller haze areas were incorrectly flagged over water areas having a slightly larger reflectance as the surrounding water. The separation of land and water in these environments is hence difficult, as can be seen in the QualityClasses in Figure 7-34, and is further detailed in the following.

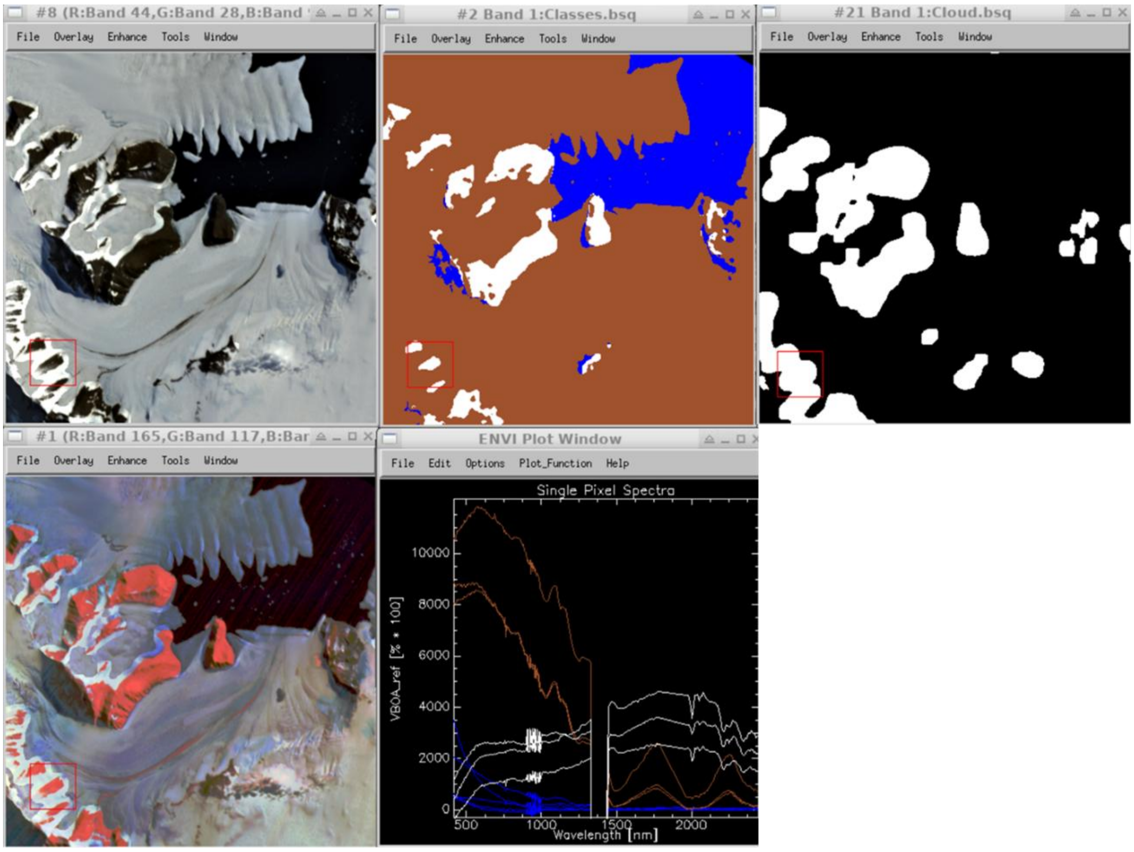

Figure 7-35 DT177995, top-Left: TrueColour Composit; Bottom-Left: IR-composite, nonlinear strecth; Top-Center: QualityClasses (blue: water, brown: land, white: other); Top-Right: Cloud Mask; Bottom-Center: singel pixel spectra where colours represent the QualityClasses.

As can be seen in Figure 7-35, parts of the image which have a similar appearance in the TrueColor image as water are indeed dark rock outcrops, as seen in the infrared composite and the related pixel spectra. Therefore, the QualityClasses separates these dark surfaces correctly.

When checking the retrieved BOA reflectances Figure 7-35, the spectral shapes and magnitudes of most surfaces is as expected, but locally surfaces exceeding 100% reflectances can be found. And as shown in Figure 7-36, most of these pixels with too high reflectance occur in areas where the terrain is steep and clouds are flagged. For pixels masked as “cloud”, a simplified correction is conducted not correcting for terrain, sometimes even causing the signal to saturate, as indicated by the red circle in Figure 7-36. This problem is even more pronounced for scenes in Antarctica having both snow/ice cover (high reflectance in the VNIR) and -due to the changing in the snow/ice, also the DEM might not be representative or of sufficient quality to accurately correct the terrain effects.

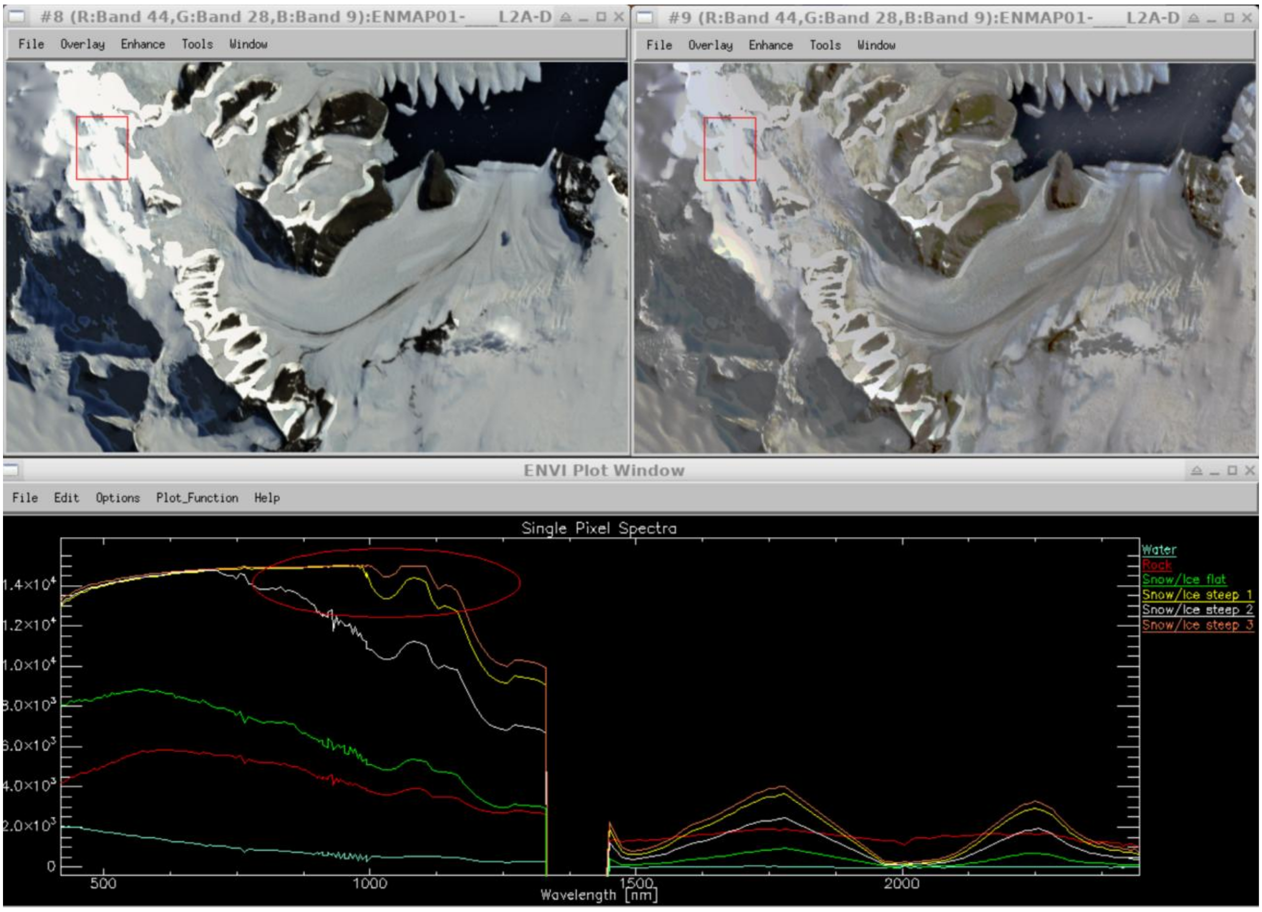

Figure 7-36 DT177995, top-left: TrueColorComposite, linear stretch; Top-right: same, but gaussian stretch; below: single pixel spectra.

To conclude, for the vast majority of this scene, both the retrieved surface reflectance values and the generated masks are as expected, and problems coming from atypical surfaces (submerged or floating ice) and terrain / cloud masking effects may limit the accuracy for certain areas.

- **Kantaunggyi, Mayanmar (DT180304, 2026-02-20)**

Beginning with tile 7 (Figure 7-37), large haze areas over the coastal area are correctly masked, including both open water, islands and marshland. A few pixels are incorrectly masked as “cloud shadow”, but these represent mangroves and/or submerged vegetation (see red spectrum in Figure 7-38), which is similar to vegetation under cloud shadow and thus can be explained. Finally, the separation between land and water in this challenging environment is correct for both inland water areas (rivers) and the coastal areas. The retrieved BOA reflectance spectra (Figure 7-38) are all plausible in shape and magnitude.

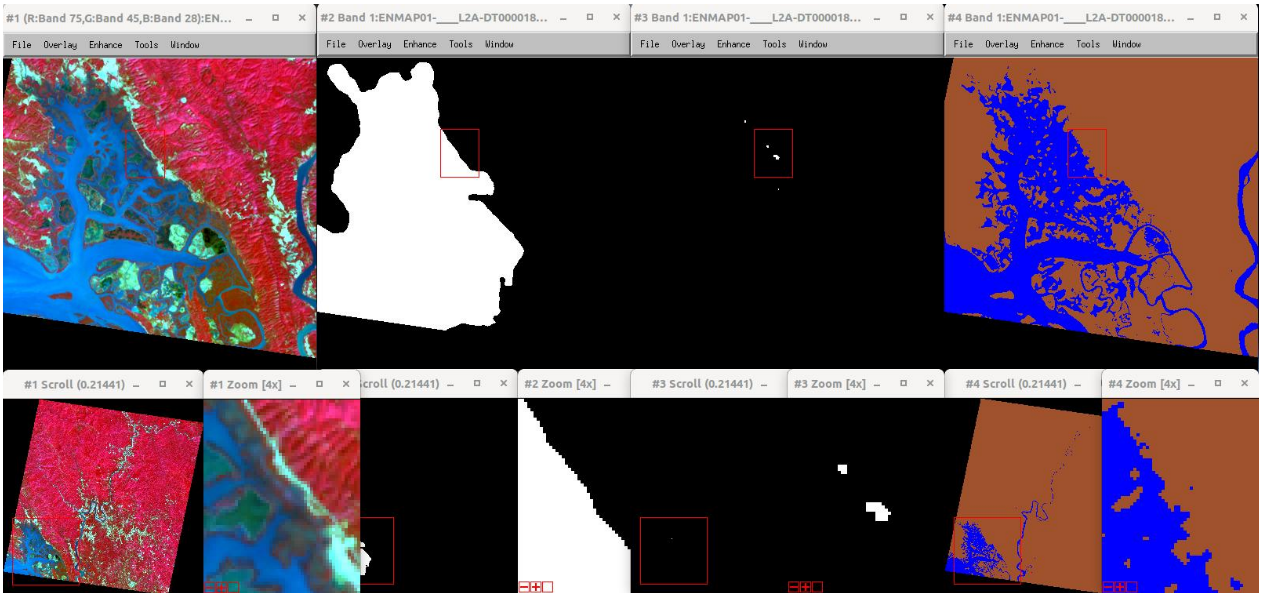

Figure 7-37 DT180304 Tile 7, from left to right: CIR composite, haze mask, cloud shadow mask, QualityClasses (blue: water, brown: land); all other masks are correctly empty.

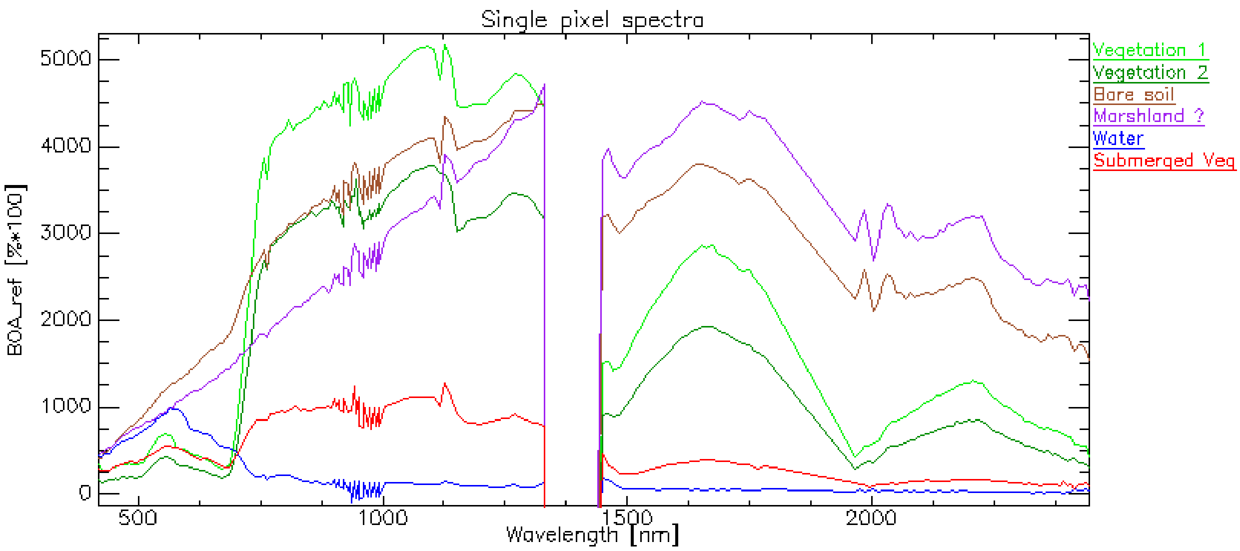

Figure 7-38 DT180304 Tile 7, single pixel BOA reflectance spectra

For the adjacent tile 8 (Figure 7-39) with larger water / marshland areas, no haze was flagged even though this would be expected based on the flagging in Tile 7. As before, cloud shadow was flagged for submerged vegetation / mangroves which is due to the spectral similarity to shaded vegetation. The land-water masks are again correct for this coastal area with many land-water transitions.

As before, the reflectance spectra shown in Figure 7-40 are as expected, showing the typical features of vegetation, soils, sand and water.

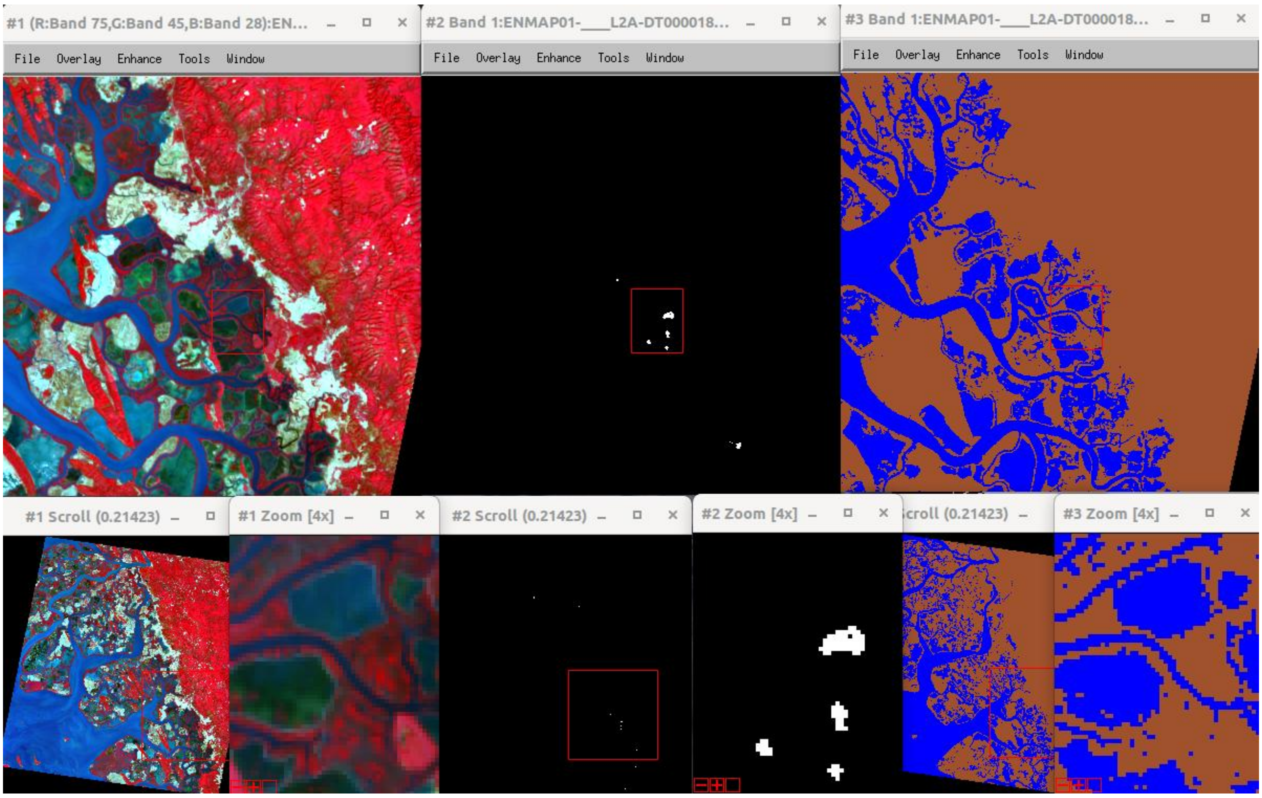

Figure 7-39 DT180304 Tile 8, from left to right: CIR composite, cloud shadow mask, QualityClasses (blue: water, brown: land); all other masks are correctly empty.

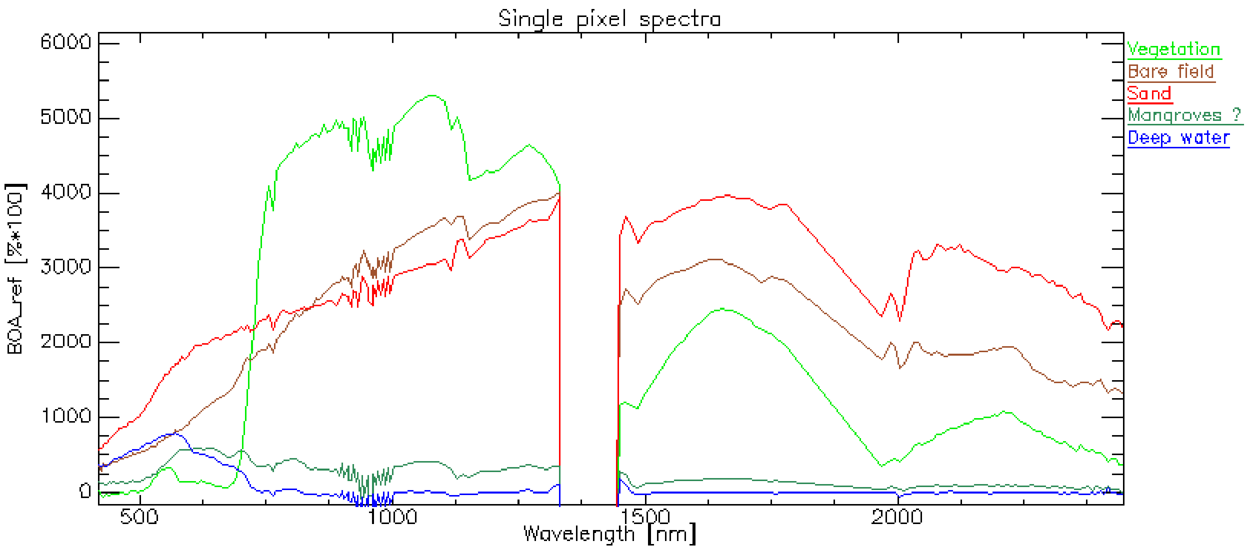

Figure 7-40 DT180304 Tile 8, single pixel BOA reflectance spectra

When mosaicking both tiles (Figure 7-41), the image impression is different for SWIR and for a TrueColorComposite: while the SWIR shows no transition between tiles, the bands in the visible show a sharp difference in brightness between tiles, and a “brighter” image impression for tile 7 than for tile 8. As the shorter wavelengths are stronger affected, this is a clear indication that the estimated aerosol values differ between tiles, as the effect of aerosol and aerosol correction is strongest in the blue, and rapidly decreases towards longer wavelengths with no influence in the SWIR. When checking the mean scene values for the AOT, tile 7 has a mean AOT of ~0.14 while tile 8 of ~0.435, while the estimated mean scene water vapor values are similar (i.e., 1.94 cm for tile 7 and 2.17 for tile 8). This is currently being investigated.

This effect can also be seen when comparing the BOA reflectance spectra of similar surfaces close to the tile borders (Figure 7-42 and Figure 7-43). In the visible spectral range, for tile 7 all surfaces show higher reflectance values than for tile 8, while in the SWIR most spectra are close to identical (note: the differences for soil in Figure 7-42 and Figure 7-43 depicted in purple are likely due to natural variabilities in the soils). When calculating the mean spectra over the areas close to the tile borders (green spectra in Figure 7-42 and Figure 7-43), this overall difference is highlighted, having a close match in the SWIR and a higher reflectance in the VIS for tile 7 w.r.t. tile 8. Note that for tile 8, slightly negative reflectance values occur for the ~25 bands, indicating a slight overcorrection for the aerosol effect in this tile.

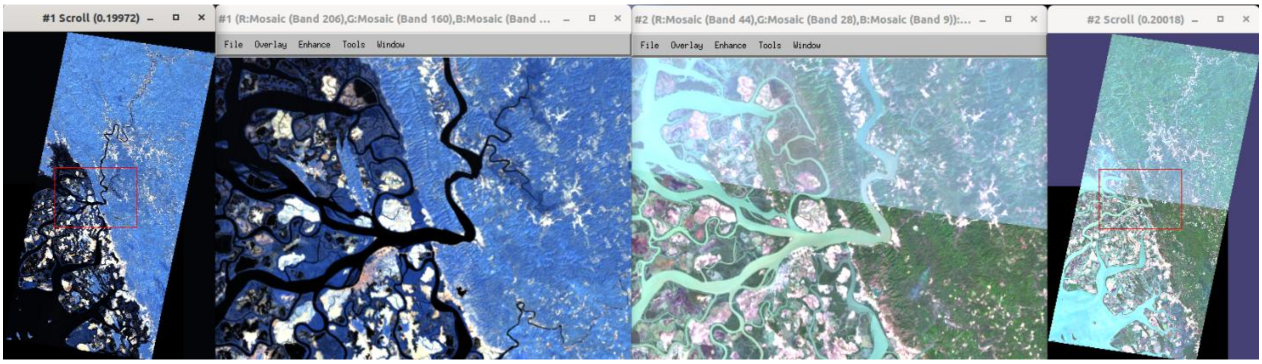

Figure 7-41 DT180304, mosaic of tiles 7 and 8, left: SWIR band composite; right: TrueColorComposite.

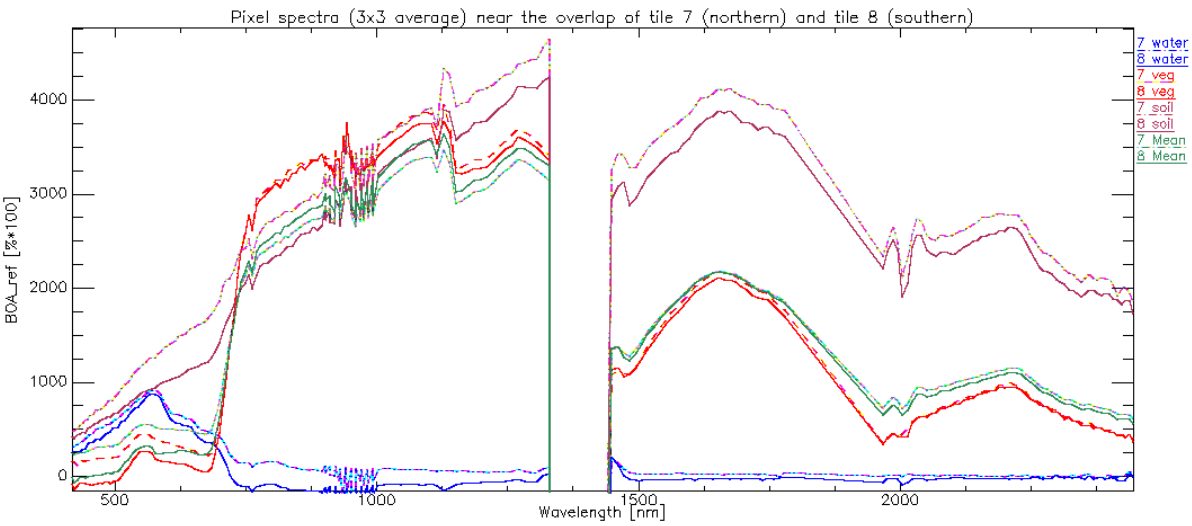

Figure 7-42 DT180304, 3x3 averaged spectra from tile 7 (dashed-dot lines) and tile 8 (solid line); the mean of areas close to the tile borders in green.

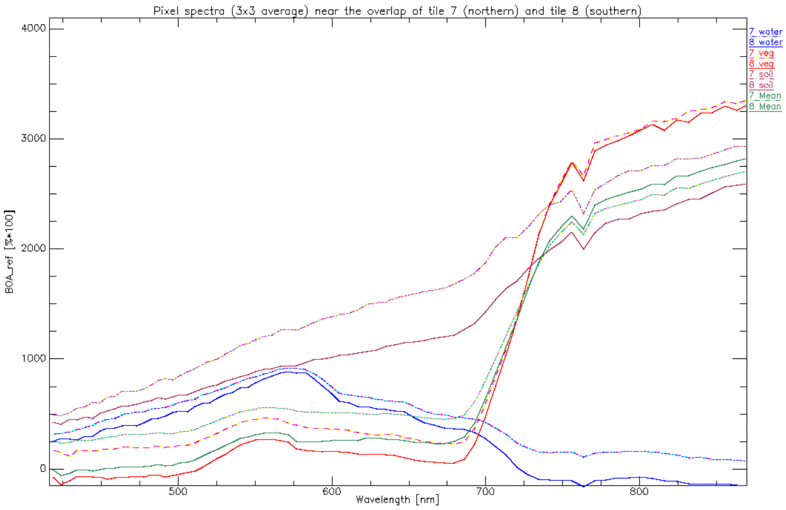

Figure 7-43 As Figure 7-42, zoom in on VNIR range.

Together with the brighter image impression of tile 7 than tile 8 in the VIS bands, and no difference in image brightness in SWIR bands, the cause can easily be explained: for tile 8, the estimated AOT value is higher, resulting in a stronger correction and therefore a lower reflectance in the aerosol-affected bands, while for tile 7, the smaller AOT results in a lesser correction and higher reflectances towards shorter wavelengths.

To conclude, for one of these tiles a slight overcorrection of the aerosol effect is observed, resulting in a visible tile border towards the following tile. But the overall shapes of the surface spectra, and the reflectances in the SWIR are estimated correct, and unlikely causing problems in the subsequent data analysis.

- **Kantaunggyi, Myanmar (DT180304, 2026-02-20), comparison of EOWeb and Geoservice products**

For the give two tiles checked before, it was additionally investigated if the on-demand L2A processing as provided in the DLR EOWeb results in the same results as the L2A data provided in the DLR Geoservice.

As expected, when setting the EOWeb processing parameters identical to the Geoservice standard (i.e., using only “land” processing), the resulting L2A datasets are identical.

And as further expected, when using the EOWeb default processing settings with “combined mode” (i.e., dedicated L2A water processing over water areas), the BOA reflectance values over land are still identical to the Geoservice product (all pixels flagged in green in the right part of Figure 7-44 showing the difference image), and all pixels flagged as water differ. Hence for land, the consistency of generated products is given also in this case.

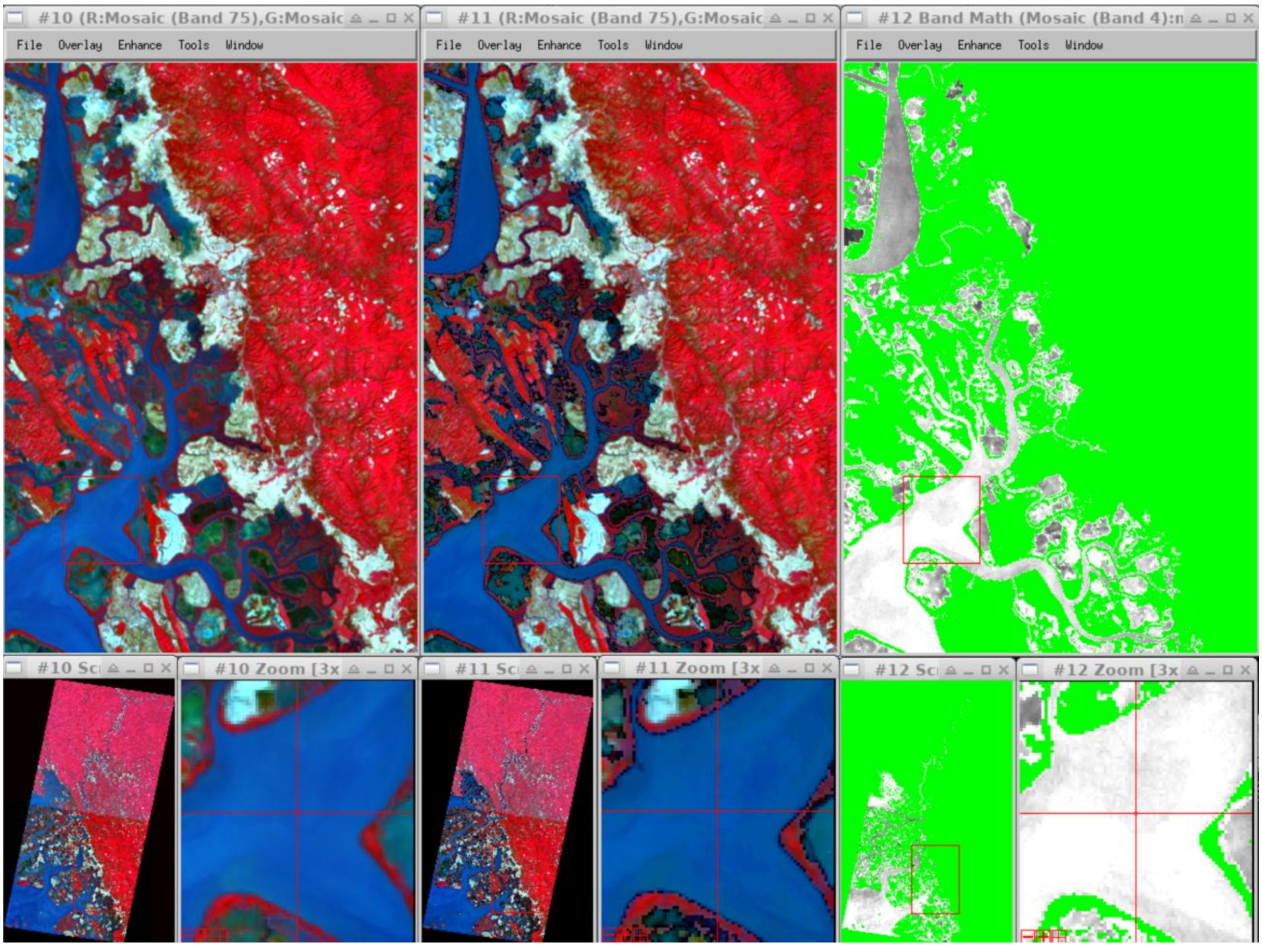

Figure 7-44 DT180304, two tiles, CIR composite. Left: Geoservice product; center: EOWEB product (standard settings not identical to Geoservice); right: difference image with identical pixel values flagged in green.

To conclude, the generated L2A products of EOWeb and Geoservice are identical when selecting identical processing parameters. And when using the standard EOWeb settings, the land processing is still identical, and areas flagged as water are differently due to the combine L2A processing scheme.

- **North Euboean Gulf, Greece (DT189005, 2026-04-21)**

The EnMAP datatake over the North Euboean Gulf (Figure 7-45 and Figure 7-46) contains open ocean and inland with vegetation as well as soil / rock outcrops (partially from open pit mines), and also a rough terrain reaching from Sea level up to ~1000 m. asl. and more.
For the masking (see Figure 7-47), land and water are correctly flagged, and also the smaller -partially artificial- inland lakes are correct, as depicted in the zoom inlay in Figure 7-47. Also, the bright non-vegetated areas in the south-eastern part of the scene (which are likely carbonate rocks due to the pronounced carbonate absorption feature at ~2.3 µm, see red spectrum in Figure 7-48) are correctly flagged as “cloud-free”.

Figure 7-45 DT167963, true color composite

Figure 7-46 DT167963, CIR composite

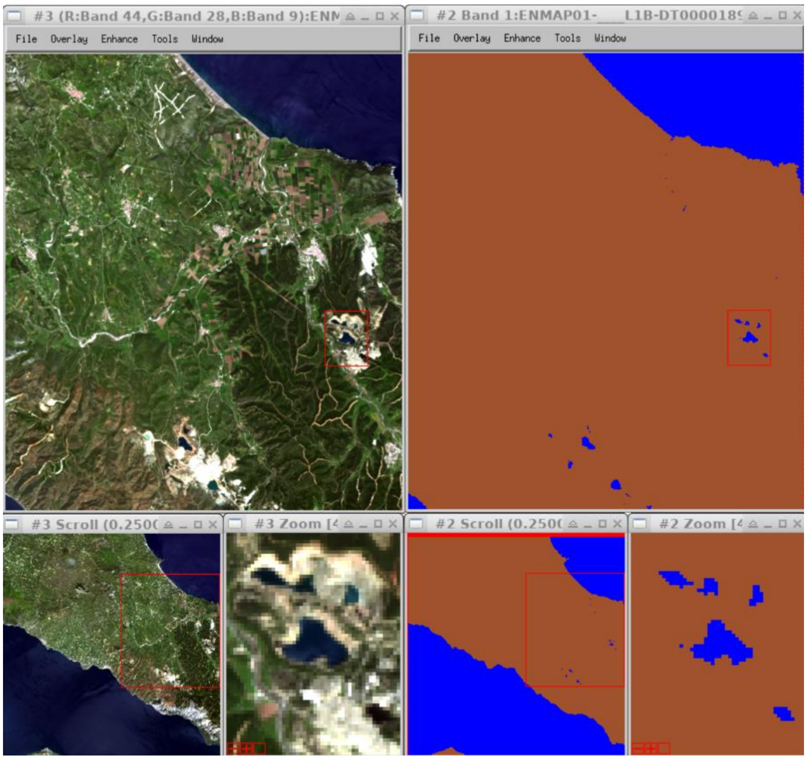

Figure 7-47 DT167963, left: true color composite; right: QualityClasses, with brown: land, blue: water. Note that all other masks are correctly empty and thus not depicted.

When having a look at the BOA reflectance spectra (Figure 7-48), the spectra of green and dry vegetation, as well as the different soils and the carbonate rock / soil are as expected regarding shape and overall reflectance. In summary, the masking and the retrieved BOA reflectance spectra are as expected.

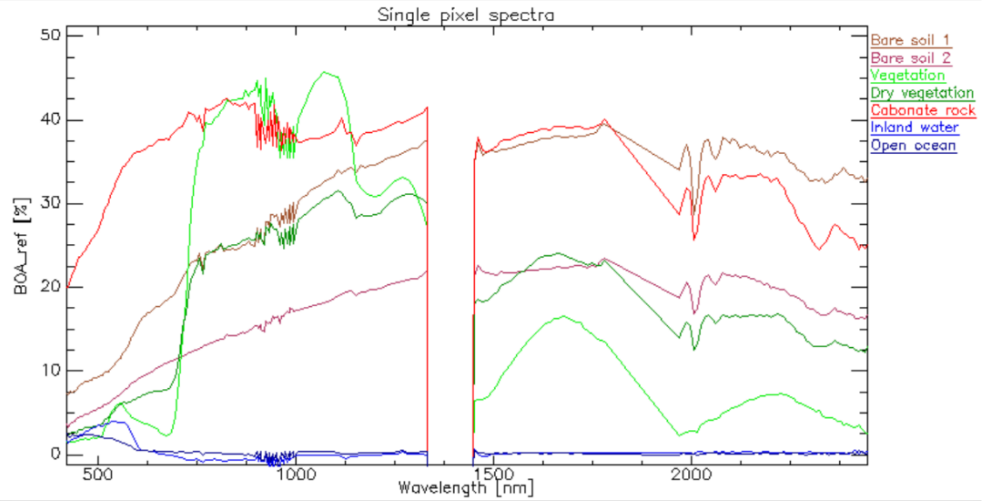

Figure 7-48 DT167963, single pixel spectra

8 External Product Validation

The standard quality parameters were validated in the external product validation process for the reporting period. The validation included 100 Level 1B, 101 Level 1C and 62 Level 2A products. All EnMAP products used for the validation were updated to the latest product version V01.05.06.

8.1 Level 1B

The following validation scenarios were performed to validate Level 1B products:

- TOA Radiance
- Signal-to-Noise Ratio (SNR)

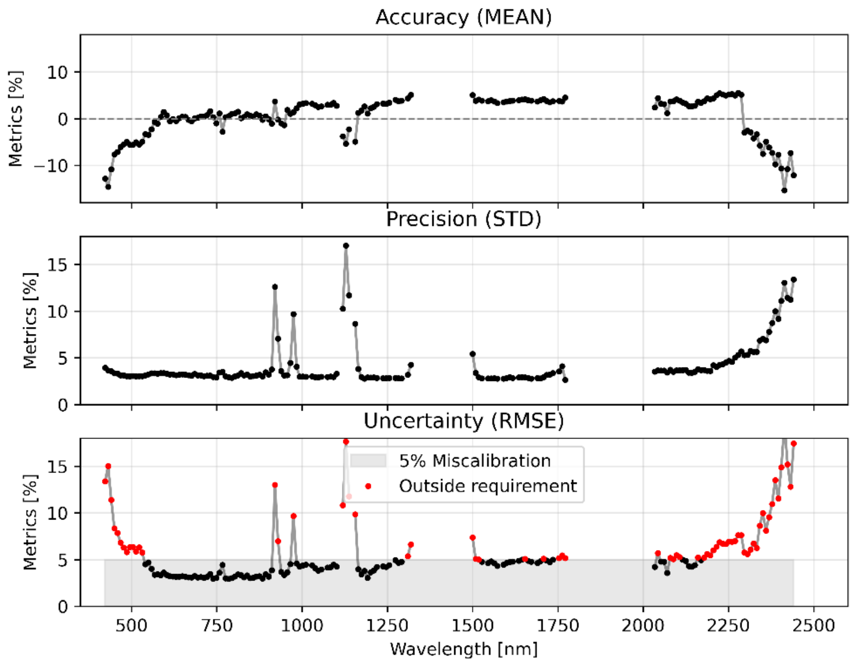

Figure 8-1 Errors between EnMAP TOA radiance and propagated TOA radiance from in situ measurements against wavelength for all arid validation sites based on 44 matchups

Two new matchups have been added to the Level-1B TOA radiance validation, including one matchup each for the RadCalNet station Gobabeb (GONA) and the HYPERNETS station Gobabeb (GHNA). This increased the number of available matchups for the TOA radiance validation from 42 to 44. Despite the larger sample size and the updated product version, the results remain consistent with those reported in the previous Mission Quarterly Report (MQR14): in the wavelength interval 550–1300 nm, the relative RMSE is within 3–4%, well below the mission requirement of 5%. In the 1500–1750 nm range, RMSE values of around 5% are observed and thus at the requirement threshold. Slight exceedances (<7%) occur in the 2000–2300 nm region, while larger deviations are visible at the detector edges (<600 nm and >2300 nm) (Figure 8-1).

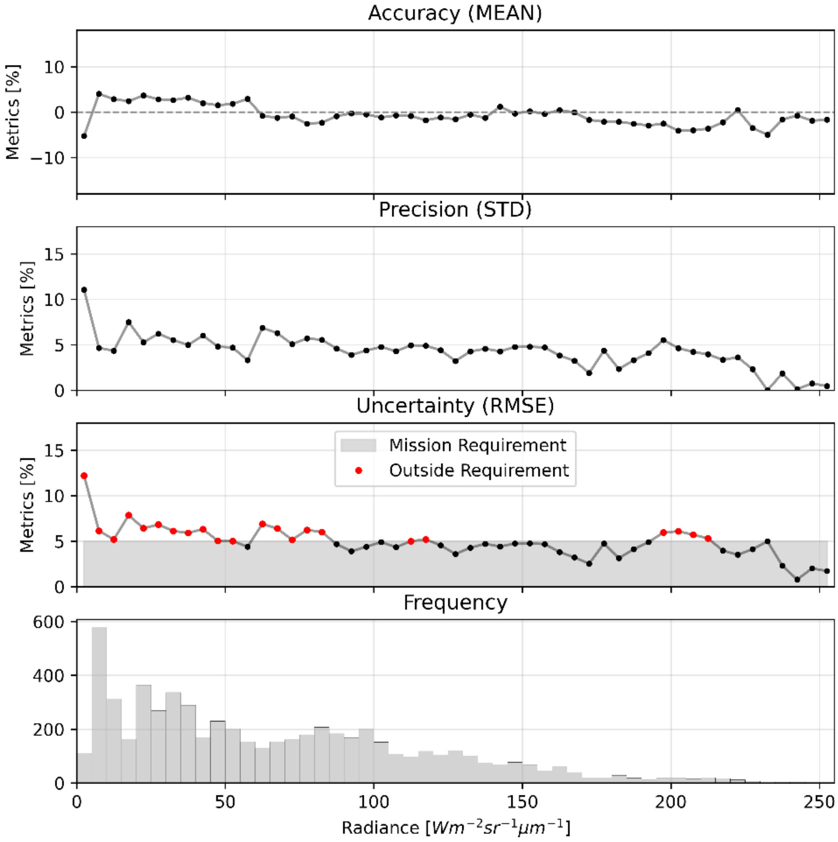

Figure 8-2 Errors between EnMAP TOA radiance and propagated TOA radiance from in situ measurements against radiance level for all arid validation sites based on 44 matchups.

The main update during this reporting period is the implementation of a revised noise model for the SNR calculation, which accounts for both signal-dependent photon noise and an additive, signal-independent noise component.

To enable direct comparison with mission requirements defined for a 30% reflective target, the scene-based SNR estimates are converted to a reference-equivalent SNR (SNR_{ref}). In previous reports, the observed SNR, directly derived from EnMAP imagery, was scaled to the reference radiance assuming a quadratic relationship between SNR and radiance. In the updated approach, the additive noise component is explicitly derived from the observed SNR and the corresponding L_{TOA}.

For this purpose, the L_{TOA} is converted into electron counts using a wavelength-dependent coefficient ccc, obtained from the latest radiometric module of the EnMAP end-to-end simulator (EeteS). The additive noise component is then calculated as:

$$additive\ noise\ [e]\ =\frac{\left({L_{TOA}}^2c^2-\ SNR^2L_{TOA}\ c\right)}{SNR^2}$$

For the VNIR bands, two distinct clusters of additive noise are observed, corresponding to high-gain (low radiance) and low-gain (high radiance) operation modes (Figure 8-3 a). The threshold separating both regimes, derived from instrument characterization (Figure 8-3 b), clearly distinguishes these clusters.

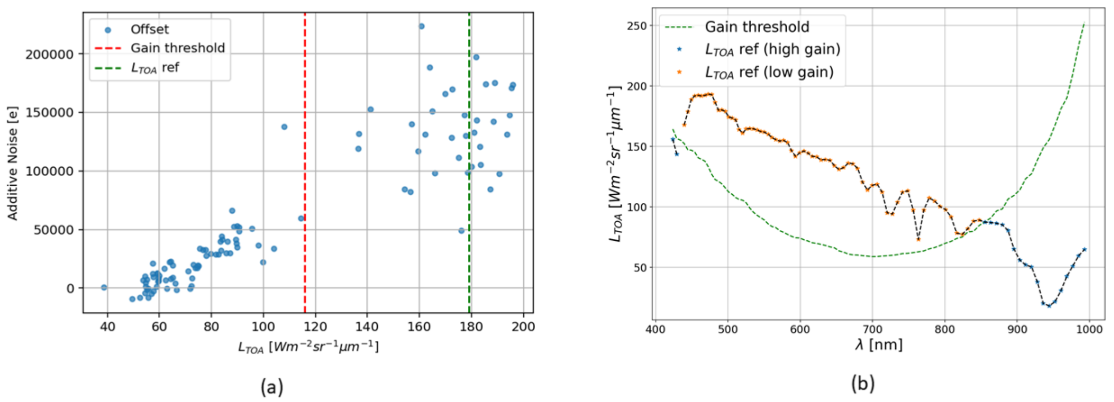

Figure 8-3 Additive noise vs. LTOA at 496 nm with gain threshold (red dashed) and reference LTOA (green dashed) (a). The gain threshold and reference LTOA for all VNIR channels are shown in (b).

The median additive noise is used to estimate the reference-equivalent SNR:

$$SNR_{ref} = \frac{L_{TOA_{ref}} * c}{\sqrt{additive\ noise + L_{TOA_{ref}} * c}}$$

Here, L_{TOAref} corresponds to the radiance of a 30% reflective target, a solar zenith angle of 30°, columnar water vapor of 2 cm and a visibility of 40 km. Only observations with consistent gain conditions are considered, i.e., low-gain measurements are used when L_{TOAref} falls within the low-gain regime and vice versa.

Additionally SNR_{ref} is normalized to a spectral sampling interval (SSI) of 10 nm by scaling the radiance-to-electron conversion coefficient c to enable a direct comparison with mission requirements:

$$SNR_{ref} = \frac{L_{TOA_{ref}} * c * \frac{10}{SSI}}{\sqrt{additive\ noise + L_{TOA_{ref}} * c * \frac{10}{SSI}}}$$

The SSI is defined as the difference between the center wavelengths of two consecutive spectral channels.

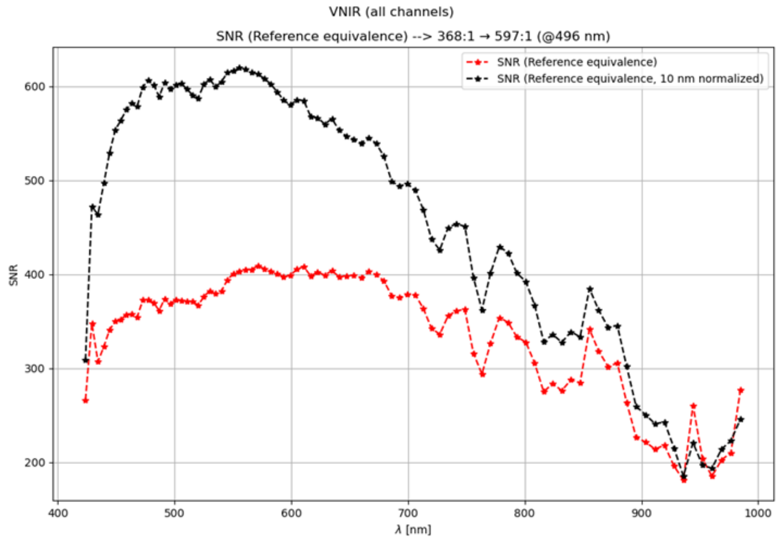

(a)

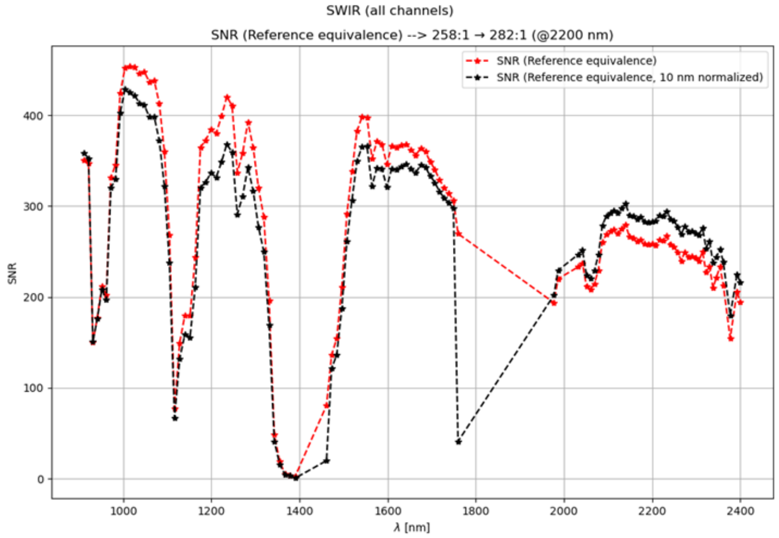

(b)

Figure 8-4 (a) SNR estimation for VNIR based on 52 tiles; SNR (reference equivalent) 368:1 @ 496 nm and (b) SNR estimation for SWIR based on 48 tiles; SNR (reference equivalent) 258:1 @ 2200 nm.

The SNR assessment is based on 100 tiles (VNIR: 52; SWIR: 48) from product version 01.05.06. Figure 8-4 shows SNR_{ref} (red) and the normalized $SNR_{ref10nm}$ (black) for VNIR and SWIR channels. Both correspond to a 30% surface reflectance target, enabling direct comparison with mission requirements.

At 496 nm (Figure 8-4 a), SNR_{ref} reaches 368:1, while the normalized value reaches 597:1, well within the mission requirements (>343:1). At 2200 nm (Figure 8-4 b), SNR_{ref} reaches 258:1 and the normalized value 282:1, thus also fulfilling the SWIR requirement.

8.2 Level 1C

The following Level 1C validation scenarios have been performed:

- VNIR-to-SWIR spatial co-registration
- Absolute spatial accuracy

The spatial co-registration between VNIR and SWIR was analysed for 101 products processed with product version 01.05.06. Compared to the previous report, the RMSE in X direction slightly improved to 5.5 m, while the RMSE in Y direction remained stable at 6.4 m. Overall, the spatial co-registration performance remains stable and is well within the mission requirement of less than 30% of a pixel.

The absolute spatial accuracy also slightly improved. Based on 101 tiles processed with product version 01.05.06, RMSE values of 9.7 m in X direction and 12.1 m in Y direction were achieved. These values are well within the mission requirements of <30 m for scenes with GCPs and <100 m for scenes without GCPs.

8.3 Level 2A

Land

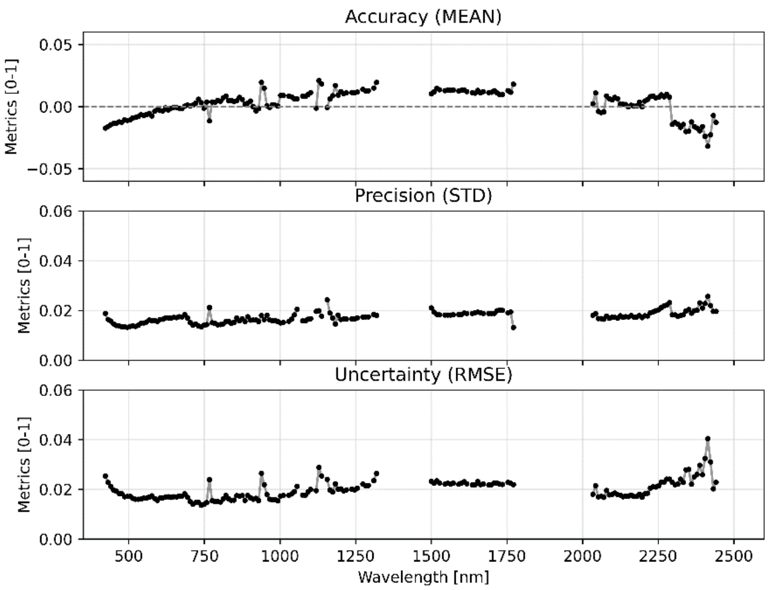

Figure 8-5 Errors between EnMAP and in situ BOA reflectance against wavelength for all validation sites based on 62 matchups.

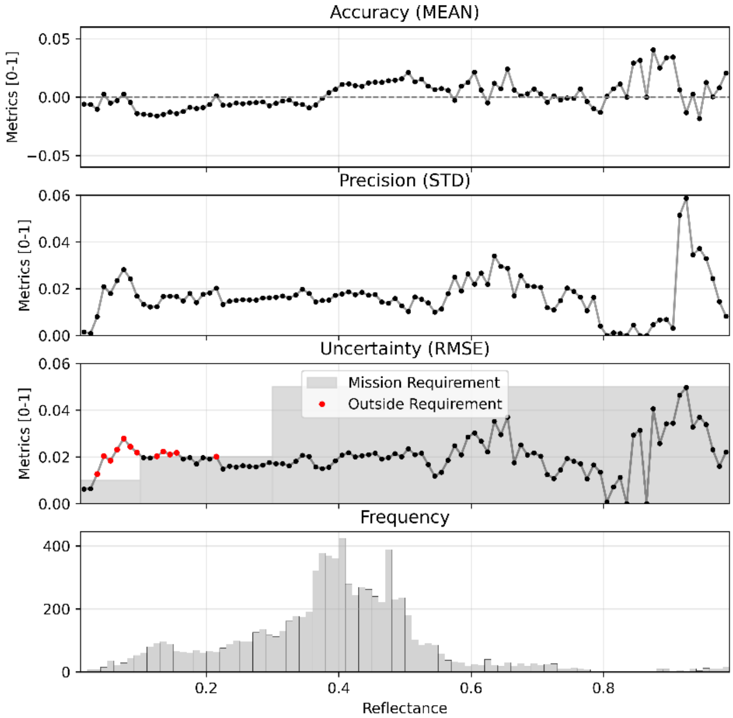

Figure 8-6 Errors between EnMAP and in situ BOA reflectance against reflectance level for all validation sites based on 62 matchups.

Three new matchups have been added to the Level-2A reflectance validation, including one matchup each for the RadCalNet station Gobabeb (GONA), the HYPERNETS station Gobabeb (GHNA), and the HYPERNETS station Järvselja, Estonia (JAES). This increased the total number of matchups to 62. The results of the Level-2A BOA reflectance validation remain consistent with previous reports. For low reflectance levels (< 0.02), the RMSE is slightly outside the mission requirements, while for all other reflectance ranges the results remain well within the mission requirements.

Water

Four new matchups have been incorporated into the water validation since the previous report. These include one additional matchup each for Lucinda and Trasimeno, and two additional matchups for Lake Garda. This increases the total number of available matchups to 90. The results show that the error between 700 and 800 nm has improved and is now well within the mission requirements for most wavelength ranges. Small overshoots can still be detected between 650 nm and 700 nm (Figure 8-7).

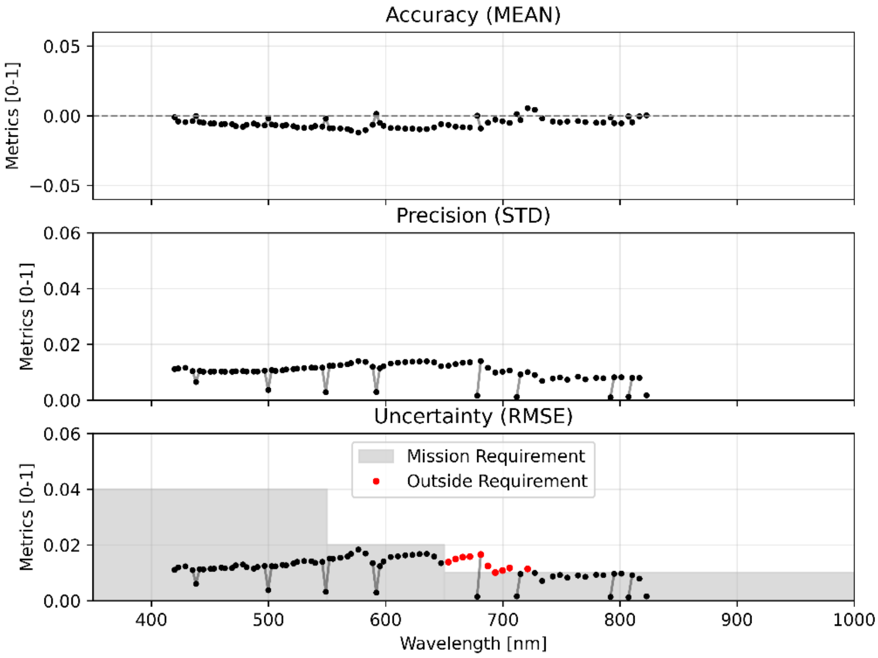

Figure 8-7 Errors between EnMAP and in situ BOA Normalized Water-Leaving Reflectance against wavelength based on 90 matchups.

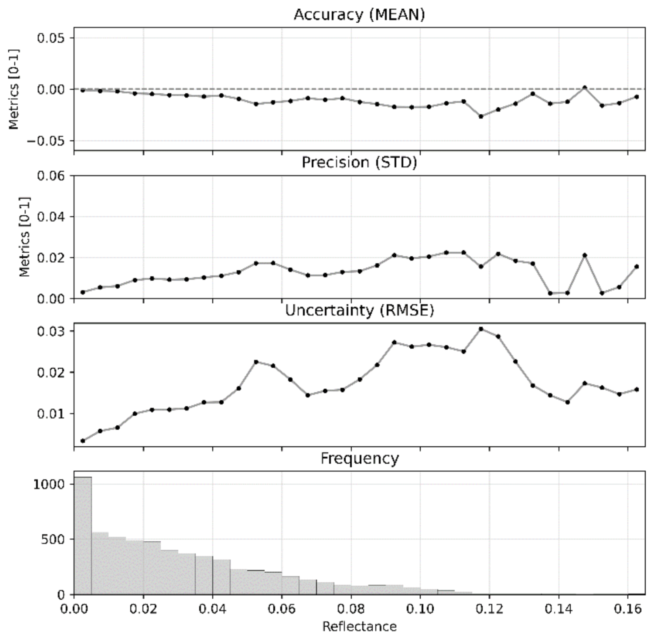

Figure 8-8 Errors between EnMAP and in situ BOA Normalized Water-Leaving Reflectance against reflectance level based on 90 matchups.

8.4 Summary of External Product Monitoring

The standard quality parameters were validated for Level-1B, Level-1C, and Level-2A products processed with the latest EnMAP product version 01.05.06. The validation results confirm a stable and overall high radiometric, spectral, and geometric data quality consistent with previous reporting periods. The Level-1B TOA radiance validation remains well within the mission requirements across most wavelength ranges, while the updated SNR assessment based on a revised noise model confirms compliance with the VNIR and SWIR mission requirements. In addition, the Level-1C geometric validation and the Level-2A water reflectance validation show slight improvements compared to the previous reporting period, while the Level-2A land reflectance validation remains stable and overall within the mission requirements.

9 Others

EnMAP Mission Operations and Status Publications:

- Brell, M., Reiners, P., Guanter, L., Segl, K., Chabrillat, S., Scheffler, D., Soppa, M., Bohn, N., Gorrono, J., Kokhanovsky, A., Bracher, A., Bachmann, M., Pato, M., Schneider, M., de los Reyes, R., Langheinrich, M., Holzwarth, S., Carmona, E., Storch, T., Pinnel, N., Kokaly, R., Ong, C., Green, R.O., Moreno, J.F., Gascon, F., Hank, T., Ben-Dor, E., Di Mauro, B., Colombo, R., Milewski, R., Brede, B., Schmid, T., Anderson, C., Schickling, A., Krieger, V., Bock, M., La Porta, L., Fischer, S. (2026). Assessment of EnMAP data quality through global product validation activities, Remote Sens. Environment, 342, 115459. https://doi.org/10.1016/j.rse.2026.115459

EnMAP Mission Operations and Status Presentations:

- **Mehr als alle Farben – EnMAP: Erfolg und Vision (Bonn, Germany, 10 March 2026)**
  - “EnMAP-Wissenschaft und Anwendungen”. Presentation by S. Chabrillat (GFZ)
  - “EnMAP Calibration as a Reference for Current and Future Hyperspectral Missions: Why Data Quality is Key for the Future”. Presentation by E. Carmona (DLR) and J. Nieke (ESA)
  - “Zeitserien & Langzeitdaten: Von der Forschung zur operationellen Nutzung am Beispiel Vegetation“. Presentation by A. Okujeni (GFZ) and L. Leist (U. Marburg)
  - “EnMAP – Abbildende Spektroskopie auch bei Nacht“. Poster by M. Bachmann(DLR)
  - “EnMAP Kalibrierung: Spektrale und Radiometrische Leistung“. Poster by D. Marshall Ingram (DLR)
  - “EnMAP Foreground Mission über Deutschland und Europa”. Poster by N. Pinnel (DLR)
- **GSICS Annual Meeting (Ottawa, Canada / Hybrid, 23 March 2026)**
  - The hyperspectral EnMAP and DESIS missions: status, processors, calibration and quality control. Presentation by M. Bachmann (DLR)